Addis Ababa University

አዲስ፡አበባ፡ዩኒቨርሲቲ

Seek Wisdom, Elevate your Intellect and Serve Humanity

School of Earth Science

Application of resistivity and magnetic method for characterizing type and depth of aquifers favorable for groundwater potential along Shashimene-Kofele road, central main Ethiopian rift.

By: Tariku Degife

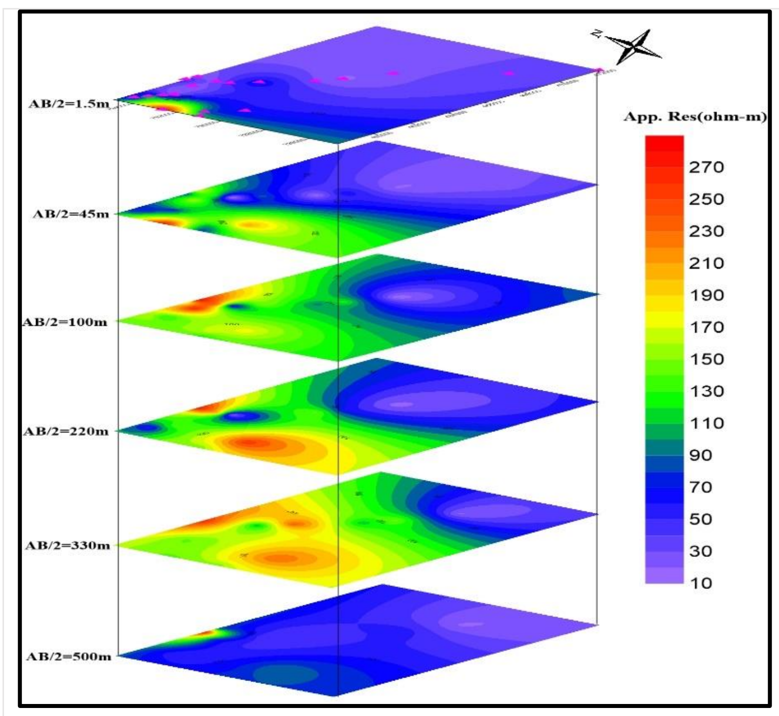

A Thesis Submitted to the School of Earth Sciences of Addis Ababa University in Partial Fulfillment of the Requirements for the Degree of Master of Science in Exploration Geophysics

Addis Ababa, Ethiopia

Jun, 2018

ADDIS ABABA UNIVERSITY

SCHOOLE OF GRADUATE STUDIES

Application of resistivity and magnetic method for characterizing type and depth of aquifers favorable for groundwater potential along Shashimene-Kofele road, central Main Ethiopian Rift.

By: Tariku Degife Haligamo

School of Earth Sciences

Approved by board of examiners:

Dr. Balemwal Atnafu	____________________	______________
Chairman, School of Earth Sciences	Signature	Date
Prof. Tigistu Haile	____________________	______________
Advisor	Signature	Date
Dr. Bekele Abebe	____________________	______________
Co- Advisor	Signature	Date
Dr. Abera Alemu	____________________	______________
Internal Examiner	Signature	Date
Dr. Dessie Nadew	____________________	______________
External Examiner	Signature	Date

Abstract

In this study resistivity and magnetic methods are applied for characterizing type and depth of aquifers favorable for groundwater potential along Shashimene-Kofele road, in central Main Ethiopian Rift. The fast growing population, and expansion of industrial activities in the study area demanded to assess groundwater potential and aquifer character. This study is aimed at assessing hydrogeological conditions of the area with the view of delineating subsurface layers and structures. Geophysical methods employed in this study are, Vertical electrical sounding and magnetic survey technique. Electrical sounding was used to investigate and ensure the potentiality of the groundwater. On the other hand, magnetic survey was used to delineate geological structures which control the groundwater flow system.

The geophysical survey comprises, twenty VES readings by using Schlumberger array along five survey lines, and above two hundred magnetic reading at about 30meter interval along two profiles. The field data obtained was processed and analyzed by using special computer soft wares. Information from nearby boreholes were incorporated to constrain resistivity and 2D model with geological layers and to enhance the result. The results of the geophysical survey are presented in the form of interpreted VES curves, sliced stacked map, pseudo depth section, geoelectric section, magnetic anomaly plot and 2D model.

The study result revealed four to five main geoelectric layers that differ in degree of weathering and fracturing. The highly weathered and fractured ignimbrite with sandy soil is the main water bearing horizon which has good groundwater potential. The aquifer thickness in the area is obtained to range between 50m and 160m. The result also revealed, the area is transected by several subsurface geological structures that are important for the movement and occurrence of groundwater. From the overall results, eight well sites are recommended for drilling based on their priority order. Detail geophysical survey and geochemical analysis are recommended along the proposed sites for farther studies.

Key words: Aquifer, Groundwater potential, VES, Geoelectric section, highly weathered and fractured ignimbrite.

Acknowledgment

My first and foremost gratitude goes to the almighty God for His unending blessing, mercies and graces throughout my life.

I would like to express my heartfelt thanks to my advisor, Prof. Tigistu Haile for his crucial comment, encouragement, supports and fatherly approach in order to accomplish this thesis successfully. My heartfelt thanks also extend to Dr. Bekele Abebe for his fatherly approach, encouragement and positive comments.

My gratefully thank goes to Dr. Shimeles Fissiha for his unreserved support, crucial comments and providing valuable VES data.

I would like to greatly thanks my classmate Getachew Belay for his support and devote much of time and energy specially during field data collection.

I am also thankful to the DH consult where I got hydrogeological report and lithological logs of the study area.

Last but not the last, my deepest heartfelt gratitude goes to all my family members, friends and instructors who credited their own role in my academic success.

Table of contents

List of figure

List of table

Acronyms

DC------------------------Direct Current

GPS-----------------------Global Position System

IGRF----------------------International Geomagnetic Reference Field

ITCZ---------------------- Intertropical Convergence Zone

Km ------------------------Kilometer

l/s-------------------------- letter per second

m.a.s.l----------------------- meter above sea level

MER-----------------------Main Ethiopian Rift

MOWE--------------------Ministry of Water and Energy

m----------------------------meter

N-S-------------------------North-South

nT---------------------------nanotesla

NW-------------------------North-West

SE-------------------------- South- East

SWL------------------------Static water level

TDS-------------------------Total dissolved solids

TMI-------------------------Total magnetic intensity

VES-------------------------Vertical Electrical Sounding

WFB------------------------Wonji fault belt

WHO------------------------World Health Organization

Ω-m-------------------------Ohm-meter

^{0}C--------------------------degree Celsius

CHAPTER ONE

1.Introduction

1.1. Background

Water is one of the prime necessities of life in the order of importance for the survival of man and other living things. The availability of quality water resources has always been the primary concern of societies in all over the world, even in the areas of more abundant rainfall. The problem of obtaining adequate supply of quality water is generally becoming more acute due to increasing industrialization and population. As a result of this, surface water cannot be dependable throughout the year due to variation in season and surface water contamination, hence, it needs to look for other alternatives. This makes the world depend on the largest available source of quality fresh water, which lies underground and this is referred to as groundwater. It is the water held in the subsurface within the saturation zone under hydrostatic pressure below the water table (Ariyo and Banjo, 2008). Fresh groundwater is very important, as in many countries, it is the main source of public water supply and its role in domestic and drinking water supply balance is growing every year because of continuing contamination of surface water (Igor et. al, 2004).

In 2004, World Health Organization(WHO) estimated that 1.1 billion people (17% of the world population) lacked access to fresh water resource. In the Ethiopian setting, people in many areas of the country lack fresh, drinkable water essential to their survival. Access to the fresh water resources development is beyond the reach of the overwhelming majority of the Ethiopian population. The fast growing population and the recurrent drought in many parts of the country has demanded such an effort more than ever.

The study area is found in the main Ethiopian rift which has many N-S trending normal faults which determines groundwater movement and occurrence. Groundwater circulation pattern and recharge source have also been the subject of a few studies in the southern MER. Large fault systems in the valley create conditions that allow very deep percolation of infiltrating surface water (Craig et al., 1977).

Groundwater occurrence around the area can be variable due to geological structures, abrupt discontinuity in lithology, the properties of the overburden and the weathered bedrock. Consequently, groundwater exploration within such complex geologic setting requires integration of geophysical investigation to effectively characterize the hydrogeologic zones and to enhance successful identification of productive well locations.

A geophysical measurement responds to some change in a physical, or chemical property. Geophysical methods are increasingly being used to characterize the subsurface. They offer the potential to derive basic characteristics, state variables, and properties of geological formations. Many geophysical methods employed in groundwater exploration include electrical resistivity, gravity, seismic, magnetic, electromagnetic and others, out of which the resistivity method, and magnetic method are the most effective for groundwater potential assessment and locating productive well. The vertical electrical sounding (VES) technique can provide information on the vertical variation in the resistivity of the ground with depth. Resistivity profiling provides a means of determining interval or lateral variation in the resistivity of the ground (Olayinka and Mbachi, 1992). The electrical resistivity of a formation depends mainly on the salinity of its fluid content, saturation, aquifer lithology and porosity (Shaaban, 2002). This technique has been successfully used in the world to explore groundwater and its condition. The electrical resistivity technique is also widely used to estimate the depth and the nature of the alluvium, aquifer boundaries and its location (Young et al., 1998).

1.2. Description of the Study area

1.2.1. Location and accessibility

The study area is located in West-Arsi Zone of the Oromia region on eastern margin of the central Main Ethiopian Rift (MER) at a distance about 250 km from Addis Ababa. It extends from Shashemene in the northwest to Kofele in the southeast direction (Figure 1.1). It is bounded by geographical coordinates of approximately 785000-800000 Northing and 455000-475000 Easting with elevation ranging 1900-2700 meter above sea level (m,a.s.l). The study area is accessed by asphalt road that runs from Addis Ababa-Shashemene 240km and that run from Shashemene-Kofele 25km long. Most of the study area covers the low lying plain land along Shashemene, and the ground surface elevation increases generally towards southeast direction of the study area.

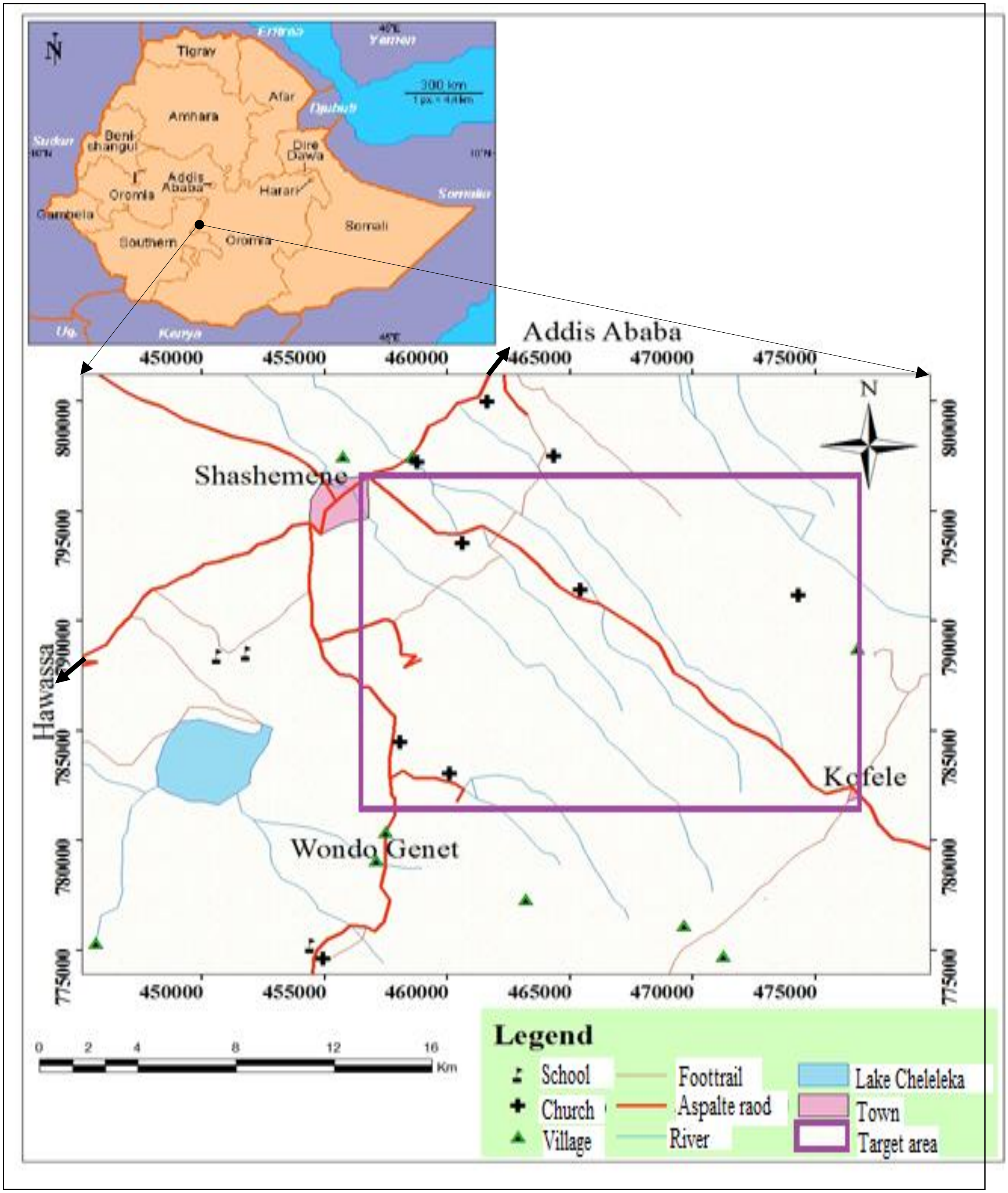

Figure 1.1: Location map of the study area

1.2.2. Physiography and drainage pattern of the study area

The geomorphology of the area is highly variable and is the result of volcanic and tectonic events with the associated erosion of volcanic rocks and deposition. The study area is found on the eastern margin of the central main Ethiopian rift. Three physiographical regions(zones) are found around the study area. The northwestern part belongs to the rift floor region, central part is dominated with rift escarpment and the Southeastern part belongs to the eastern highlands of the central main Ethiopian rift.

In the MER floor Quaternary deposit form a flat plain and eroded along river banks. Elevation in the MER floor fluctuates between 1580 to 1800 m.a.s.l. The hills are mostly in the shape of cone and semi-conical crests that leave the traces of past volcanic activity. The rift escarpment rises on the edges of the rift connecting the rift floor with the eastern highlands. The escarpment area altitudes vary between 1700-1900 m.a.s.l. The eastern margin of the rift characterized by a few widely spaced faults with very large vertical displacements to the rift bottom. The eastern highlands have altitudes exceeding 2000 m.a.s.l. The landform in this region is a result of major regional tectonics and associated volcanism. Residual landforms also dominate this region due to the weathering of volcanic landforms and products. Figure 1.2 shows physiography of the study area. The physiographic map was produced from digital elevation model (DEM) data of the area by using surfer10 and Arc GIS softwares.

Drainage pattern of the study area is divided by the main surface water. The study area is part of the rift valley lake closed basin. Drainage system generally belongs to Hawassa and Shala lake catchments. The Wesha, Werka Gomesho, and Wedesa rivers drain water from the eastern escarpment and feed the swampy area of the former Lake Cheleleka which is sub-basin of Hawassa lake. In the other hand, Debaba, Laftu, and Denbi rivers feed lake Shala. The lakes represent the drainage basin of the area. The drainage system form dendritic pattern with moderate drainage density on upland volcanics and low drainage density in the plain.

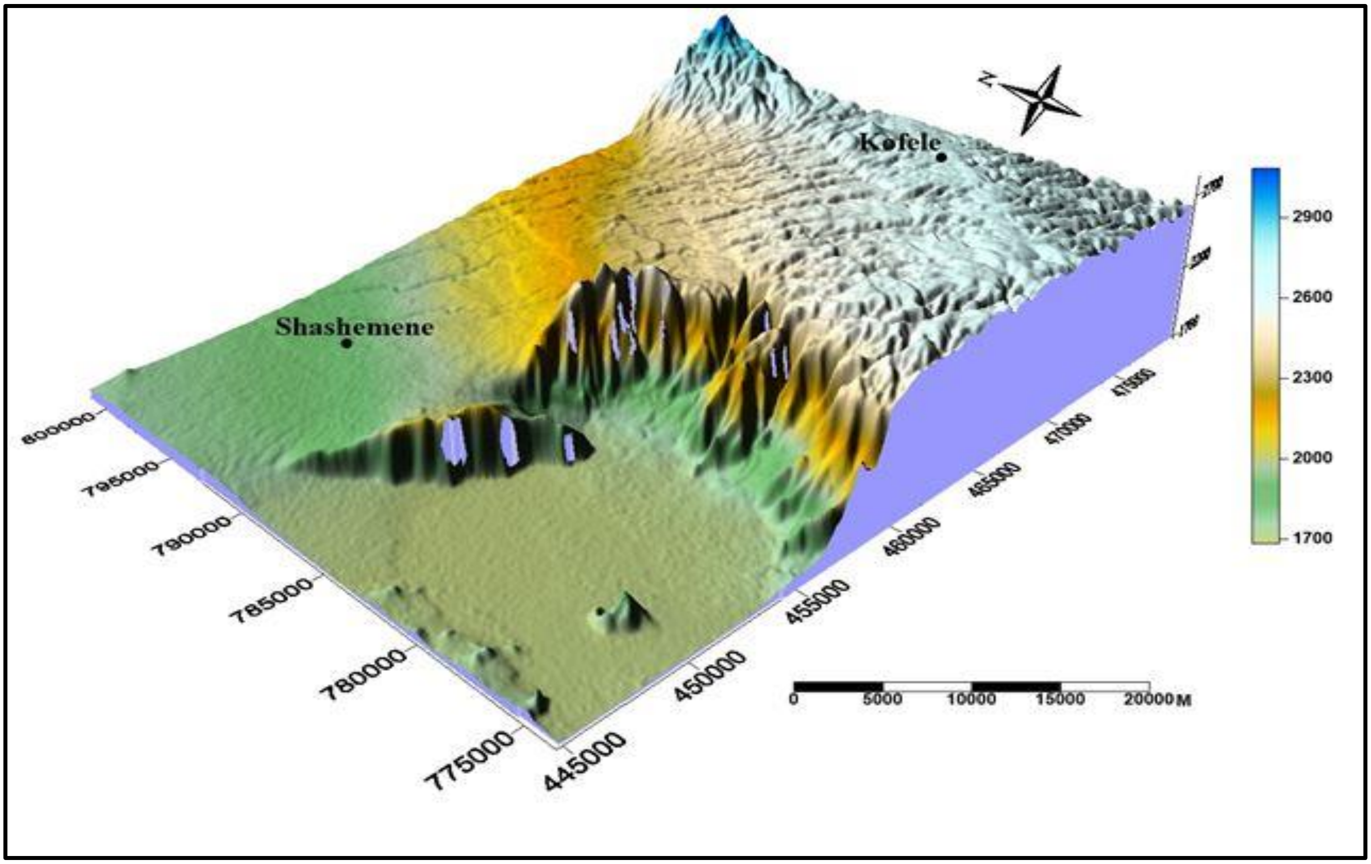

Figure 1.2: Physiographic map of the study area.

1.2.3. Vegetation

Vegetation type of the study area varies from the rift floor towards the rift margin. Rift floor vegetation ranges from bushed grassland to open woodland whereas, rift escarpment is characterized by bushed grassland, Eucalyptus, Juniper, Acacia and other long trees. Some dense forests, like Arsi forest are found in the study area.

1.2.4. Climate

The climate of the area is highly variable and mainly characterized by the subtropical Weyna Dega on the rift floor and the temperate to humid Dega climate zones on the escarpment and the adjacent highlands. The modern climate of the Shashemene area is mainly characterized by alternating wet and dry seasons following the activities of the Intertropical Convergence Zone (ITCZ) which separates air streams of the southeast and northeast monsoons (Nocholson, 1996).

The climate is warm and temperate in Shashemene area. The Köppen Climate Classification subtype for this climate is "Cwb" (Oceanic Subtropical Highland Climate). As shown in figure1.3 below the red line is the temperature of the Shashemene.

The average temperature of the study area is 18.1 ^{0}C. The warmest month of the year is April, with an average temperature of 19.5 ^{0}C. In December, the average temperature is 17.1 ^{0}C which is the lowest average temperature of the whole year.

Climograph (Figure 1.3) shows in winter, there is much less rainfall than in summer. The driest month is December, with 14 mm of rainfall. Most precipitation falls in July, with an average of 178 mm.

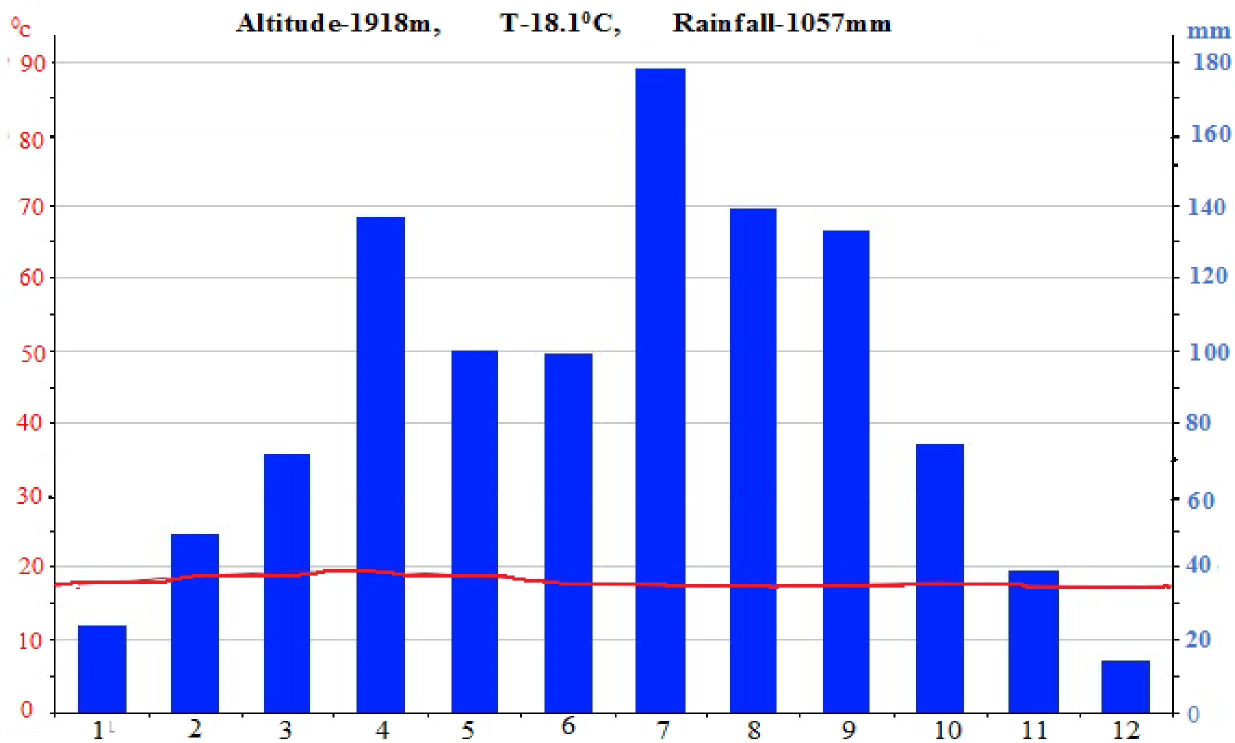

Figure 1.3: Climograph and temperature graph of Shashemene (http://www.weatherbase.com)

The rain gauges and annual rainfall averages are shown in table 1.1 below.

Stations	Cooordinates		Altitude (m.a.s.l.)	Average Rainfall
	X	Y		
Shashemene	455884	795851	1934	835

Hawassa	442915	780888	1765	969
Wondo Genet	457547	782775	1765	1135
Kofele	476356	782064	2679	1184

Table 1.1: Climatic stations of Shashemene and surrounding area (Brehanu, et al. 2014).

1.3. General discussion on application of geophysical methods for groundwater potential assessment.

For groundwater assessment, the most significant parameters that are used to describe aquifer system are ones that relate to the porosity and permeability of the aquifer and surrounding aquitard. Electrical conductivity, or its inverse resistivity, is the proportionality factor relating the electrical current that flows in a medium to the electric filed. The relationships between conductivity and material properties of an aquifer have been discussed by Mazac et al, (1990). Direct current (DC) electrical resistivity method for conducting a vertical electrical sounding (VES) has proved very popular with groundwater studies. Barker et al. (1992) and Carrithers and Smith (1992) all have demonstrated the use of electrical techniques for sitting boreholes in crystalline basement aquifers throughout Sub-Saharan Africa. VES techniques are typically limited in the shallow surface to exploration depths less than 50m due to spacing of the electrodes and the strength of currents required (Young et al., 1998). Recent development in computing power have led to advancements in electrical techniques that have opened up the opportunities of conducting 2D geoelectric cross-sections (Barker, 1996a and b).

Magnetic surveys are also used to identify faulting and other locations of weakness zone that determines occurrence of groundwater system and preferential fluid flow paths. Ground based magnetic surveying results mostly shows that the major faults and shear zones provided higher yield aquifers which could be mapped in relatively sparse groundwater regions.

1.4. Objective of the study

1.4.1. General objective

The main objective of this study is to use practical application of resistivity and magnetic method for groundwater potential assessment and aquifer characterization along Shashemene-Kofele traverse, in central MER.

1.4.2. Specific objectives

- ✓ To determine subsurface layers, their thickness and their resistivity's and magnetic susceptibility's.
- ✓ To map subsurface structures along the traverses that may control the flow of subsurface water from rift escarpment to the rift floor.
- ✓ To investigate the hydrogeological conditions of the area with the view of delineating the potential area(site) for groundwater development.

1.5. Statement of the problem

Availability of quality water (fresh water) resources has been always the primary concern of societies in all over the world. The problem of obtaining adequate supply of quality water is generally becoming more acute due to ever increasing population, climate change and industrialization. Ethiopia is being substantially affected by climate change, whose impact is to be seen in marked seasonal variations of climatic, hydrometric parameters and El Nino effect which result in drought for millions of people. The study area is situated in the Oromia regional state and fast growing population and the recurrent drought in the area demanded to assess the groundwater potential.

Therefore, a detailed study to illustrate the subsurface groundwater flow system and groundwater potential are indispensable in this area. Lack of understanding on groundwater system resulted in poor groundwater productivity of the wells, and drying of wells. The exploration of groundwater done so far is not adequate to solve the problem in relation to the demand for clean water raised in the society. Furthermore, due to population growth and the expansion of industrial and infrastructural activities, the groundwater reserve is decreasing and water demand is increasing at an alarming rate.

Therefore, the principal objective of this study was to gain a better investigation and assessment of ground water potential problem with respect to its aquifer character by using resistivity and magnetic method in order to support groundwater issues along Shashemene-Kofele road.

1.6. Review of previous work

A number of studies have been carried out in central main Ethiopia rift valley. Most of the studies have been carried out so far around and in the study area which directly or indirectly are related to this thesis. Among those, some of the works are briefly described as follows.

In the rift the localization of groundwater is strongly controlled by the rift faults. They have contrasting role in the movement and occurrence of groundwater. Most of the faults acts as conduit for groundwater flow. In contrast to the high hydraulic conductivity of the rift fractured volcanics, some faults act as barriers of groundwater flow. This is a common case in areas of structures where the faults dip against the topographic slope forming local grabens and horsts. Beyond the barrier faults most volcanic rocks do not form large extended aquifers, even if they are highly permeable. (Shimels Fikre, 2006).

Groundwater circulation patterns, groundwater recharge source identifications and interactions between lakes and ground waters have also been the subject of many important studies in the East African Rift System (EARS) (Craig et al., 1977; Darling, Brhanu, Arusei, M.K.1996....etc). Many of these studies shows that groundwater flow system in the main Ethiopian rift is from adjacent highlands towards the rift.

Berhanu et al., (2014) have compiled a set of geological and hydrogeological maps of the Shashemene sub-sheet 0738-D3. This project study focused on the geology, tectonic, and hydrogeology of the area. The final outcomes of the study briefly described as follows:

Groundwater flow is in general parallel with surface water flow system and is from the highlands through the escarpment to the rift floor. On the rift floor itself, the groundwater flow direction is governed by the relative elevations between the individual sub-basins. Groundwater (drilled and dug wells) remains the main source of water supply for towns and villages within the Shashemene sub-sheet.

According to Berhanu et al., (2014) the lithological units of the sub-sheet were divided based on the hydrogeological characteristics of various rock types using water point inventory data into the following aquifers/aquicludes.

- Extensive and moderately productive or locally developed and highly productive porous aquifers.
- Local and moderately productive fissured aquifers. The aquifers consist of basalts, ignimbrite, and rhyolite.

- Extensive and highly productive mixed porous and fissured aquifers. The aquifers consist of sequences of sedimentary, pyroclastic rocks and pumice fall.
- Formation consisting of a minor fissured aquifer with local and limited groundwater resources– Aquiclude.

Groundwater well drilling programs has been initiated over the last decades, but groundwater provision is often unsuccessful because of poor groundwater productivity of wells, difficult drilling conditions, drying of wells and springs after prolonged drought, or sometimes due to poor quality. This is hampered by lack of understanding of groundwater systems. Groundwater development is being conducted without a good understanding of its role in the hydrology of the basin. (Znabu G/Mariam and Elias D., 1989).

1.7. Methodology

The study was conducted through several different consecutive steps to achieve the final set goals. The methodologies are carried out in the following steps.

Initially, relevant literatures reviewed in order to have a general overview about geological and hydrogeological aspect of the study area and surrounding regions. This part provides important information about the area what other authors did and recommended to be done earlier. Generally, before the geophysical surveys were conducted; desk studies, interpretation of available aerial photos and terrain evaluation studies were conducted to make geophysical studies more easy and effective.

The second phase involves geophysical data acquisition, processing and interpretation in light of existing background information harvested from initial phase. Field work were carried out to collect primary data of resistivity and magnetic susceptibility of subsurface layers. In the field resistivity, and magnetic data acquisition were carried out with gathering all necessary information in a systematic manner. In order to acquire all the above data and information; appropriate instruments are used. Resistivity data is collected by using the PASI-16 GL plus p-100 Energizer. Magnetic data was acquired by using proton precession magnetometer.

After returning from the field, geophysical data correction(filtering), analysis and synthesis was conducted to process the raw data using different geophysical software and computer. The softwares that are used are: - Surfer, WinResist, Ip2win, Oasis Montaj, and others. Then after, geophysical maps and plots are produced and the correlation between geophysical methods and geological work was made. Maps and plots are interpreted to give the geological meaning which leads to the discussion and conclusion about the final result. Finally, after integrating the previous geological and geophysical work with current work, the draft report prepared. The above objectives reach properly and timely by using appropriate methodology and steps. The methodology and steps followed to conduct this research is presented as follows by the flow chart.

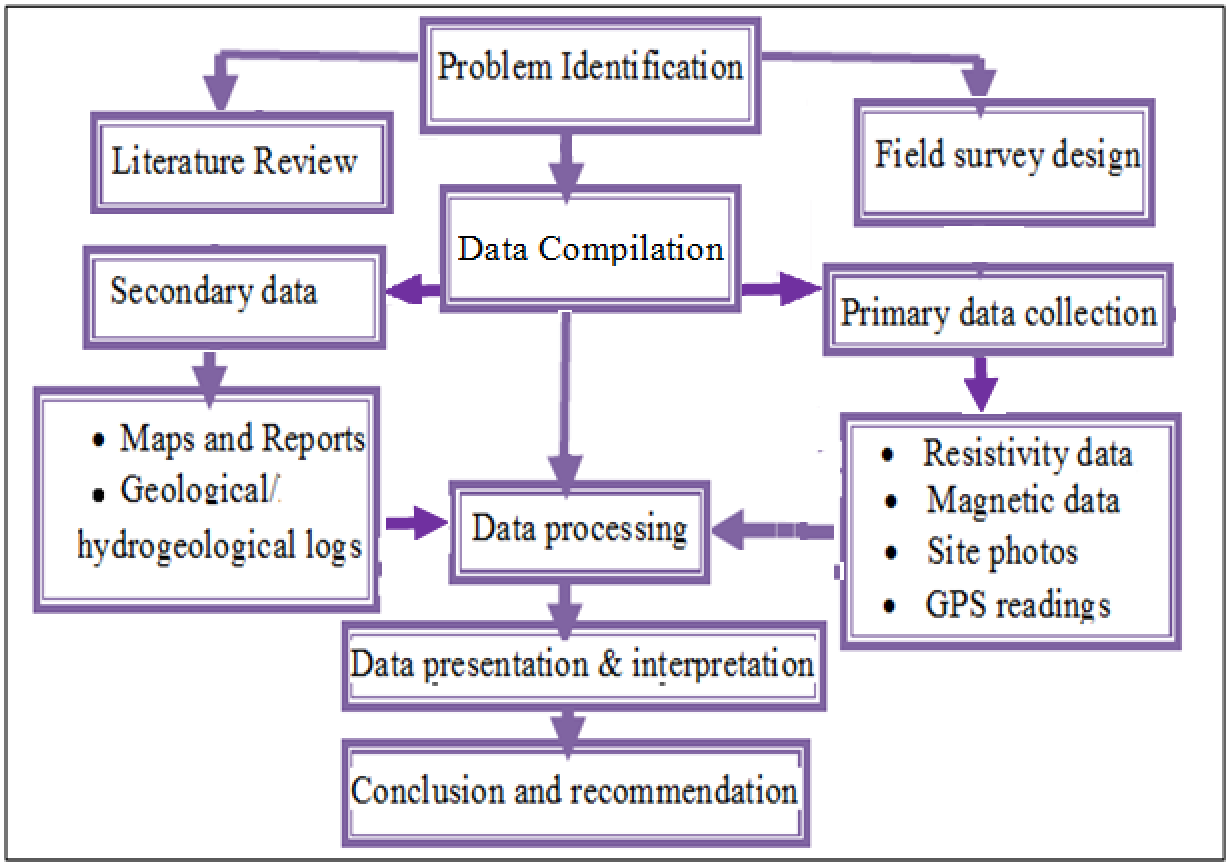

Figure 1.4: Flow chart of methodology

1.8. Significance of the study

This research project is particularly designed to better investigation of groundwater potential and aquifer character in the study area. It is significant to map structures (such as fault, and weak zones) and also define the vertical electrical/geological stratification of the study area by using integrated geophysical methods and their role in the groundwater flow system. So that, the study has following significances; -

- It gives some initial information for the future detailed study in the area which leads intended researchers for further research activity.
- It gives practical experience for the researcher.

- The result help and services as a great resource for the respective sectors.
- The study enhances understanding of the geology and geological structure of the area.
- It provides information about the hydrogeology, aquifer zone, its depth as well as the drilling point of high potential zone of groundwater in the study area.
- It develops the researcher's ability on geophysical software.
- This research work fills the existing gap of detail information and its usage in the geophysical methods in the country.

1.9. Limitation of the study

Every research study has to undergo some form of limitation. The major problems that encountered during the research study are: -

- ✓ Lack of well published documents, well organized books and previous studies.
- ✓ Scarcity of previous geophysical work on the area which are source for required data.
- ✓ Shortage of field materials like geophysical instruments and transport.

1.10. Layout of the thesis

The thesis is organized generally in six chapters. The first chapter is general introduction of the study which include description of the study area, statement of problem, objectives, methodology and previous work. The second chapter concerned mostly with previous studies that includes local and regional geology, tectonic setting and hydrogeology of the study area and the surrounding. Chapter three covers the theoretical background for the geophysical methods and its fundamental principle employed in this study. Chapter four deals data acquisition and data analysis which consists of selection of traverse, types of array and data acquisition and reduction, processing and presentation of the VES, and magnetic data. Chapter five deal with the discussions and interpretation of the processed and presented data or results. The last chapter deals with the conclusions and recommendations of the study based up on the result.

CHAPTER TWO

2. Geological and Hydrogeological Settings

2.1. Geological Setting

2.1.1 Regional Geology

The study area is part of the central Main Ethiopian Rift, a segment of the Miocene-Quaternary intra-continental extensional system which extends from Mozambique to Afar (Abebe et al., 2007). The Ethiopian rift system, which represents the northern half of the East African Rift System (EARS), consists of three rift zones with distinct tectonic and volcanic setting that are at different stages of rifting (Abebe et al., 2007). These are the Main Ethiopian Rift(MER), the rifted zone of southwestern Ethiopia, and the Afar Rift Systems. The width of the MER increases from the south(30-60km) to the central(65-80km) and the northern(80-120km) sectors, and in the southern part of the Afar Rift it is even more than 200km wide. MER developed over a span from the Oligocene to Quaternary. During the period, major volcanic episodes are recognized in Oligocene, middle Miocene, late Miocene, early-middle Pleistocene and Holocene. The oldest volcanic activities are basalt and rhyolite flows in Oligocene, exposed in and around the rift margins, which formed lava plateau in the surrounding area. By middle Miocene, the rift was formed in some parts with basaltic flows. In Pliocene, a huge pyroclastic flow covered the rift floor in central MER. (WoldeGebriel et al., 1990).

In Plestocene, Wonji Fault Belt(WFB), which is the main spreading axis of MER is formed at the rift floor. Rift floor basalt and rhyolite are erupted along WFB. The WFB is 2-8km wide with NNE trending zone disposed En-echelon in the rift floor within which are deep open, and consists of young faults. The volcanic activities are characterized by peralkaline fissure basaltic eruptions and rhyolitic eruptions which make volcanoes and calderas. Upper Miocene to Pliocene volcanic rocks of the Nazret Group composed by prevailing rhyolite and ignimbrites with intercalated basalt unit form the basement of the wider area of the MER. Lower Pleistocene volcanic rocks of the Dino formation composed of rhyolitic ignimbrites, crystal rich rhyolite, and trachyandesite, belonging to the volcanic activity of the Hawassa caldera.

The volcanic sequence of the Middle Pleistocene age- Corbetti ignimbrites is exposed in eastern half of the Shashemene sub-sheet map, whereas to the west it is covered by Holocene pyroclastic deposits. The youngest deposits of the Upper Pleistocene to Holocene show generally low thickness, most below 10m but cover a significant area of the sub-sheet. Extensive cover of colluvial and polygenetic to lacustrine sediments is exposed in the south-western corner of the Shashemene sub-sheet. (Berhanu et al., 2014).

The MER was created by a complex of NE-SW trending system of tensional faults, cut by more recent system of NNE-SSW trending faults known as Wonji Fault Belt. Structural relations of volcanic rocks along both rift escarpments of MER indicate a two-stage rift development. The early phase started during late Oligocene-early Miocene characterized by a series of alternating and opposed half-grabens evolved into a symmetrical rift during the late Miocene. (WoldeGebriel et. al., 1990)

According to Abebe et al. (2010) geological setting of central Ethiopia is classified in six lithologic units.

1. Pre-Tertiary sediments and crystalline basement: - The regional faults expose basement rocks beneath tertiary volcanic rocks in the southern sector of the MER, however in the central and the northern sectors, the rift margins are Tertiary silicic and mafic rocks. Pre-Tertiary crystalline basement and Mesozoic sedimentary rocks that are overlain by Oligocene basalt flows are exposed in the western margin of the central sector at the Guraghe Mountains (Woldegebriel et. al., 1990).

The crystalline basement is represented by altered biotite gneiss intruded by NW trending quartzo-feldspathic pegmatites. The Mesozoic sequence uncomformably overlies the crystalline basement at Guraghe.

2. Oligocene (32-29) and lower Miocene (12-8) plateau volcanics

This is the oldest volcanic unit in the central sector of MER and is found at Ambo and Agereselam, Welkite and Chilalo shield volcano. The main part of the Ethiopian plateau volcanics consists of the Trap series (Hofmann, 1997; Ukstins et al.,2002) and are in age of 32-29 Ma. Their average thickness at the Gurage margin is 600-700m. For both volcanic events widespread time-correlative basaltic units occur on the western and eastern margins of the central MER.

3. Miocene-Pliocene rift-shoulder trachytic-rhyolitic volcanics and pyroclastic layers

Several layers of pyroclastic units associated with trachytic and rhyolitic lava domes and flows together with some important central volcanoes were formed in this episode, and cover the MER shoulders and floor. This episode consists of uncompacted pumiceous fall and flow deposits, rhyolitic-trachytic lava flows, fissural basaltic lava flows with associated scoria and phreatomagmatic cones, and interbedded lacustrine deposits.

4. Plio-Pleistocene rift floor: -Volcanic rocks of Pliocene and Pleistocene age such as rhyolite, trachytes, ignimbrites and basalts are abundant within the rift floor (Kazmin, 1972). The eastern margin is covered by Pliocene to early Pleistocene(4.6-1.6Ma) shield volcanoes. These consist of trachytes with subordinate basalt (Merla et al., 1979; woldeGabriel et al., 1990). Silcic pyroclastic materials cover most of the MER floor (Mohr,1962; WoldeGabriel et al.,1990); they are Early to Middle Pliocene (4.2-3Ma, WoldeGabriel et al., 1990), mainly peralkaline rhyolitic ignimbrites intercalated with basalt and tuff.

5. Quaternary central volcanics and basaltic lava flows, associated scoria cones and phreatomagmatic deposits.

Quaternary volcanic setting was spatially associated with the Oblique faults of the Wonji Fault belt affecting the rift floor and still characterized by both silicic and basalts (Bora-Bericha Rhyolites and Wonji Basalt of Abebe et al., (2005)). Radiometric ages of this activity are generally < 1.8 Ma [e.g. WoldeGabriel et al.,1990; Abebe et al., 2005].

6. Quaternary lacustrine sediments and interbedded pyroclastics

Bimodal volcanic rocks (lava, pyroclastics and volcanoclastic strata) in the quaternary(<1.6-1.8Ma) were generally closely associated with Wonji Fault Belt affecting the rift floor (WoldeGabtiel et al., 1990). In the rift floor, interlayering of air fall pyroclastic deposits and lacustrine deposits are common. Pleiostocene-Holocene lacustrine sediments cover a significant tract of ground and were deposited in a lake whose level before 3500-2100 years used to be 100m (Kazmin et. al., 1980)

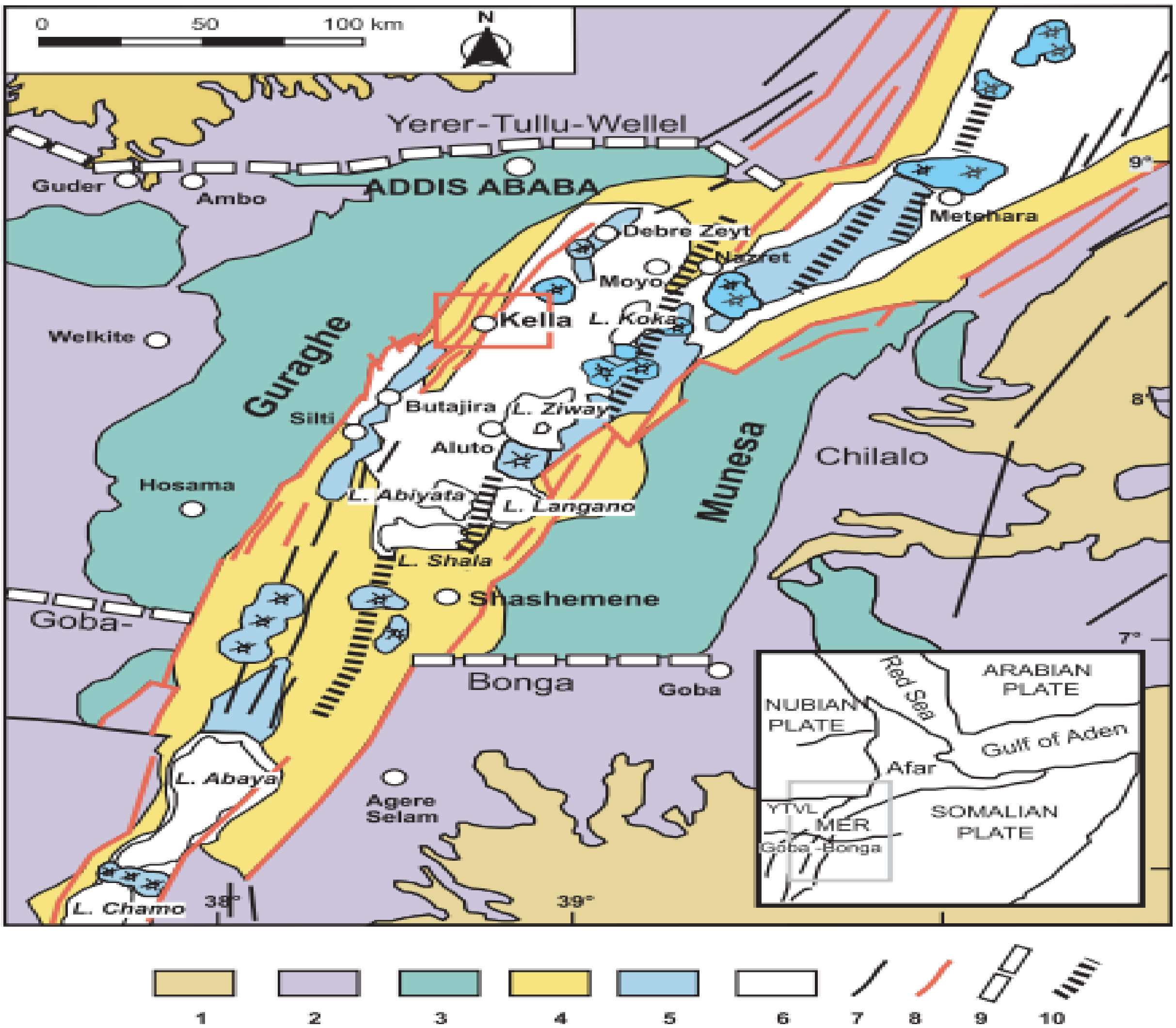

Figure 2.1: Geological map of central Ethiopia (modified after Jepsen and Athearen (1997).

(1). Pre-Tertiary sediments and crystalline basement, (2). Oligocene (32-29Ma) and lower Miocene (12-8 Ma) plateau volcanics, (3). Miocene-Pliocene Rift-Shoulder trachytic-rhyolitic volcanics and pyroclastic layers, (4). Plio-Pleostocene rift floor, (5). Quaternary central volccanics and basaltic lava flows, associated scoria cones and phreato-magmatic deposits, (6). Quaternary lacustrine sediments and interbedded pyroclastics, (7). Faults, (8). Major rift border faults, (9). Major transversal tectonic lineaments in the basement, (10). Wonji Fault Belt segments: Red square area show Kella area. In the inset: YTVL refers Yerer-Tullu-Wellel volcano tectonic lineament.

2.1.2. Local Geology

Detail study of the geology of the study area was conducted by corporation of Geological Survey of Ethiopia and Czech Geological Survey in 2014. Lithologic units of the study area are discussed in detail based on the previous reports conducted in the site and field observations. According to Berhanu et al. (2014) the lithological units described in the following text are arranged in stratigraphic order from the oldest to the youngest with descending order.

2.1.2.1. Basalt

Basalt of the rift floor is one of the latest volcanic manifestation in the Wonji group. This basalt was erupted from fissures during the Late Pleistocene and Holocene. Most of the eruptions are concentrated along the Wonji fault belt. The eruption fissures are obviously controlled by extensional fractures. The chains of scoria cones follow the lines of the fractures. Recent flows follow depressions of relief or over the fault escarpment. The eruption of basalt usually followed the silicic pantelleritic volcanoes, but some basalt is associated with the latest stages of their development. Effusions of basaltic lavas were associated with scoria cones. (Debebe et al., 2014). This rocks seem to be correlated with alkaline olivine basalts and scoria cones of the MER. (MOWE,2014).

2.1.2.2. Corbetti rhyolitic ignimbrite

Represents the complex of volcanic deposits of rhyolitic composition which dominates in the surface geology of the southeastern part of the study area. Ignimbrite is characterized by closely spaced discontinuity and as a consequence it is affected by weathering. The stratigraphic relations indicate that the complex can reach about 700m thickness. The ignimbrite sequence consists of welded and non-welded facies alternating many times. Welded facies are formed by gray to pinkish color typical stratified ignimbrite with abundant subhedral fragments of the phenocrysts of quartz. Sole quarry which is located in the vicinity of Sole village in the east of Shashemene exploits welded facies of Corbetti rhyolitic ignimbrite. It is very fresh and hard. The ignimbrite contains lithic fragments of quartz crystals. Non-welded facies are yellowish or grayish tuffs representing pumice-ash fall deposits and co-ignimbritic ash fall deposits.

Figure 2.2: Ignimbrite unit

2.1.2.3. Phreatomagmatic tuff

This unit covers nearly the entire area especially northwestern side of the study area, except stream gorges where the tuff was washed out by erosion. It belongs to the youngest volcanic deposits most probably of the Upper Pleistocene age. The tuff is loose and poorly solidified, but the textures allow interpretation of depositional process. The exposed deposit is documented by 2m thick units of matrix supported yellowish to brownish tuff with small clasts of pumice. The matrix supported unit overlays paleosol developed in Corbetti ignimbrite and contains in its basal part pieces of this paleosol. These two units are separated by a sequence of well-sorted massive ash layers with abundant accretionary lapilli altering with diagonally bedded layers. The horizon of the paleosoil with a deep brown color is developed on the top of the tuff sequence, mostly covered by a layer of the youngest pumice fall originating from Wondo Koshe volcano or from the Fike volcano between the lake Shala and Abijata.

Figure 2.3: Phreatomagmatic tuff unit

2.1.2.4. Pumice fall

The fall deposits were undoubtedly result of violent explosive event of the Wendo Koshe volcano. The pumice deposits are greyish to whitish color, loose, well-sorted and clast-supported. The thickness of the deposits increases continuously from ESE to WNW. The maximum size of the clasts correlated well with the thickness of the deposits and with the distance from Wondo Koshe volcano. The poorly developed recent soil lay upon the pumice unit.

2.1.2.5. Lacustrine sediments

The sediments are characterized by alterations of beds and successions with various origins. It fills the channel basin of the former lake Shala and lake Hawassa basins. Cheleleka lake in the southwest and Shala lake in the northern direction, are completely filled by sediment, and its remnants are represented by a network of irregular channels surrounded by an extensive swamp. The character of the sediments is a result of tectonic, volcanic and exogenous processes. They are a mixture of re-sedimented loose pumice or mixtures with a low portion of silt and sand.

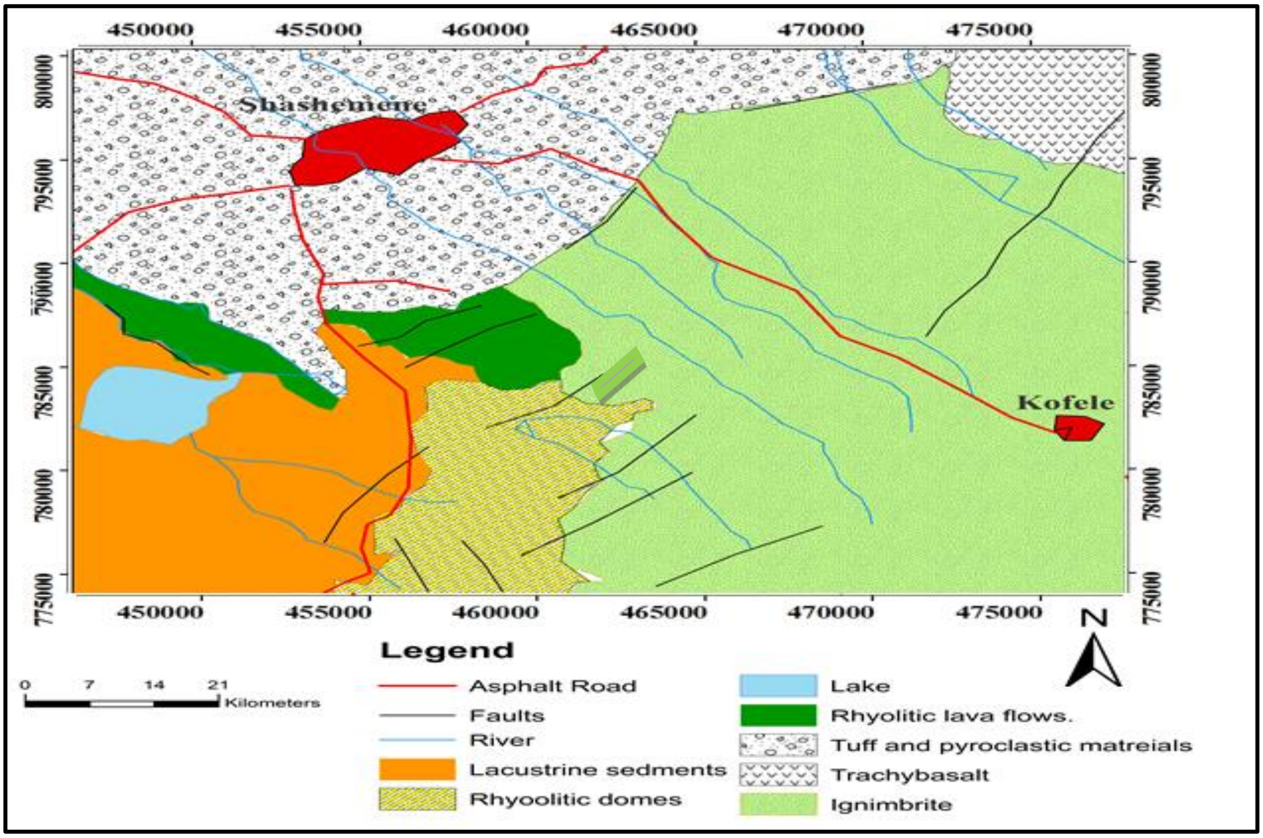

Figure 2.4: Geological map of the study area (modified after GISE, 2012).

2.2. Tectonic Setting

The Main Ethiopian Rift accommodates the active extension between the Somalian and Nubian plates since late Miocene (Ebinger, 2005). The study area has been confined to a complex of NE-SW trending system of tensional faults, cut hundreds of NNE trending more recent normal faults and volcanic centers along the rift floor closer to the eastern escarpment, and arranged in en-e'chelon fashion. This volcano-tectonic axis which is considered to be the current axis of crustal extension is known as the Wonji Fault Belt. (WoldeGabriel et al., 1990). Faults along this active zone form numerous minor horst and graben structures. As a result of this volcano-tectonic activity, geological structures of the study area can be classified majorly into brittle and ductile structures.

As shown in the figure 2.4, across the study area a number of normal and strike-slip faults were observed. The faults dip steeply to approximately E or W bearing well developed steeply plunging slickensides. These faults are almost parallel to the East African Rift System. Subordinate sets of faults predominantly have: - WNW-ESE trend mainly bearing dextral strike-slip kinematic indicators, approximately NE-SW trend showing a dextral strike-slip movement and approximately N-S trend with sinistral kinematics indicators. (Berhanu et al.,2014)

Extensional joints also occur in the study area. The main trends of their orientation are mostly parallel to the regional faults, predominantly NNW-ESE, WSW-ENE and also in WNW-ESE. In figure 2.5 below fractured ignimbrite exposed along Shashemene- Kofele road.

Along the NNE-SSW regional faults the original flow-banding was folded into asymmetric folds. Corresponding fold limbs dip under various angles to the ESE or WNW and the fold axis and associated stretching lineation plunge under low angles towards the NNE or SSW. The axial planes have a steep to moderate orientation dipping to the ESE. Ignimbrites display well-developed flow-foliation dipping to the SSE, N or NW. (Berhanu et al. ,2014).

Figure 2.5: Fractured ignimbrite

2.3. Hydrogeology of the Study area.

Most of hydrogeological information of the Study area were adopted from (Berhanu et al., 2014). According to the paper, the eastern plateau area is covered with various volcanic rocks forming undulating plain receives adequate rainfall resulting in good infiltration. Aquifer outcropping in the plateau area feed deeper fissured aquifers developed in underlying volcanic and sedimentary rocks. The escarpment area in the south east is steep for infiltration. However, in some parts it provides water to percolate and feed the aquifers. The groundwater flow system and direction is mainly controlled by faults in the escarpment area. There are also some faults which act as barriers to flow and some faults are access hot water to circulate from deep regional flow to the surface as hot spring. Groundwater flowing from the eastern escarpment feeds the aquifers of the rift floor.

Groundwater flow is in general parallel with the surface water flow system and is from the highlands through the escarpment to the rift bottom. Even on the rift floor groundwater flow direction is governed by elevation difference between the sub-basins. Two drainage systems of Hawassa and Shala lake basins are found in the study area, and groundwater flow is contained within these basins. Groundwater flows from east to west towards Hawassa lake catchment and from southeast (Kofele area) to the northwest (Shashemene area). (MOWE, 2014).

According to Tesfaye (1982) the large part of the MER area is characterized by Lucustrine Sediments and Volcano-Sedimentary rocks. The geology of the upper soil profile has good primary and secondary porosity and permeability characteristics which enables continuous groundwater recharge.

Lithologic units of the area were divided into groups with dominant porous and fissured permeability. This division served for a definition of the aquifer system of the Shashemene and its surrounding areas. The hydrogeology of the area shows aquifers and aquicludes defined based on the character of the ground water flow (pores and fissures), the yield of spring and the hydraulic characteristics of boreholes. According to Berhanu et al (2014) the following aquifers/aquicludes were defined.

2.3.1. Extensive and Moderately Productive Porous Aquifers

Classical porous unconsolidated sediments of the Quaternary age are represented by re-sedimented pyroclastics and fluvial and colluvial sediments. The porous aquifer is a very good source of groundwater depending on the thickness, sorting and recharge. Vocano-sedimentary rocks are developed in shallow depressions and represented by volcaniclastic strata, which have hydrogeological characteristics of sedimentary materials. The yield of drilled boreholes to the aquifer varies from 1 to 5 l/s. The average thickness of the aquifer is about 50m.

2.3.2. Local and Moderately Productive Fissured Aquifer

Permeability is largely a function of the primary(porosity) and secondary structures (joints and fractures) within the rock. Extensive volcanic ash beds may form semi-horizontal barriers to water movement resulting in lower productivity of basaltic units located at greater depth. Quaternary volcanic rocks like basalt, rhyolitic ignimbrite and rhyolite have dominant fissured permeability and represent fissured aquifers of the area. Welded ignimbrites usually alternate with non-welded facies and are intercalated with tuffs, pumice and lacustrine sediments.

Groundwater flow through joints, fractures and pores of non-welded layers and interbedded sediments. However, fissure flow is the dominant hydrogeological characteristic of these rocks. Fault systems may also provide significant groundwater flow paths. Outcrops of ignimbrites are mostly well jointed providing good possibility for direct infiltration as well as indirectly by overlaying porous aquifers within the Corbetti sequence. The continuity of fractures in both horizontal and vertical planes provides the aquifers their hydraulic continuity with adjacent units and aquifers. Wells developing groundwater from fissured aquifers located on the Shashemene sub-sheet have a yield ranging from 0.3 to 18.3 l/s. The level of groundwater is about 15 to 30 m below the surface at the foot of escarpment in the eastern part of the area.

2.3.3. Extensive and Moderately Productive Mixed Porous and Fissured Aquifers

Volcanic rocks of rift valley are often mixed with sediments in between lava flows of different volcanic episodes. The rocks are also intercalated with relatively thick layers of unwelded tuffs, ash and pumice deposits. Porous materials can significantly contribute to the safe yield of wells when they are developed together with volcanic rocks. The porous sediments in between lava flows form a body that can accumulate large volumes of groundwater by draining the surrounding fissured aquifer.

The mixed aquifers are exposed in northern part of the area where they form gently sloping eastern to north-eastern plains of the rift floor and the eastern part of the area where they form the eastern escarpment. The aquifers are recharged directly by percolating rain water and by overlaying porous aquifers of the Corbetti complex. Wells developing groundwater from mixed aquifers located on the area have a yield about 0.3 to 2.2 l/s. The groundwater level is about 100 to 150m below the surface in the eastern part of the area.

2.3.4. Formation Consisting of a Miner Fissured Aquifer- Aquiclude

Volcanic rocks with local limited groundwater resources. Aquicluds are unites where groundwater neither stored nor transmitted(flow) through the rock. These are groundwater resources with poor or no exploration potential and are represented by Hawassa obsidian. The fissures in the obsidian are well developed but they are open and the infiltrated water is transmitted very fast and the unit has no ability to store water. Groundwater development for limited individual water supply is very difficult.

2.3.5. Well Log Reports

A total of 22 well data have been collected from previous works and reports. As shown in appendix:2, eighteen water source inventory data points were collected. Their depth varies from 24 to 316m. Static water level (SWL) varies from 21 to 94.5m and the borehole yield is 0.3 to 18.8 l/s. Three boreholes have lithologic log (Appendix 3) which used to model geoelectric section, correlate and interpret nearby geophysical results. The well log data were used to extend surface geophysical measurements and to validate model.

CHAPTER THREE

3. Theory of Geophysical methods

3.1. General

Geophysics is the scientific method that uses the science of physics with high degree of technological development employed to observe the hidden subsurface of the earth. Geophysics is majorly subdivided as solid earth geophysics and applied geophysics. In applied geophysics, geophysical methods are employed to delineate the subsurface structure and to explore underground resource including groundwater. Nowadays, geophysicists are well equipped with geophysical instruments which are capable of exploring deep to several kilometers into the interior part of the earth. Geophysics is not only applied for subsurface investigations but it also used to investigate the ocean and land surface of the earth, which gives rise to the environmental application.

Many geophysical techniques have been applied to groundwater exploration with some showing more success than the others. Geophysical surveys greatly help in studying of groundwater potential in any hydrogeological setting and locate preferred borehole locations and determine the characteristics of aquifer. Depending up on the source signals, geophysical methods fall into two major groups: those that make use of natural fields of the earth refers to passive methods, and those that require artificially generated energy as source signals are called active methods. In all geophysical methods, there is always physical property for which a particular method is sensitive as such determines its specific range of applications. However, integrated geophysical methods may be applied simultaneously in solving certain geological problems. This approach greatly reduces the problem of ambiguity, which is inherent drawback in the interpretations of results of one method. Moreover, surface and bore hole geological information are vital important for the successful analysis and interpretation of geophysical data.

Of the several geophysical methods employed in groundwater exploration; the electrical, and magnetic methods of prospecting are the most effective for groundwater investigations. This is because; the electrical method is the most suitable to investigate saturation zones in the subsurface. Magnetic method in addition to several advantages they offer, the best tool that could map subsurface fractures detrimental for groundwater movement. These two methods have been used over the Shashemene-Kofele road for groundwater potential assessment and aquifer characterization. The theoretical foundations of the methods are therefore briefly discussed in the following sections.

3.2. Electrical Method

Electrical methods of geophysical prospecting are well established and the most important method for groundwater exploration. Electrical resistivity method is one that has been widely used because of the theoretical, operational and interpretational ease. The advantages of electrical methods also include control over depth of investigation techniques, portability of the equipment, availability of wide range of simple and elegant interpretation techniques, and related software etc.

According to Roynold (1997) the electrical resistivity methods were developed in the early 1900s but becomes widely used since 1970s due to primary availability of computers to process and analyze the data. Sharma, (1997) stated that the technique of resistivity survey was developed by Conrad Schlumberger who conducted the first experiments in 1912 in the field of Normandy. Real progress in applying electrical methods to groundwater exploration began during world war II (Zohdy et al., 1990).

There are two procedures of subsurface resistivity measurement. These may be either sounding survey or profiling survey. The methods vary in the type of target they are looking for and their measurement layout. While sounding survey also known as Vertical Electrical Sounding(VES). VES measures vertical variation of the subsurface at a point by assuming horizontal layer of the earth while, profiling survey measures the lateral variation of the subsurface by assuming vertical variation in electrical properties of the earth. VES survey is the technique which is widely and commonly employed for groundwater resources potential studies

3.2.1. Principles of Vertical Electrical Sounding (VES) Survey

In vertical electrical sounding(VES), the positions of electrodes are changed with respect to a fixed point known as sounding point and the measured values reflect the vertical distribution of resistivity values on geologic setting. The technique is extensively used in hydrogeological investigation to define horizontal zones of porous strata (Kearey et al., 2002).

Vertical electrical sounding consists of a symmetrical electrode array used to determine vertical variation in resistivity of the subsurface which is assumed to be consisting of horizontally stratified media. It also called electrical drilling or commonly vertical electrical sounding. As shown in figure 3.1 below it is achieved by symmetrically expanding the distance between current electrodes about the point called the sounding point, while keeping the potential electrodes(MN) at the same position, provides sounding curve corresponding to the apparent resistivity versus depth. As the current electrode spacing increases, the depth of investigation also increases.

The most commonly used arrays in electrical drilling survey are the Schlumberger and Wenner arrays. Schlumberger array as shown in figure 3.1 is used to collect data in this research work. The distance between the potential electrode is not greater than one tenth of the current electrodes spacing

Increasing the potential electrode spacing produces a 'step' in the apparent resistivity curve. It is common to obtain overlap between the curve segments by obtaining two reading at different potential electrode spacing for two adjacent current electrode spacing.

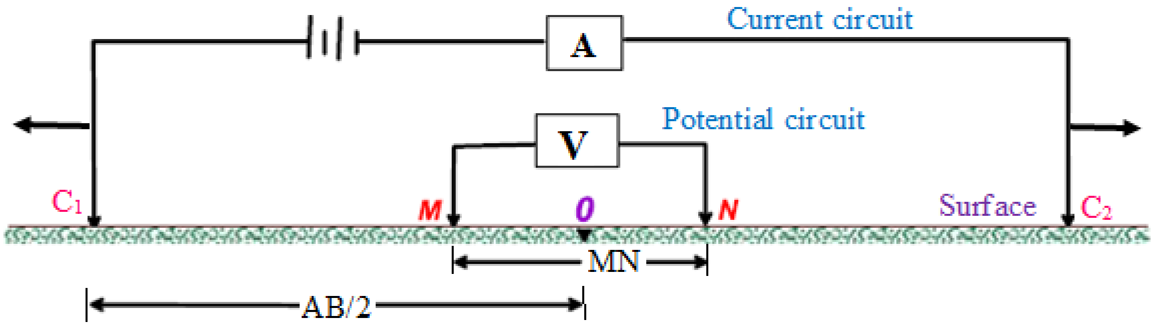

Figure 3.1: The Schlumberger configuration.

Let as to consider the subsurface consists of finite number of layers separated by horizontal boundary plane with the deepest layer extending to infinite depth, $(hn \rightarrow \infty)$,the other layers have finite thickness hi=h1,h2.... and each of the layers are electrically homogeneous and isotropic. The field is generated by point source of current located at surface.

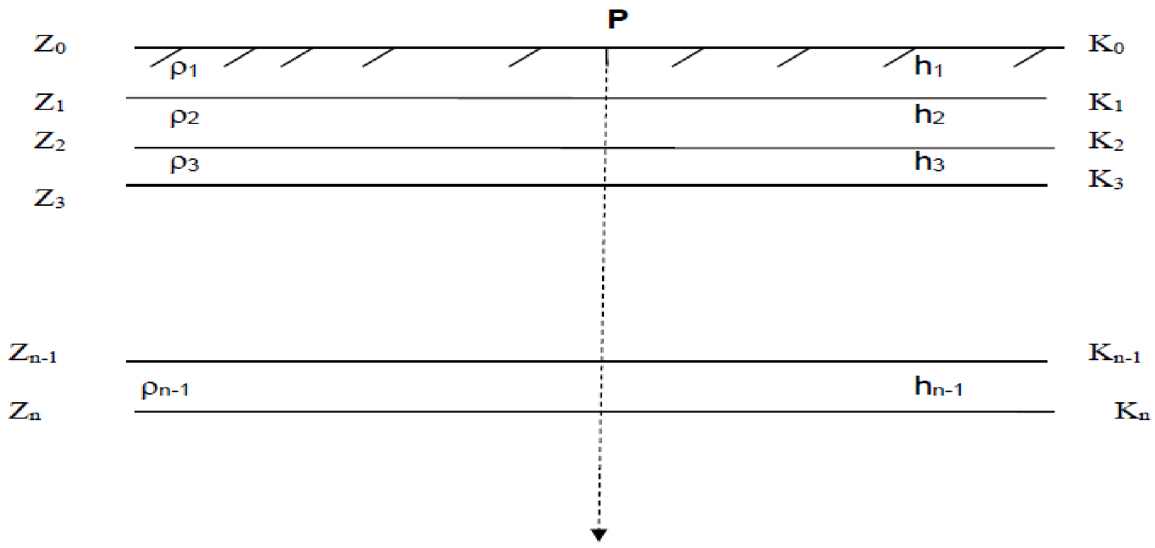

Figure 3.2: A multi-layer earth and problem presentation for solution of the potential

The derivation of potential based on the above conditions was first due to Stefanesu et. al (1930).

The electrical potential (V) for direct current satisfies the Laplace equation. The potential field has a cylindrical symmetry with respect to the vertical axis/line through the current source. Therefore, the Laplace equation in cylindrical coordinate is most appropriate.

$$\text{s}\frac{\partial^2 V}{\partial r^2}+\frac{1}{r}\frac{1\partial V}{\partial r}+\frac{\partial^2 V}{\partial z^2}+\frac{1}{r^2}\frac{\partial^2 V}{\partial \theta^2}=0 \tag{3.1}$$

For a solution symmetrical with respect to the vertical axis, $\frac{dv}{d\theta}=0\ and\,\frac{d^2v}{d\theta^2}=0$ so the equation(3.1) becomes

$$\frac{\partial^2 \mathrm{V}}{\partial r^2}+\frac{1}{\mathrm{r}}\frac{1\,\partial \mathrm{V}}{\partial \mathrm{r}}+\frac{\partial^2 V}{\partial z^2}=0 \tag{3.2}$$

The particular solution of equation (3.2) is obtained from method of separation of variables by making the assumption that there exist solutions that have the form:

$$V\,(r,\mathrm{z}) = U\,(r)\,W\,(\mathrm{z}) \tag{3.3}$$

Substituting equation (3.3) into equation (3.2) and dividing throughout by the product $U\,(r)\,W\,(\mathrm{z})$ gives

$$\frac{1}{\mathrm{U(r)}}\frac{d^2\mathrm{U(r)}}{dr^2}+\frac{1}{\mathrm{U(r)r}}\frac{\mathrm{dU(r)}}{\mathrm{dr}}+\frac{1}{\mathrm{W(z)}}\frac{d^2\mathrm{W(z)}}{dz^2}=0 \tag{3.4}$$

Equation3.4 is satisfied if and only if

$$\frac{1}{\mathrm{U(r)}}\frac{d^2\mathrm{U(r)}}{dr^2}+\frac{1}{\mathrm{U(r)r}}\frac{\mathrm{dU(r)}}{\mathrm{dr}}=-\lambda^2 \tag{3.5}$$

And

$$\frac{1}{\mathrm{W(r)}}\frac{d^2\mathrm{W(z)}}{dr^2} = \lambda^2 \tag{3.6}$$

Where λ is arbitrary real constant

The solution of equation (3.6) can be written as

$$W(z) = C_{2^e}{}^{-\lambda z} \quad and \quad W(z) = C_{3^e}{}^{+\lambda z} \tag{3.7}$$

The solution of equation (3.5) is then;

$$U(r) = CJ_0(\lambda r) \tag{3.8}$$

Where J_0 is Bessel function of order zero.

The combination of equation (3.7) and (3.8) gives the particular solution of the differential equation given by equation (3.2), which is

$$V(r,z) = Ce^{+\lambda z}J_0(\lambda r) \text{ and } V(r,z) = Ce^{-\lambda z}J_0(\lambda r) \tag{3.9}$$

Where C and X are arbitrary constants.

In equation(3.9) both ϕ (λ) and ψ (λ) are arbitrary function of λ.From the basic theory of the potential generated by a point source of current if intensity I, located at a point p is given by

$$V(r,z) = \frac{\mathrm{I}\rho}{2\pi}\left[\frac{1}{\sqrt{\mathrm{r}^2+\mathrm{z}^2}}\right] \tag{3.10}$$

Equation (3.10) can be written in Lipschitz integral formula that is;

$$\left[\frac{1}{\sqrt{\mathrm{r}^2+\mathrm{z}^2}}\right] = \int_0^\infty \mathrm{e}^{-\lambda \mathrm{z}} J_0(\lambda r)d\lambda \tag{3.11}$$

So that equation (3.10) can be written in the form of

$$V(r,z) = \frac{\mathrm{I}\rho}{2\pi}\int_0^\infty \mathrm{e}^{-\lambda \mathrm{z}} J_0(\lambda r)d\lambda \tag{3.12}$$

The general solution of differential equation (3.9) can be written in the form

$$V(r,z) = \frac{\mathrm{I}\rho}{2\pi}\int_0^\infty \left[\mathrm{e}^{-\lambda \mathrm{z}} + \theta(\lambda)e^{-\lambda z} + X(\lambda)e^{+\lambda z}\right]\mathrm{J}_0(\lambda \mathrm{r})\mathrm{d}\lambda \tag{3.13}$$

Where θ_i (λ) *and* χ_i (θ) are arbitrary functions of λ.

In the case of a point source of current at the surface of a horizontally layered earth we must thus write separate expressions for the solution in different layers that is;

$$V_i(r,z) = \frac{Ip_{\mathrm{i}}}{2\pi}\int_0^\infty \left[e^{-\lambda zi} + \theta_i(\lambda)e^{-\lambda z} + \chi_i(\lambda)e^{+\lambda zi}\right]J_0(\lambda r)d\lambda \tag{3.14}$$

The equation (3.14) is called Stefanesco integral and the subscript "i" refers to several layers of the subsurface.

3.2.2. Boundary Conditions

The following boundary conditions are fulfilled, for a potential setup by a single source of current at the surface of a horizontally stratified earth.

1. At each of the boundary planes in the subsurface, the electrical potential must be the same

$$V_i = V \text{ at } Z = h_i \tag{3.15}$$

2. The vertical component of the current density must be continuous on each boundary plane

$(J_i)_N = (J_{i+1})_N$

$$\frac{1}{\rho_i}\frac{\partial V_i}{\partial Z} = \frac{1}{\rho_{i+1}}\frac{\partial V_{i+1}}{\partial Z} \quad (3.16)$$

3. At the surface(Z=0) the vertical component of the current density J_v must be zero everywhere except in the infinitesimal neighborhood around the current source. In air $J_{air}=0$ and from condition (2), the vertical component of the current density at the surface must be zero. Near the current source the potential must not approach infinity as;

$$V = \frac{IP}{2\pi}\frac{1}{\sqrt{r^2-Z^2}} \quad \text{at depth Z=0, as } r \longrightarrow 0 \quad (3.17)$$

4. At infinite depth, the potential must approach zero, i.e. $V \longrightarrow 0$ as $Z \longrightarrow \infty$

3.2.3. Resistivity of Earth Materials

Resistivity of rocks of earth materials(rocks) mainly depends up on the water content(porosity), the resistivity of the water, the clay content and the content of metallic minerals (Bernard, 2003). The following consideration help in the determination of the resistivity of earth materials.

- ✓ Dry sand without water is very resistive.
- ✓ A hard rock without pores and fracture is very resistive.
- ✓ Porous or fractured rock bearing free water has resistivity, which depends on the resistivity of the water and on the porosity.
- ✓ Impermeable clay layer, which is wet, has low resistivity but may not contain enough yields for successful groundwater exploration.
- ✓ Mineral ore bodies (sulphides) have very low resistivity (much lower than 1ohm (Bernard, 2003).

Igneous and metamorphic rocks have high resistivity values. The resistivity of these rocks is dependent on the degree of fracturing, and percentage of the fractures filled with groundwater. Sedimentary rocks, which are usually more porous and have higher water have lower resistivity values as compared to igneous and metamorphic rocks. The resistivity of these rocks largely dependent on the porosity of the rocks, and the salinity of the contained water (Loke, 2004).

To identify the presence of groundwater from resistivity measurements, the absolute value of the ground resistivity must be considered. Usual target for aquifer resistivity can be between 50 ohm-m to 2000 ohm-m (Bernard, 2003).

Earth Materials		Normal Resistivity(Ohm-m)	
Sandstone		200-5000	
Weathered sandstone		50-200	
Clays		1-100	
Saturated gravel		100	
Basalt		$10\text{-}1.3\times10^{7}$	
Topsoil		250-1700	
Sandclay		30-215	
Saturated Sandgravel		30-225	
Tuff		2×10^{3}(wet)-10^{5}(dry)	
Numerical values for various type of water			
Type of water	Resistivity(ohm-m)	Conductivity(micros/cm)	Salinity(mg/l)
Very fresh	200	50	35
Fresh	20	500	150
Salted	10	1000	700
Sea water	0.3	30000	35000

Table 3.1: Resistivity values for earth materials (Bernard, 2003)

3.4. Magnetic Method

Magnetic techniques measure the remnant magnetic field associated with a material or the change in the Earth's magnetic field associated with a geologic structure or man-made object. They have been used for regional surveys since the early 1900s in the hydrocarbon industry and for longer in mineral prospecting. Magnetic surveys have also been used to identify faults and other locations of crustal weakness that may represent preferential fluid(groundwater) flow paths. The method also used in a wide variety of applications ranging from small scale investigation to locate pipes, cables and metallic objects near surface and to large scale regional geological mapping(Reynold,1997).

Most of the rocks are not magnetic, however certain types of rocks contain enough mineral to originate significant magnetic anomalies. The data interpretation that reflects differences in local abundance of magnetization is especially useful to locate faults and geologic contacts (Blakely, 1995).

3.4.1. Principle of Magnetic Method

3.4.1.1. Magnetic Force

The magnetic force as given by Columb's law for magnetic poles, symbolically identical to gravitation, is expressed by:

$$F_m = \frac{1}{\mu}\frac{P1P2}{r^2} \tag{3.27}$$

Where, μ is constant of proportionality, known as the magnetic permeability of the medium surrounding the poles, p_1 and p_2 are the strength of the two magnetic monopoles, and r, is the distance between the two poles.

Then intensity of magnetization **I,** is related to the strength of the magnetic field H, through a constant of proportionality **K**.

$$I = kH \tag{3.28}$$

The constant $\boldsymbol{\mu}$ depends upon the magnetic properties of the medium in which the poles are situated. This force is repulsive if the poles are the same in sign, and attractive if they are opposite in sign.

The space in which magnetic forces act on the magnet or coil, through which a current is flowing, is called the magnetic field. The force associated with the magnetic field is characterized by the magnetic induction B; which is given by

$$B=\mu H \tag{3.29}$$

Where $\mu=\mu_0\mu_r$ the permeability of the medium, the product of relative permeability and permeability of the free space.

Thus the above equation3.29 can be written as

$$B= \mu_0(1 + K)\, H \tag{3.30}$$

By introducing $K= \mu_r -1$ and rearranging we have

$$B= \mu_0 H+ \mu_0 KH= \mu_0\,(H+I) \tag{3.31}$$

3.4.1.2. Magnetic Susceptibility

In magnetic prospecting, Susceptibility is the fundamental material property whose spatial distribution we are attempting to determine.

Magnetic Susceptibility is a measure of the degree to which a material gets magnetized. The larger the susceptibility the greater the intensity of magnetization and the anomaly produced relative to the Earth's magnetic field will be bigger. The susceptibility of earth materials is almost entirely controlled by the amount of ferromagnetic minerals, grain size. and mode of distribution.

Table 3.2. Typical magnetic susceptibilities of some common rocks and minerals in rationalized SI units (Modified from Milsom, 2003)

Common rocks	Magnetic Susceptibilities(SI)	Ores	Magnetic susceptibilities(SI)
Rhyolite	0.00025-0.01	Hematite	0.001-0.0001
Gabbro	0.001-0.1	Magnetite	0.1-20.0
Greenstone	0.0005-0.001	Chromite	0.0075-1.5
Basalt	0.001-0.05	Pyrrhotite	0.001-1.0
Granulite	0.0001-0.05	Pyrite	0.0001-0.005

3.4.2. Earth's Magnetic Fields

The Earth's magnetic field consists of three components: 1) main field, 2) external field and 3) magnetizable materials within the Earth's crust (local anomaly field).

The main field which accounts for over 99% of the earth's total magnetic field which is caused by convection currents of conducting materials (mainly iron and nickel) within the liquid outer core. The main field consists of several magnetic elements, which are important in understanding the measured magnetic anomaly patterns. These includes: 1) magnitude of the field(F), 2) magnetic inclination(I) which is the dip of a magnetic compass needle from horizontal and 3) magnetic declination(D) which is the angle between geographic and magnetic north. Figure3.3 shows the relationship between these values.

Additionally, the Earth's main magnetic field changes with time due to variations in the motion of the convection currents within the outer core. These changes (called secular variation) cause the magnitude, inclination and declination to change with time. As a result, the IGRF is updated every ten years to give the DGRF(definitive), which is current reference model of the earth's magnetic field. The DGRF can be obtained from national geophysical data center of the National Oceanic and Atmospheric Agency(NOAA,2011).

The external field (diurnal variation) is due to currents within the earth's ionosphere. These currents are mainly caused by interactions with plasmas connected with solar winds. These variations fluctuate rapidly with time (minutes to hours) with maximum amplitudes varying from 50 to 200 gammas. In some days, these fluctuations are more random with amplitudes of several gammas and are called magnetic storms which related with solar flares and sunspot activity. The magnetizable materials within the earth's crust create small amplitude magnetic fields that cause spatial variation of the earth's main magnetic field. These crustal materials are the targets of the magnetic method.

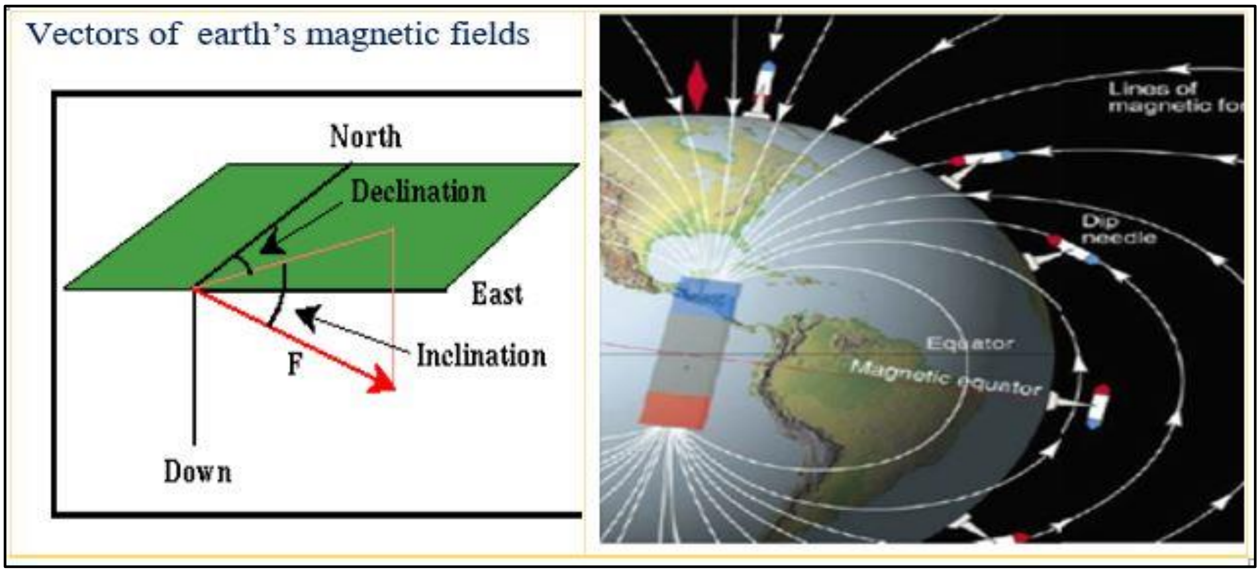

Figure 3.3: Magnetic elements of the earth's magnetic field (modified from Yahya 2011)

3.4.3. Noise and Corrections for Magnetic Variations

All magnetic data sets contain elements of noise and will require some form of correction to the raw data to remove all contributions to the observed magnetic field other than sub-surface magnetic sources. Correction for the diurnal variation is the most significant in the earth's magnetic field. The necessary corrections are mostly attempted by reoccupation of the base station which is located in or near the survey area.

$$DC = \left[\frac{BS_2 - BS_1}{T_2 - T_1}\right](T_r - T_1) \quad (3.32)$$

Where DC = Diurnal Correction T1 = Observed time of Base Station-1

BS_1 = Reading of Base Station -1 T2 = Observed time of Base station-2

BS_2 = Reading of Base Station-2 Tr = Observed time of each measuring points.

In order to produce a magnetic anomaly, the data have to be corrected to take into account the effect of latitude and, to some extent longitude. As the Earth's magnetic field strength varies from 25000nT at the magnetic equator to 69000nT at magnetic poles, the variation in magnitude with latitude needs to be taken into account (Reynold, 1997). Survey data at any given point can be corrected by subtracting the theoretical field value obtained from IGRE, from the measured value.

IGRFC = DC- IGRF

Where, IGRFC is the IGRF correction

CHAPTER FOUR

4. Data Acquisition and Processing

4.1. Data Acquisition and Instrumentation

To locate target areas for geophysical investigation; topography, vegetation, stream patterns and geological features of the study area were initially evaluated. Based on background information and careful observations, traverse lines were selected. The geophysical observations have been carried out all along the selected profile lines. The methods applied for the survey consist of the VES and magnetic geophysical technique. The layout of the geophysical observation points and profile line is shown in figure 4.1.

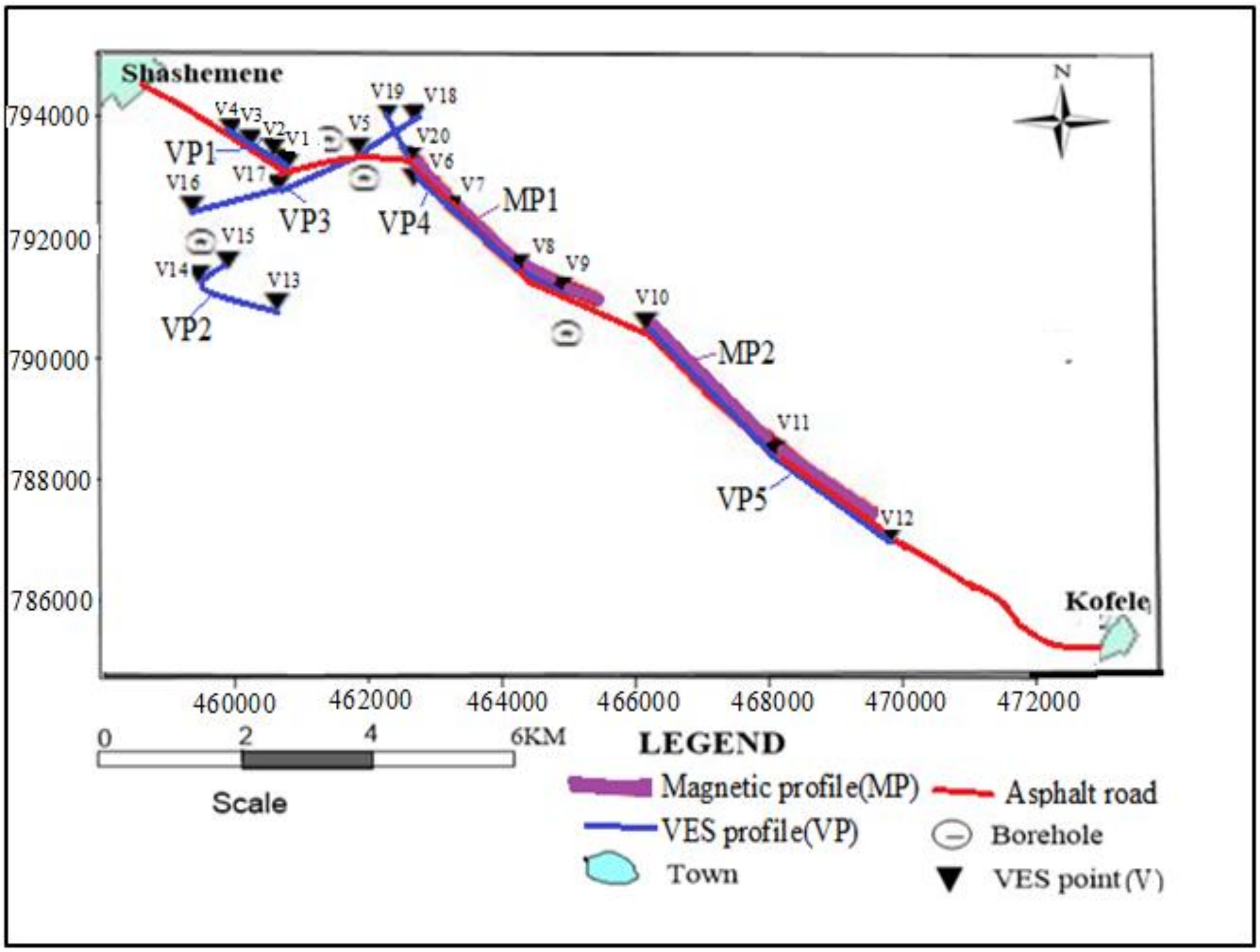

Figure 4.1: Distribution of VES points, borehole and magnetic profile lines over the study area.

4.1.1 Vertical Electrical Sounding

In this study resistivity data was collected by vertical electrical sounding (VES) technique using Schlumberger array. VES survey was carried out along five transect lines. Total of twenty VES data sets were collected on different transect lines. Twelve VES with current electrode spacing (AB/2) of 500m were collected during the field and eight VES data with AB/2 of 1000m was collected from previous work conducted by DH consultant.

PASI-16 GL equipment was setup, ensuring the electrodes were well hammered into the ground and Cables were connected to both current and potential electrode terminals. Direct current was injected in to the ground through the current electrodes and resulting potential drop is measured by a second pair of potential electrodes placed near the center of the current electrodes. Current electrode separation was progressively increased in series of measurements in order to acquire data from deeper horizons. The apparent resistivity values of each of the VES sites were recorded simultaneously. Location of each VES point were recorded in UTM coordinate. Table 4.1 shows UTM coordinates of each sounding points. In order to ensure consistent and reliable readings, measured results were plotted in the field during the measurement and inconsistent values were repeated to ensure uniformity in the readings.

Instrument employed for the Vertical Electrical Sounding (VES) survey was the **PASI-16 GL** electrical resistivity unit plus P-100 Energizer (Figure 4.2). Handheld GPS was used to record the sounding point coordinate. Other instruments are also used in VES survey which includes: -Meter, Hammer, Cable, Cable reels and others.

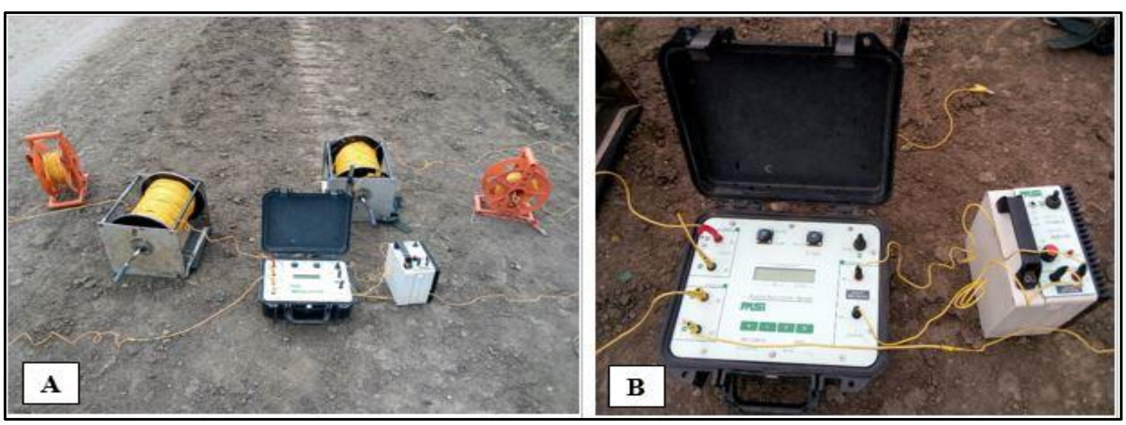

Figure 4.2: Photo((A) and (B)) showing connection for resistivity method.

Table 4.1: Location of each sounding (VES) pointes in UTM coordinate.

VES No.	UTM coordinates			Remark
	Easting	Northing	Elevation	
1	0460042	0793715	2067	
2	0459686	0793968	2061	
3	0459248	0794224	2061	
4	0458818	0794492	2032	
5	0461406	0794010	2082	
6	0462564	0793302	2164	Near Selam water
7	0463307	0792598	2212	
8	0464676	0791232	2323	
9	0465541	0790700	2345	
10	0467253	0789855	2365	
11	0469807	0786784	2501	Hurssa Simbo
12	0472201	0784736	2585	Germama
13	0459778	0790281	2104	
14	0458169	0790988	2070	
15	0458756	0791263	2076	
16	0458051	0792579	2036	
17	0459968	0793683	2066	
18	0462528	0794760	2120	
19	0461984	0794833	2106	
20	0462435	0793809	2140	

4.1.2. Magnetic Survey

The magnetic survey was conducted along two traverse lines within the study area. Over two hundred magnetic data was collected at every 30m interval of survey points. The profiles were oriented about northwest-southeast in order to cross and to detect structures determining groundwater occurrence.

Two base stations were established for diurnal correction of the magnetic data. At each station the magnetometer reading, time and its location in UTM coordinate were recorded. At every stations three suitable readings are taken in systematic manner. The observed magnetic field data were corrected for diurnal variation using the base station reading taken at the beginning and reoccupation reading after each 30 minutes.

The magnetic survey was carried out using the **Proton Percussion Magnetometer-600 (**Figure 4.3-A), which is versatile and rugged tool. Handheld GPS was used for recording position of the measured point.

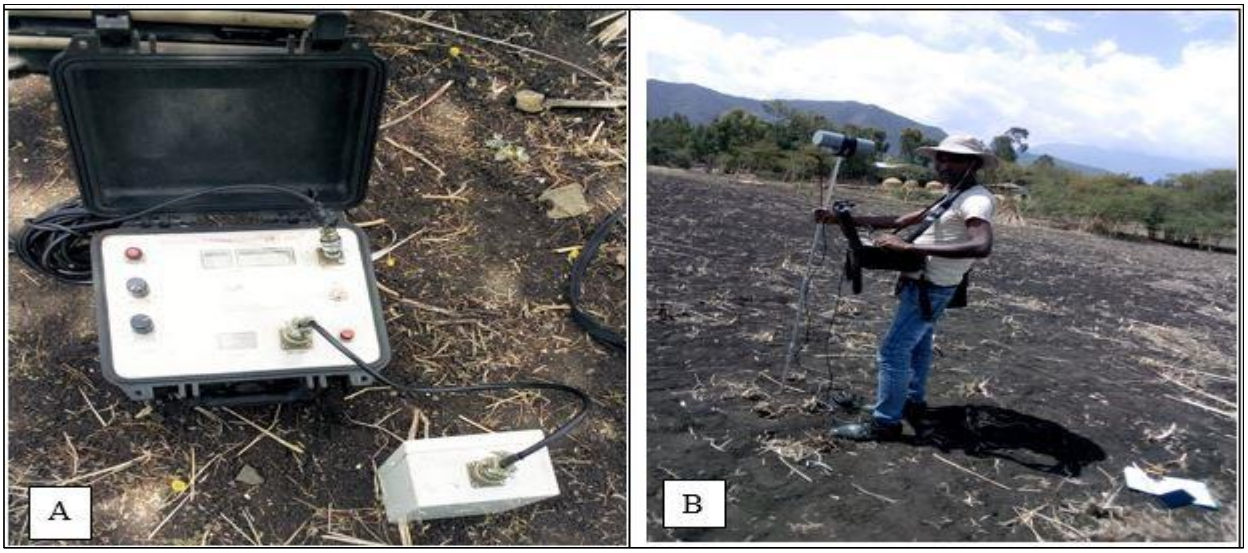

Figure 4.3: Proton Precision Magnetometer-600 ((A) and (B)) in field operation

4.2. Data Reduction and Processing

4.2.1. VES Data Reduction and Processing

The apparent resistivity values are plotted on logarithmic paper; the apparent resistivity value on the ordinaries and the electrode separation (AB/2) on the abscissa. The potential electrode distance (MN) progressively increased for large increment of the current electrode separation (AB/2). Mostly the sounding curve is segmented due to overlap measurement and it cannot be interpreted as it is. To give precise interpretations the segmented curves were shifted to the small MN curve points, so that the effect could be reduced and the data could be corrected in order to obtain a single smooth curve that be processed with the computer by using IP2WIN and WINRESIST software (Velpen, 1995). The calculated and the measured resistivity values were adjusted to reduce the error to as much as possible to the possible minimum value.

Initial step in data processing is transformation of the measured responses, to apparent resistivity values using the relation:

$$\rho = \frac{K\Delta V}{I} \tag{4.1}$$

Where: ρ – apparent resistivity, I –current electrode, K- geometric factor and ΔV- Potential difference.

Geophysical data were processed and analyzed by using geophysical software namely: Ip2win, RESIST and Surfer10(a product of golden software). For the IP2win, the data were copied and pasted on VES notepad window which is the same as Microsoft excel and logarithmic curves of the data were automatically generated. Initial model parameters such as number of layers, their depth, and resistivity values were derived from generated logarithmic curves.

Initial model parameters are arranged and analyzed with existing borehole lithologic logs of the area and used to generate interpreted VES curves of each sounding by using WinResist Software. Field data for each VES is loaded along with current electrode spacing. Initial model parameters, are fed to the model entering option and apparent resistivity curve is computed. This makes the program ready to compare the theoretical curve and the field curve. Trial and error adjustments of the layer parameters are made until the theoretical curve fit with the field curve. The iteration processes continue until the calculated error is within the prescribed limit. Interpreted VES curves of each sounding points are generated and interpreted(determined) qualitatively. The interpreted VES curves and model parameters of the selected five VES curves obtained from the software is presented on figure 5.1.

Sliced stacked map for different value of AB/2 shows lateral variation of apparent resistivity over a horizontal surface at a certain depth. These apparent resistivity contour maps for different values of AB/2 were constructed by using Surfer 10(32-bit) software and illustrated in the figure 5.2.

Pseudo sections of traverse lines are created by using Surfer 10 software. GPS coordinates of VES stations together with resistivity values and the depth at which it measured are used to create contour maps (pseudo-sections). These pseudo-section are given in figure 5.3, 5.4., 5.5., 5.6., and 5.7.

Resistivity and depth values that determined from interpreted pseudo sections and interpreted VES curves are used to construct geo-electric sections. Geoelectric sections, show the distribution of layer resistivities and thickness closer to the actual geological setting in the subsurface. Constructed geoelectric section are interpreted in terms of resistivity, and thickness of lithologic units. The geoelectric sections of all profile are given in the figure 5.8., 5.9., 5.10., 5.11., and 5.12.

4.2.2. Magnetic Data Reduction and Processing

Data correction is the series steps taken to remove spurious noise from the data that are not related to the geology and hydrogeology of the area. Magnetic data collected at the field was recorded in Microsoft excel. Diurnal correction was done by subtracting the diurnal variation of each reading point. The main magnetic field of the study area is obtained from international reference field (IGRF) and subtracted from diurnal corrected total field, then the anomalous field values are gridded by using Oasis Montaj software 7.0.1 and Microsoft Excel Software.

Data enhancement techniques were applied in order to produce magnetic profile section 2D model, which helps to recognize more features to aid qualitative interpretation. Processed magnetic profile plot and 2D model is used for qualitative and quantitative interpretations in order to get clear view of the subsurface, and to estimate the relative depth of the magnetic anomalies sources. Processing and analysis were done by Oasis Montaj software V.6.4.2 and GM-SYS software.

CHAPTER FIVE

5. Results, Interpretations and Discussions

Geophysical data is presented and interpreted in different forms, based upon the objective of the survey that we need to achieve and method employed. The output of geophysical data was used to produce different anomalies which indicates contrast in the physical property of the subsurface material. In this study; interpreted VES curves, sliced stacked plot, pseudo section, and geoelectric section were prepared from VES data, while from the magnetic data; 2D model and magnetic profile plots which show residual anomaly of the area were prepared and presented. Results of resistivity sounding survey are presented in the form of interpreted VES curve and pseudo depth sections for qualitative interpretations and vertical geoelectric section for quantitative interpretations. Interpretation of these maps and profiles are discussed in the following section.

5.1. Interpreted VES Curves

Apparent resistivity versus current electrode spacing was plotted on a bi-log scale and interpreted by using IP2Win to obtain initial model parameters to be used in RESIST software. Accordingly, iteration software (WIN RESIST) is used to iterate curves of the all VES.

As interpreted field curves shows that a very good correlation between the field data and interpreted model parameters are obtained for all the VES points. This is supported by quadratic mean error (RMS error) obtained for all sounding ranges from 0.9 to 4.4 %. Five VES points were sampled from each of the survey traverse, and given in figure 5.1. In the five VES curves, 5 to 6 subsurface layers are observed (with the AB/2 of 500m for VES-1, VES-8 and VES-12, and 1000m for VES-14 and VES-18). Interpreted VES curves of the rest soundings are found at Appendix-1.

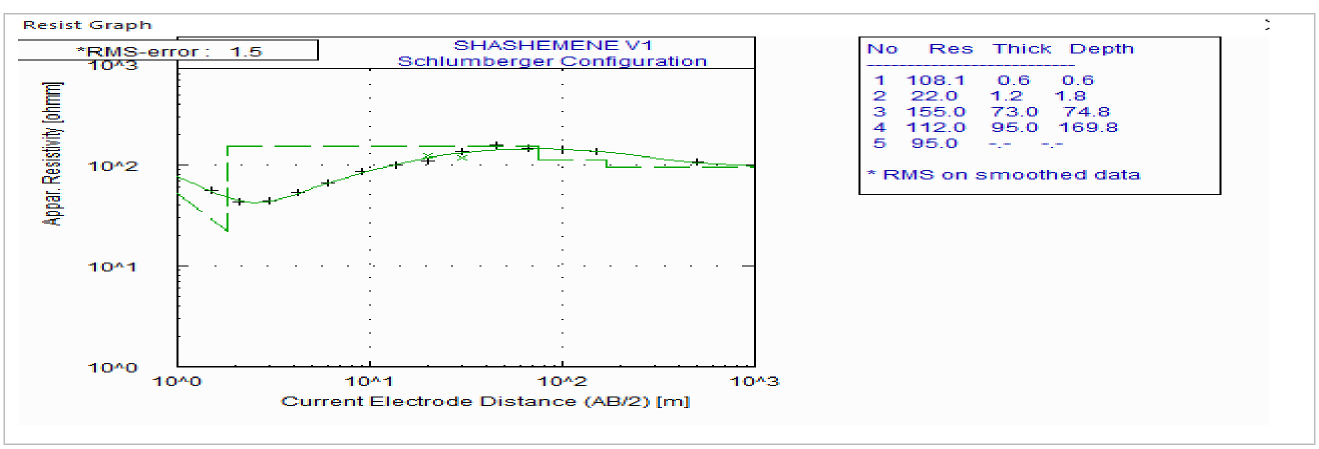

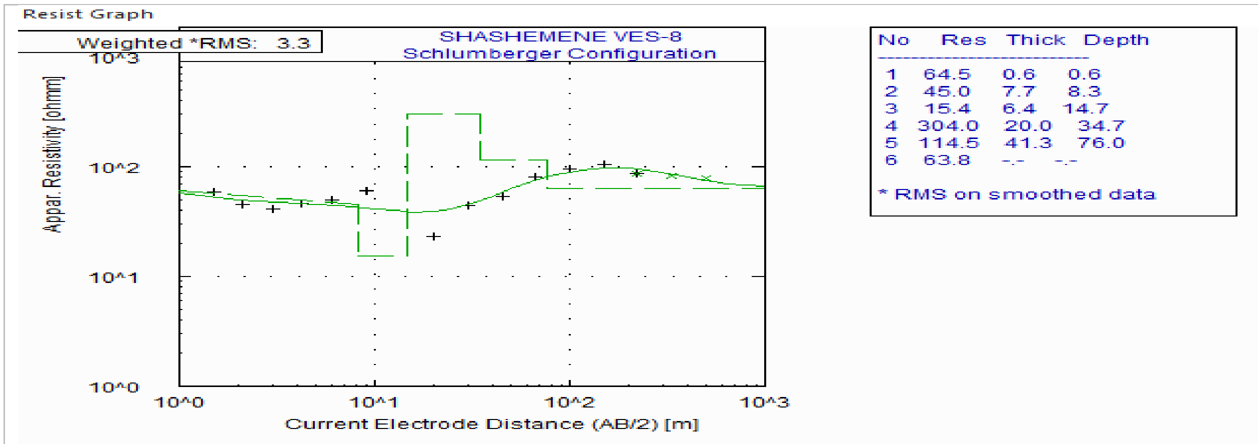
Resist Graph
Weighted *RMS: 3.3
SHASHEMENE VES-8
Schlumberger Configuration
Appar. Resistivity [ohmm]
10^3
10^2
10^1
10^0
10^0
10^1
10^2
10^3
Current Electrode Distance (AB/2) [m]
No Res Thick Depth
1 64.5 0.6 0.6
2 45.0 7.7 8.3
3 15.4 6.4 14.7
4 304.0 20.0 34.7
5 114.5 41.3 76.0
6 63.8 -.- -.-
* RMS on smoothed data

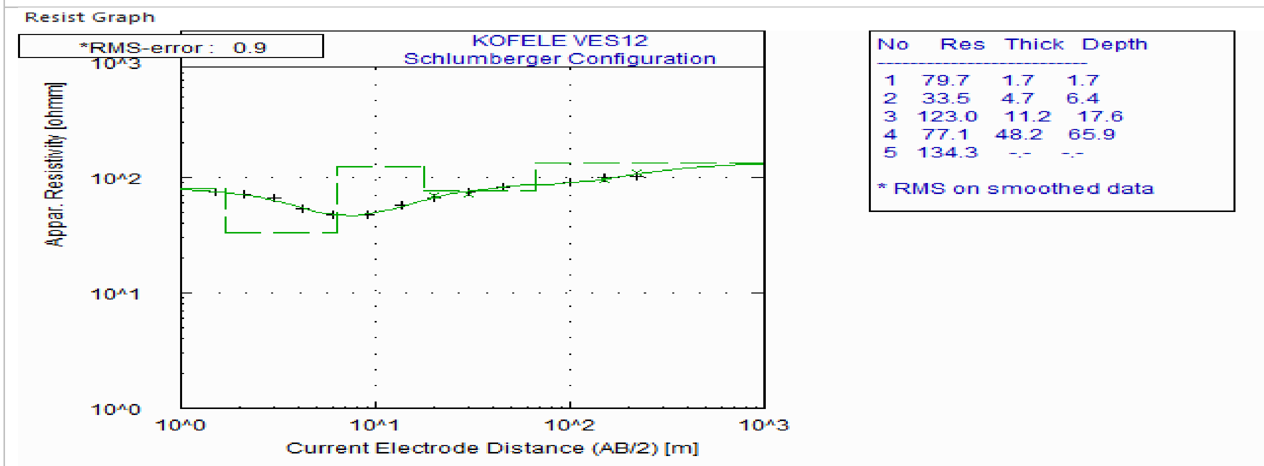
Resist Graph
*RMS-error : 0.9
KOFELE VES12
Schlumberger Configuration
Appar. Resistivity [ohmm]
10^3
10^2
10^1
10^0
10^0
10^1
10^2
10^3
Current Electrode Distance (AB/2) [m]
No Res Thick Depth
1 79.7 1.7 1.7
2 33.5 4.7 6.4
3 123.0 11.2 17.6
4 77.1 48.2 65.9
5 134.3 -.- -.-
* RMS on smoothed data

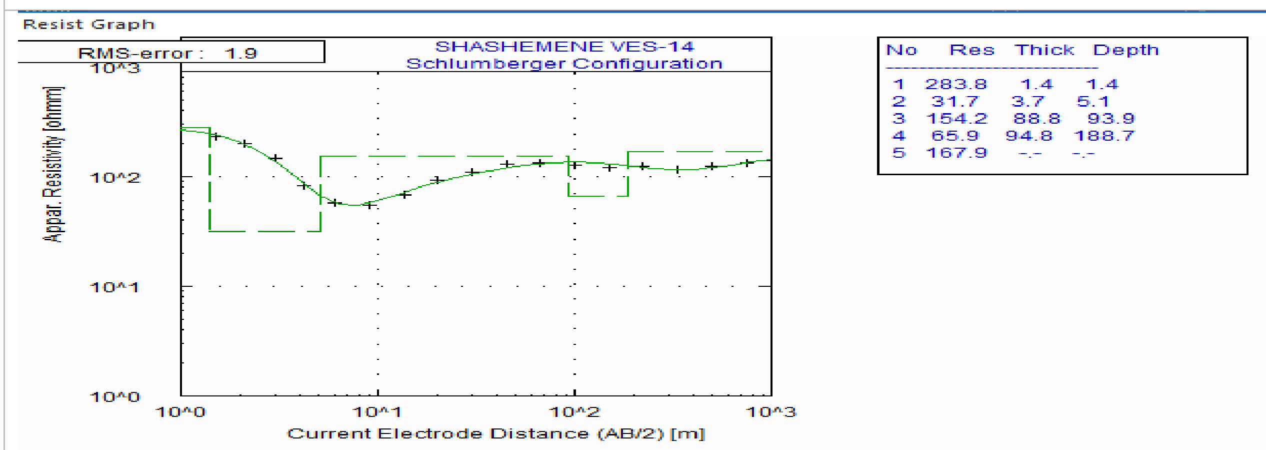
Resist Graph
RMS-error : 1.9
SHASHEMENE VES-14
Schlumberger Configuration
Appar. Resistivity [ohmm]
10^3
10^2
10^1
10^0
10^0
10^1
10^2
10^3
Current Electrode Distance (AB/2) [m]
No Res Thick Depth
1 283.8 1.4 1.4
2 31.7 3.7 5.1
3 154.2 88.8 93.9
4 65.9 94.8 188.7
5 167.9 -.- -.-

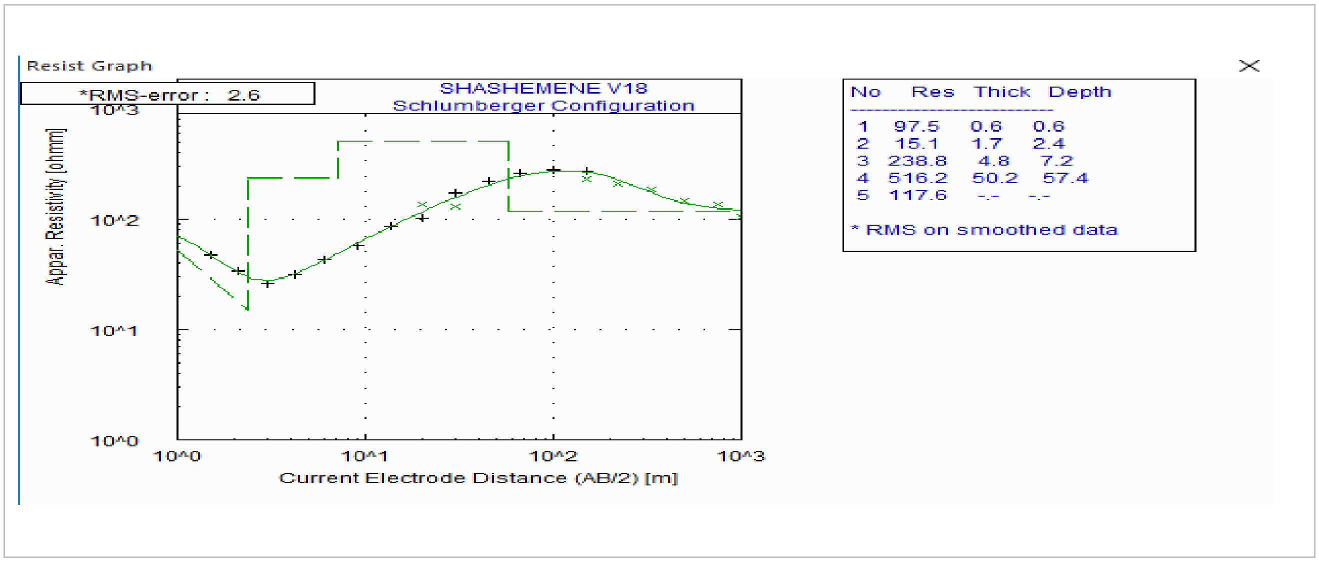

Figure 5.1: Interpreted VES curves of five sounding points

5.2. Sliced-Staked Map for Different AB/2

Sliced-stacked plot provides visualization of the overall picture of subsurface electrical parameters and their variation both in vertical and lateral directions. Lateral distribution of the electrical resistivity at the subsurface gives additional information for complete understanding of the hydrogeological frame work of the study area. It serves only for qualitative interpretation, since it gives nature between largely spaced point values from individual soundings, and the contribution from such presentation for the completeness of our interpretation is beyond doubt.

In figure 5.2, the sliced stacked maps were constructed for AB/2=1.5,45, 100, 220, 330, and 500m. The choice of such separation depends on their variability and to show the horizontal variations of the resistivity at different pseudo depth. Specially, the map shows the relative variation of the apparent resistivity value of the whole area both vertically and laterally at different depths of current electrodes spacing. It is found that the resistivity value varies from 10-300 Ω-m.

Various zones of contrasting apparent resistivity values, separated by a narrow and medium resistivity ranges, appear as prominent features in the figure bellow. According to the figure the most interesting feature of this sliced plot is the low resistivity zone (<120Ω-m) that occupies southeastern side of the map region and extends to central region of the area for all AB/2. On the other hand, relatively high resistivity zone (>120Ω-m) appears in western side of all AB/2 except at AB/2=500m and in northwestern corner of AB/2=500m. Relatively high resistivity region is demarcated from the low resistivity region by narrow zone of intermediate resistivity values. Such narrow features are thought to designate geological structures, fault zones or contacts.

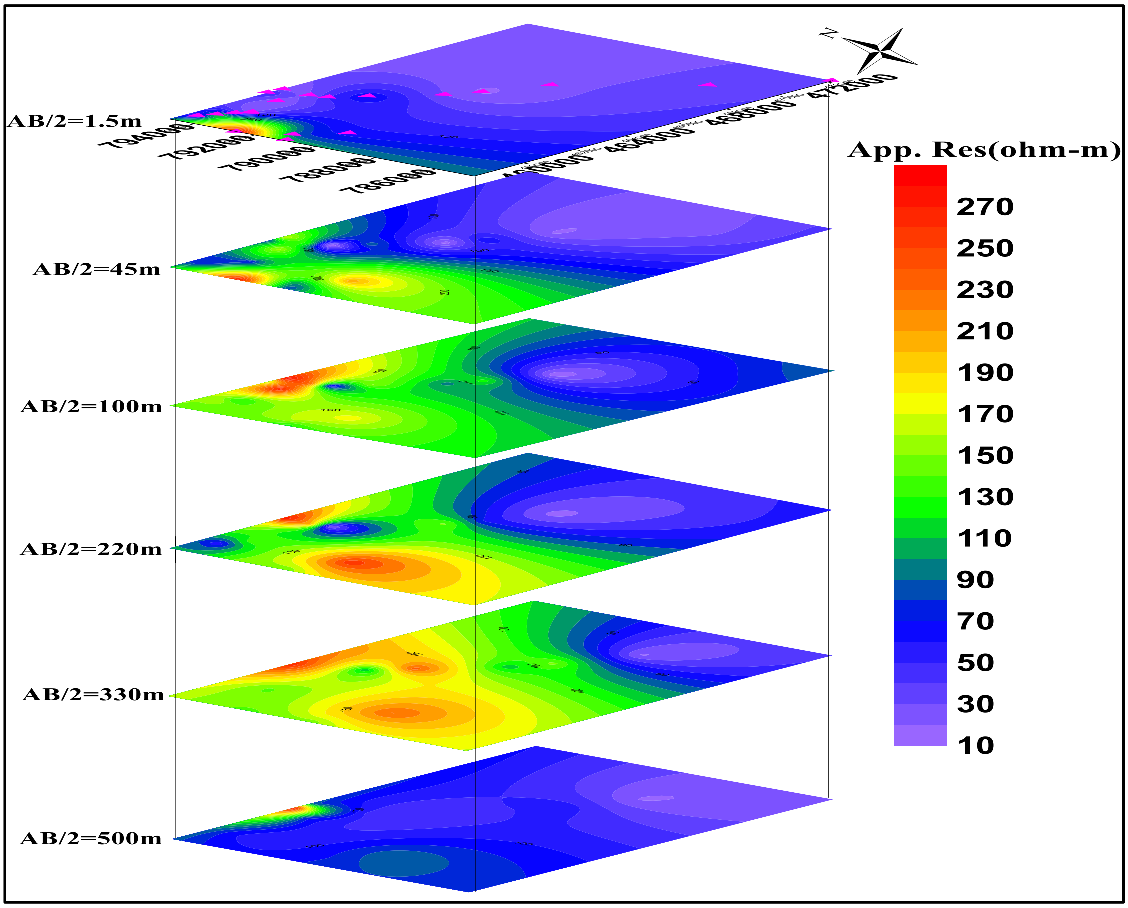

Figure 5.2: Sliced stacked map for different AB/2.

5.3. Pseudo Depth Sections

Pseudo section is one way of presenting the measured apparent resistivity values. The field data collected from each sounding is gridded and displayed as regular contour maps, showing areas of high or low anomalous value. Pseudo sections have been generated for the VES profiles by using Surfer 10(32-bit) software.

5.3.1. Pseudo Depth Section of Profile One

The pseudo depth section generated from apparent resistivity data of VES-1,2,3, and 4 that lay on survey line one is given in figure 5.3. The projection line runs in NW-SE direction. According to the figure below the apparent resistivities are not high but still show a considerable variation with depth. Around northwestern side of profile line (VES-3 to VES-4), the pseudo section shows relatively medium to high resistivity region which extends to VES-2 and below VES-1 high resistivity zone is found below the top layer. The region between VES-1 and VES-2 the ground section is represented by a relatively conductive horizon, which progressively dips to the position of VES-4.

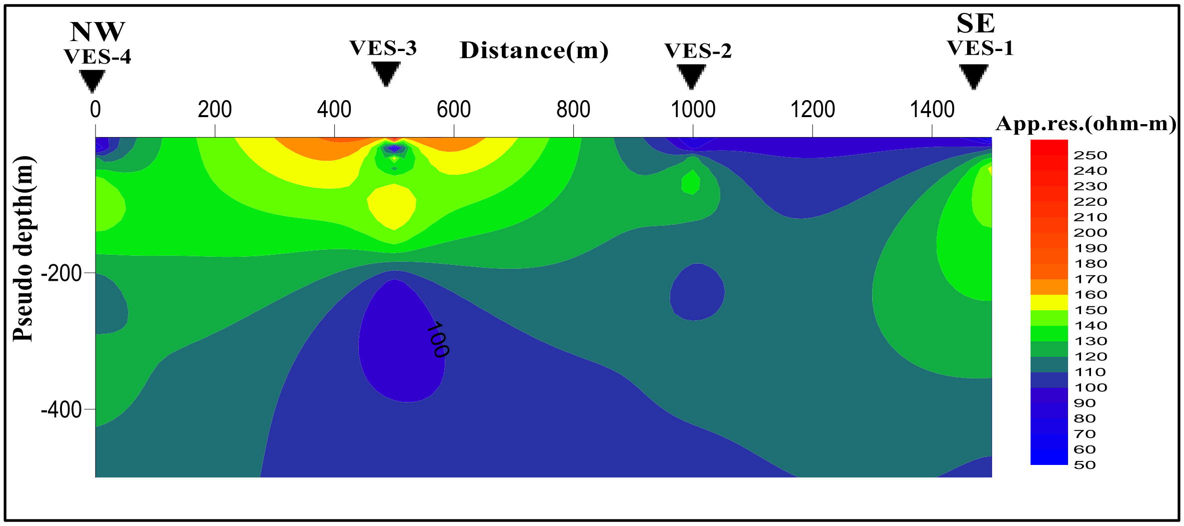

Figure 5.3: Pseudo depth section of profile one

5.3.2 Pseudo Depth Section of Profile Two

The pseudo depth section constructed for VES-13, 14 and 15 that lie on profile line two are given in figure 5.4. The survey line runs in NW-SE direction. According to the figure resistivity value decreases with increasing the depth of investigation. High resistivity ranging from 130-240Ω-m covers upper most layer of the section. This high resistivy shallow region extends to depth and exhibit a gratual decrease in resistivity response with depth. Low resistivity (saturated) zone is maped at the foot of VES-15 and 13. Bellow VES-14 low resistivity region found at shalow section which dips to VES-13 interprated as weak zone.

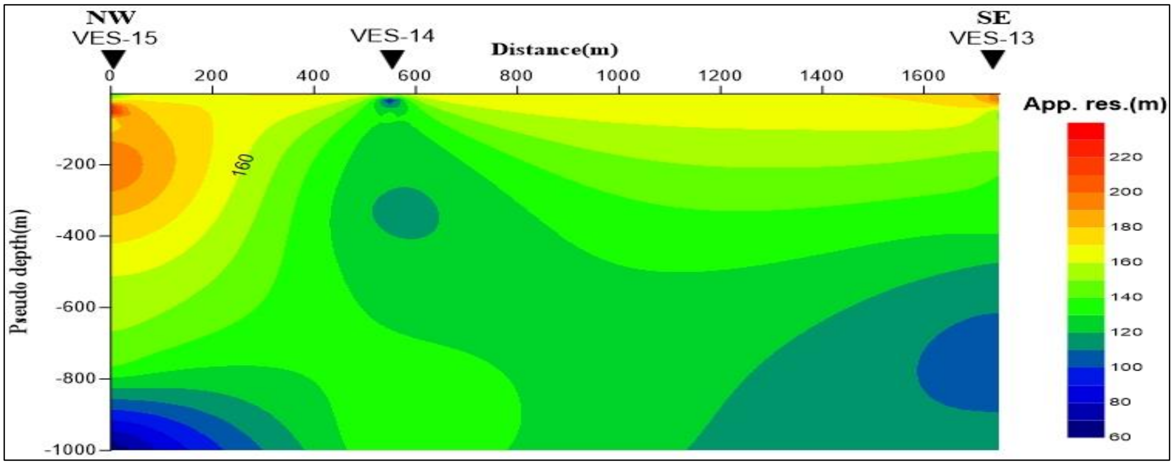

Figure 5.4: Pseudo depth section of profile two

2.3.3. Pseudo Depth Section of Profile Three

The pseudo section was constructed by using VES-17,18 and 5 of survey line-3 which projected in SW-NE direction. According to the section, there is a lateral variation in resistivity in the upper most part of the section with prominent high resistivity top regions mapped beneath VES-17 and below the upper layer of VES-5 and VES-18. This relatively high resistivity zones are not extend to greter depth. The rest of the section shows extensive coverage of the low resistivity horizon. The low resistivity region(0-120Ω-m) which cover the vast region of the section potential water saturated horizon. VES-16 which lay on this profile can not be used to construact pseudo depth section and geo-electric section scince unlike other VES it does not exihibit smooth variations in apparent resistivity.

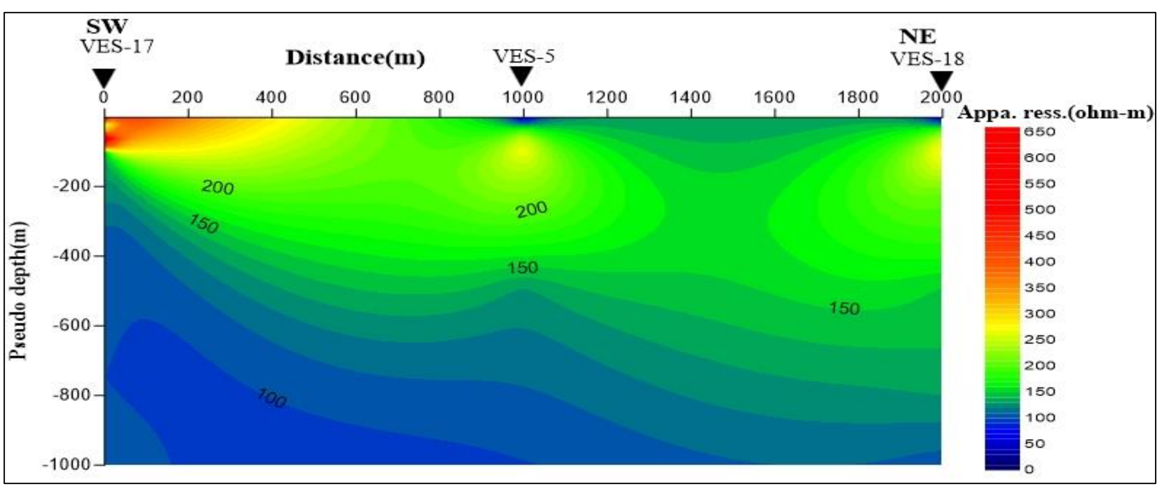

Figure 5.5: Pseudo depth section of profile three

2.3.4. Pseudo Depth Section of Profile Four

This profile line runs over in NW-SE direction of the study area. There are six resistivity sounding points such as VES-6,7,8,9,19, and 20. The apparent resistivity pseudo section for this line is given in figure 5.6.

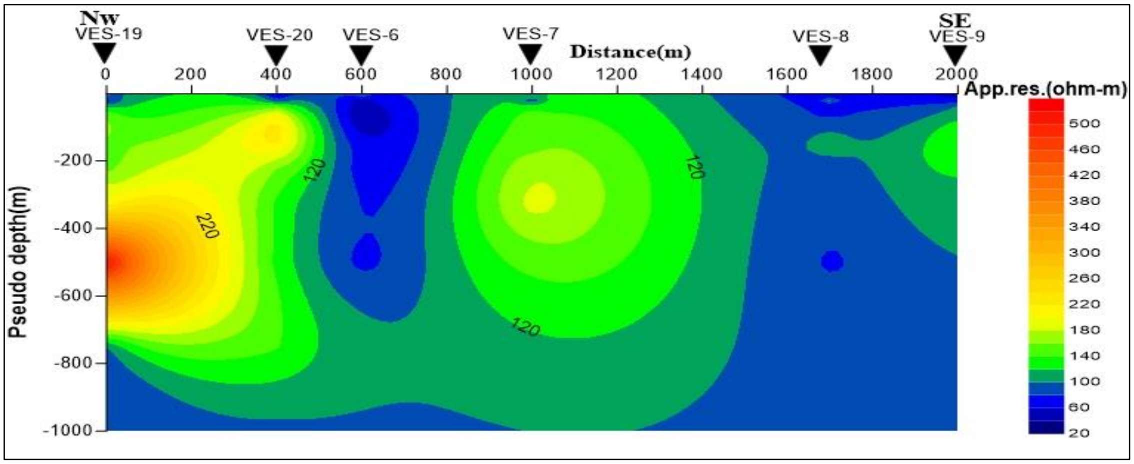

Figure 5.6: Pseudo depth section of profile four

As the pseudo section of figure 5.6 of this profile shows, relativily high resistivity region below the uper most layer of the area were maped between VES-19 and 20, beneath VES-7 and VES-9. This high resistivity zone is not extending to grater depth. Otherwise, the vast region of the section shows extensive coverage of a relatively conduvtive horizon. The the resistivity of low resistivity zone which covers the wide region of the section ranges from 20-120Ω-m whereas, resistivity of unsaturated zone ranges from 130-500Ω-m.The low resistivity region is intepprated as presence of saturated groundwater potential.

2.3.5. Pseudo Depth Section of Profile Five

The pseudo depth section generated from the apparent resistivity data of VES-10, 11 and 12 is given in figure 5.7. The projected line runs over in NW-SE direction of the study area. From top, down to the end, the the ground section between VES-11 and 12 is represented by a relativily high resistivity region. Towards the NW along this projected line between VES-10 and 11, the shallow portion of the ground section appears to be more resistive and exhibit a gradual decrease in resistivity with depth. Below the shallow layer of VES10 low resistivity horizon which dips towards VES-11 is mapped.

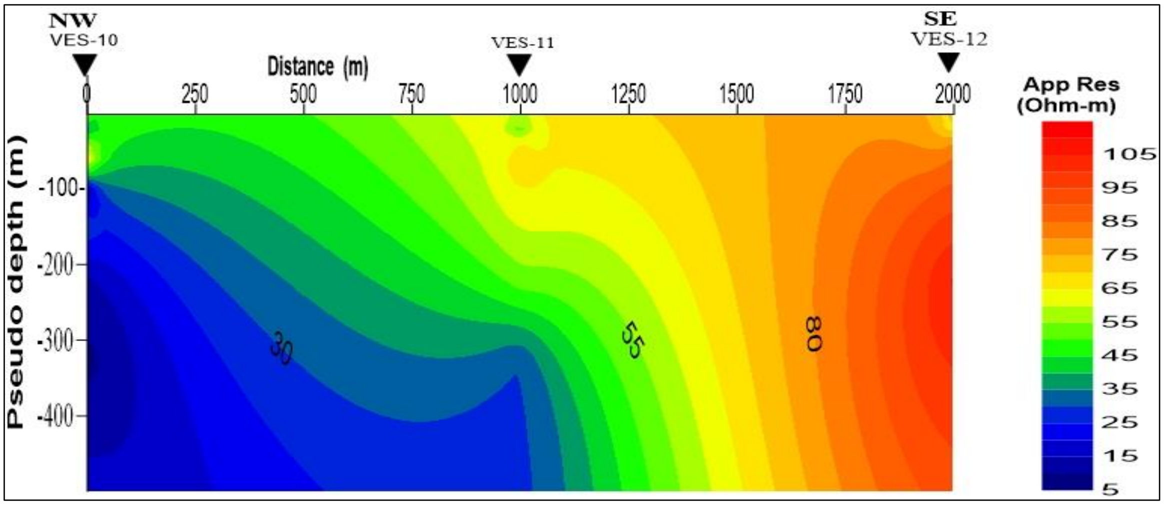

Figure 5.7: Pseudo depth section of profile five

5.4. Geoelectric Sections and Magnetic Profile Plots

The final interpretation of VES results indicate subsurface sequence of the area in the form of layers with different thickness and resistivity values. These results have been used in depicting valuable form of geoelectric section representations to aid the interpretation and to identify the distribution of different lithology units in vertical direction. These sections can reveal good idea about geologic and hydrogeologic situations of the area.

WIN RESIST and IP2WIN software's were used for inversion of the VES data whereas geoelectric plotting was carried by using AutoCAD (V 2007). Five geoelectric sections were constructed along survey lines. Layers with small thickness are not quit apparent on the geoelectric section due to a scale factor. Lithologic logs of the boreholes that are lying near the survey lines were used to fix the thickness of each subsurface layers. However, it is not possible to constrain the depth of each geoelectric layers all over the survey lines on the basis of borehole logs, rather, it is possible to derive trail-and-error models that match VES data sets, coincident with borehole data.

5.4.1. Geoelectric Section of Profile One

Figure 5.8 represents the geoelectric section constructed using the interpreted layer parameters of sounding data from VES-1, VES-2, VES-3 and VES-4, plus the lithology log from nearby borehole, especially near VES-1. The lithological description of the borehole depth section used for modeling is given in Appendex-3. The subsurface beneath the projected line, is represented by four geoelectric layers.

A very thin clay soil with varying resistivity response is due to the varying moisture content and/or grain size, is mapped as the first layer along the line. This is underlain by a high resistivity(155-350Ω-m) layer with thickness varies from 30m bellow VES-1 to 80m near VES-4. The high resistivity response of this layer may be attributed to dry weathered and fractured ignimbrite, presumably devoid of water. The third broad horizon of the geoelectric layer corresponds to moderately saturated layer. The formation resistivity varies from 72-110Ω-m and thickens from 45m to 60m. The layer may represent that of paleosol with highly weathered ignimbrite, possibly water saturated ignimbrite.

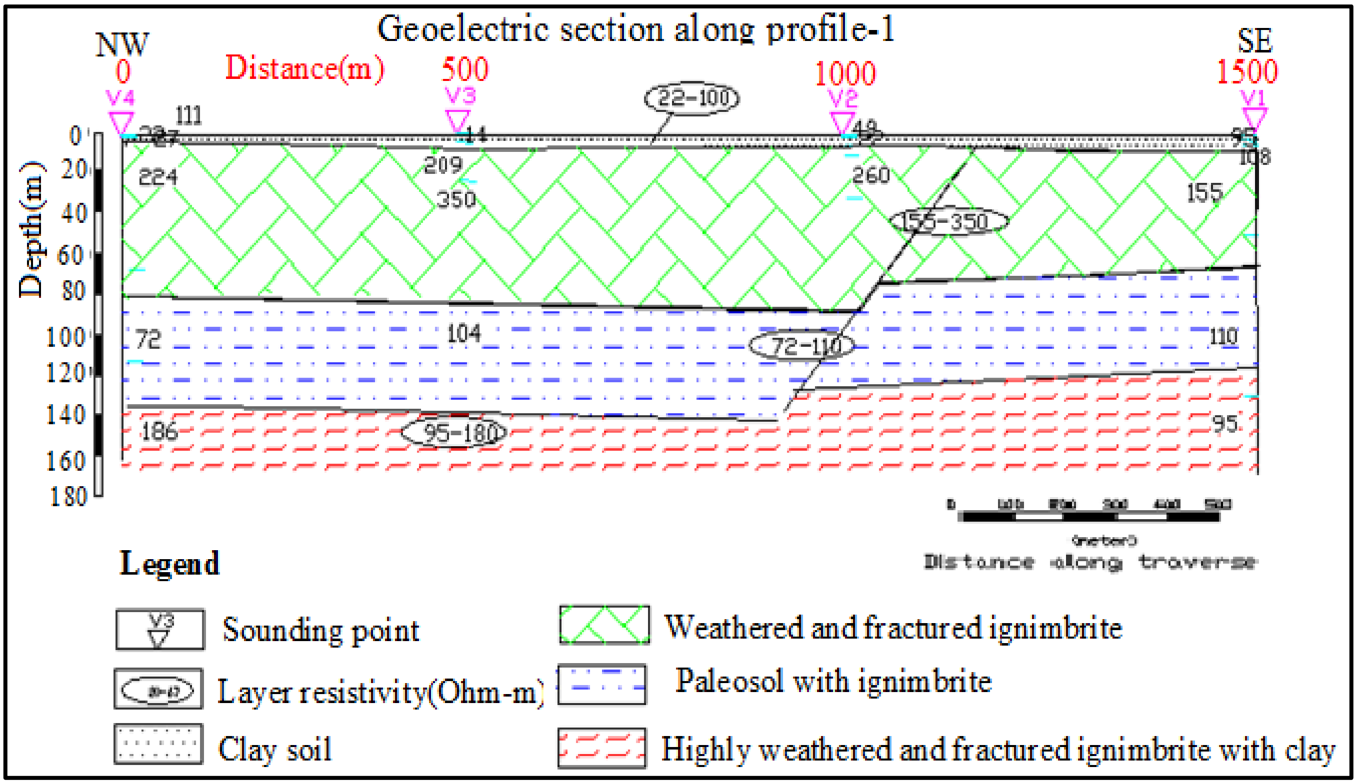

Figure 5.8: Geoelectric section of profile one

The fourth, bottom, layer which is moderately saturated is characterized by resistivity value ranging from 95-186Ω-m. This resistivity response represents highly weathered and fractured ignimbrite with sand. Inferred geological structure (normal fault) is shown in the figure 5.8 above by broken line. It is found at approximate distance of 500m along the projected survey line. Geology of the area and geoelectric layers of this profile is highly correlated based on their lithologic units and their weather condition.

5.4.2. Geoelectric Section of Profile Two

According to figure 5.9, the subsurface, beneath the projected line, is represented by four distinct geoelectric layers. The top two layer, marked by resistivity values ranging from 123-326Ω-m has thickness of about 20m. This layer is likely interpreted as highly weathered and fractured ignimbrite with clay.

The second broad horizon of the geoelectric layer that corresponds to the moderately saturated layer with resistivity values varying between 118 and 220Ω-m. The layer thickens from 60m at VES-14 to 110m at VES-13. According to the lithology log from the nearby well that is found near to VES-15 and the resistivity response, of this horizon corresponds to undifferentiated succession of scoracious basalt with sand and the other felsic rocks forming vast zone of saturation.

The third geoelectric layer is characterized by relatively low resistivity values varying between 55 and 69Ω. Its thickness varies from 40m at VES-13 to 60m at VES-14. This highly conductive layer could be interpreted as saturated highly weathered ignimbrite with coarse sand which has relatively a good ground potential.

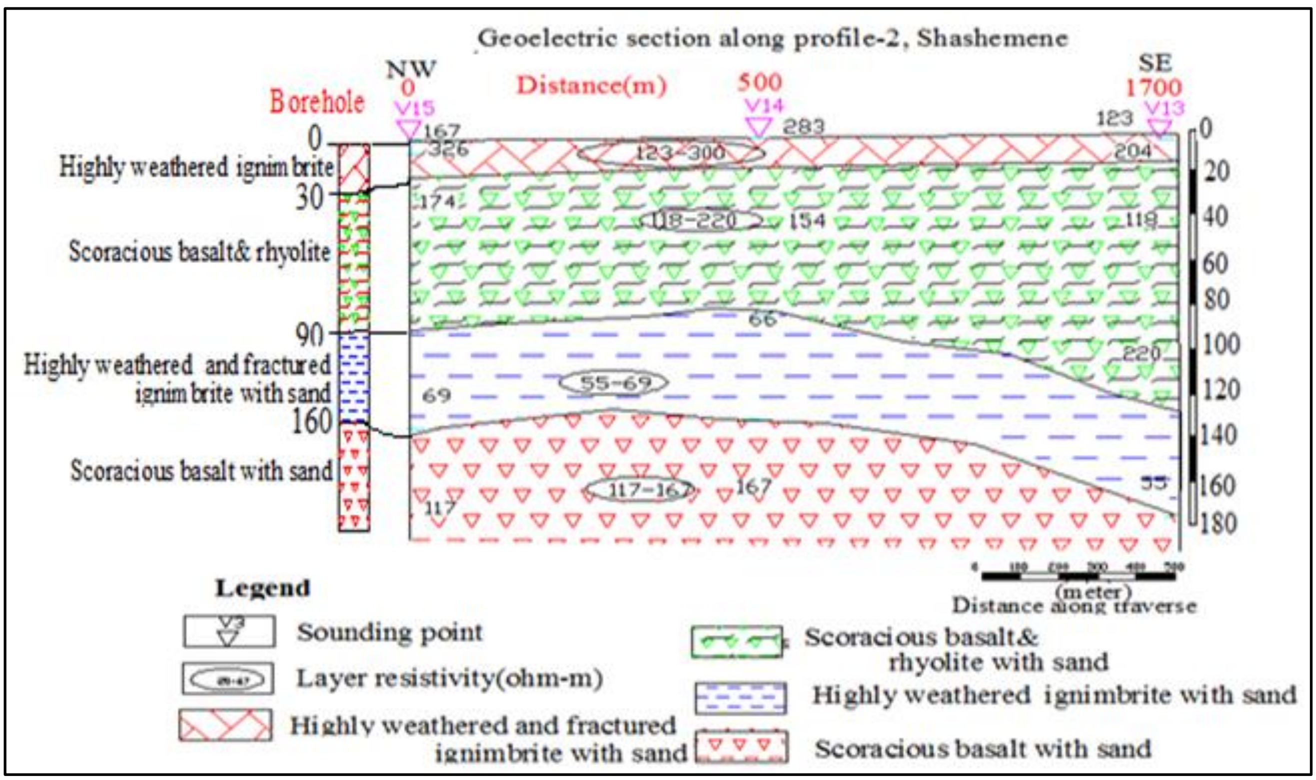

Figure 5.9: Geoelectric section of profile two

5.4.3. Geoelectric Section of Profile Three

The geoelectric section along profile line-3 is constructed from the interpreted layer parameters of VES-5, VES-17 and VES-18. The geoelectric section as shown in figure 5.10, the subsurface is represented by four distinct layers

A very thin top geoelectric layer having resistivity values that ranges from 11-90Ω-m with thickness variations from 3-5m. This conductive layer is inferred as clay soil. The high resistivity variation is due to moisture content. The second horizon of the geoelectric section thickens from 10m at VES-17 to 20m at VES-5. The formation resistivity ranges 170 to 316Ω-m and interpreted as highly weathered and fractured ignimbrite with clay. The third layer in the sequence is characterized by relatively high resistivity values varying between 460 and 567Ω-m and its thickness also varies from 40m at VES-17 to 60m at VES-18. This unsaturated horizon is also presented on the nearby borehole at this depth range and interpreted as moderately weathered ignimbrite, presumably devoid of water.

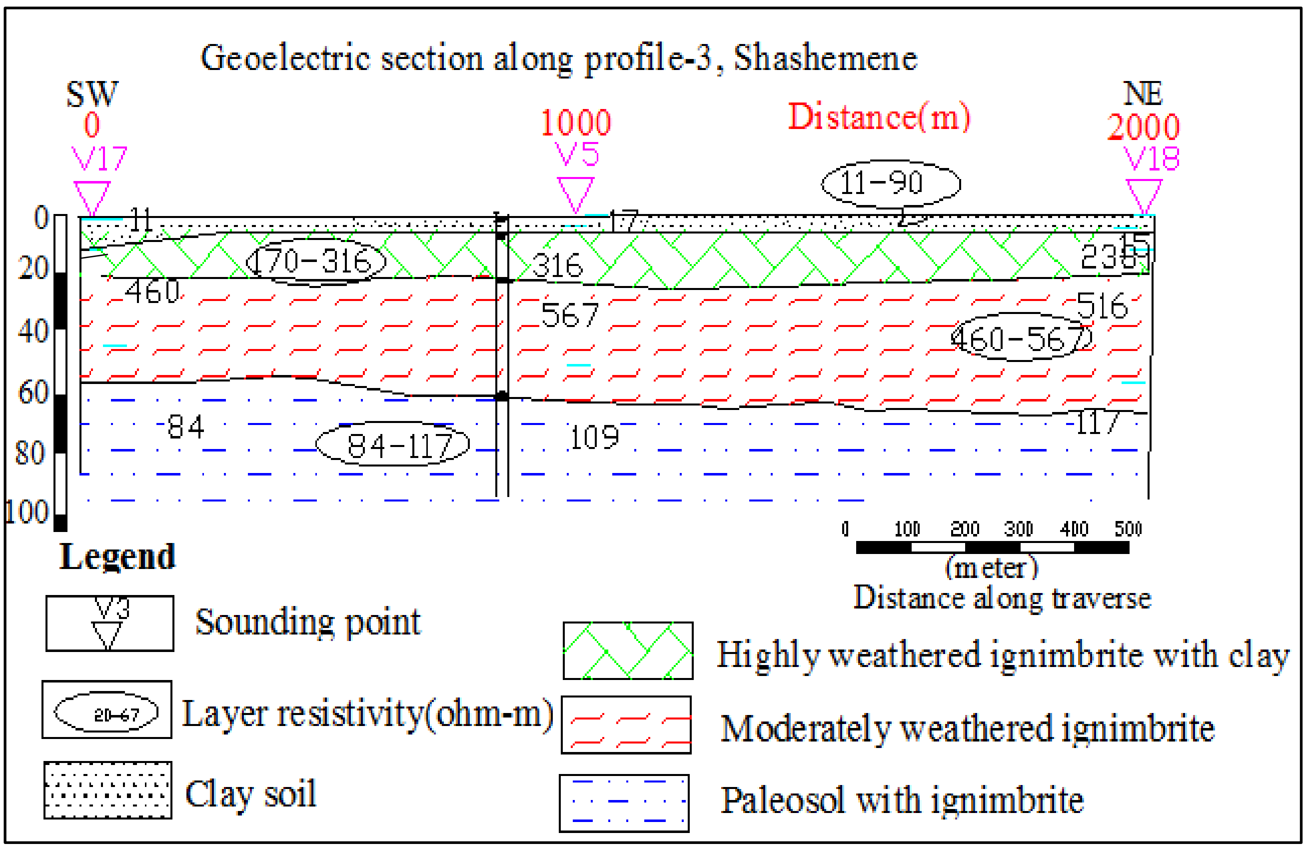

Figure 5.10: Geoelectric section of profile three

This is underlain by a fourth, geoelectric layer, with resistivity range of 84-117Ω-m, and could be interpreted as the response of paleosol with ignimbrite. It is bottom layer in the geoelectric section. The layer corresponds to moderately saturated horizon with good groundwater potential.

As shown in the figure 5.10 geoelectric layers and lithologic units of the borehole that is found on the survey line are coincident (fit) to each other in terms of depth and weathering

5.4.4. Geoelectric Section of Profile Four and Magnetic Profile Plot One

The geoelectric section along this profile line is constructed by using interpreted layer parameters of VES-6 to 9, VES-19 and VES-20. The geoelectric section as shown in figure 5.11, the subsurface is represented by five distinct layers.

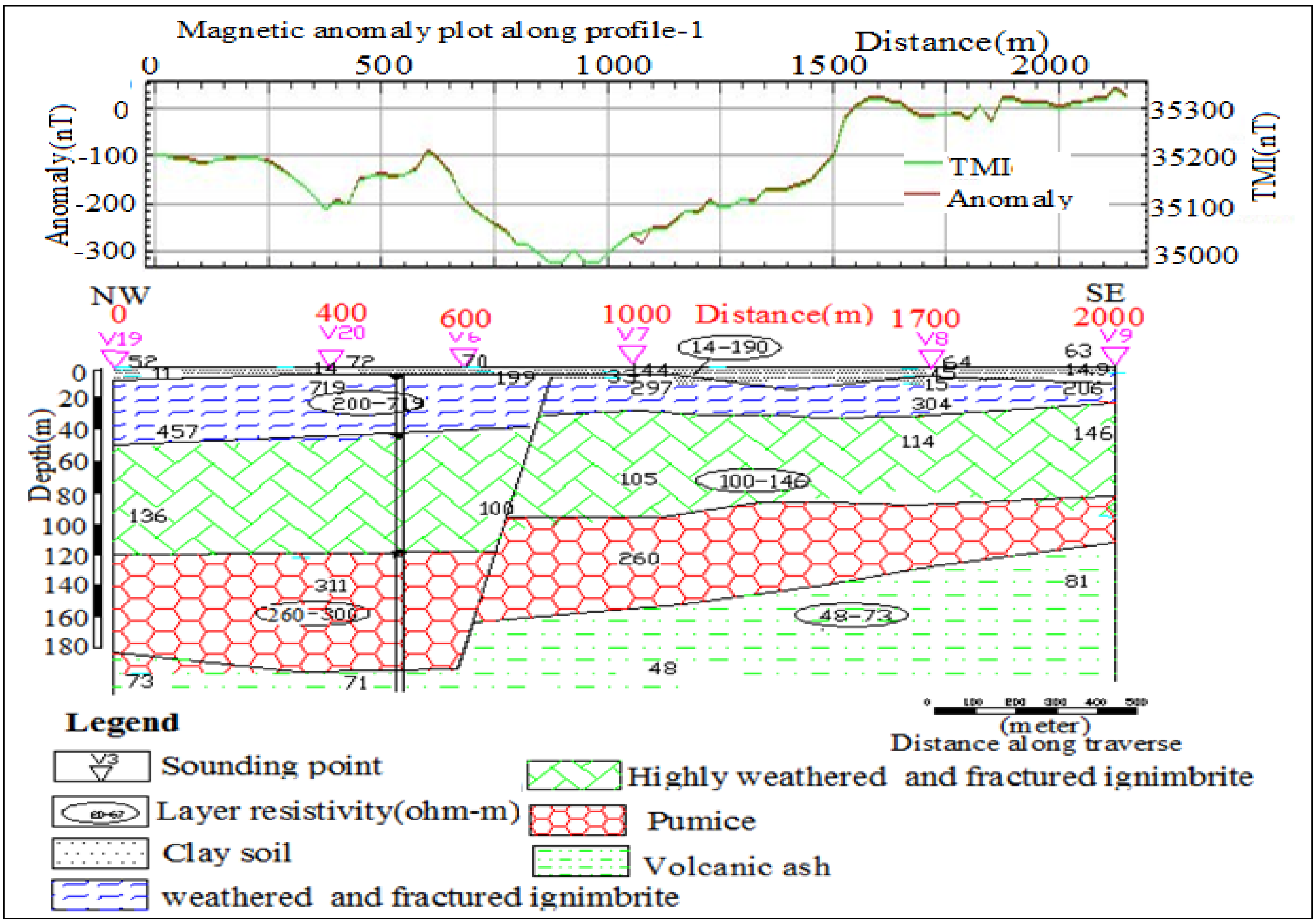

Figure 5.11: Geoelectric section of profile four and its magnetic anomaly plot

The uppermost geoelectric layer which has high resistivity variation, corresponding to the varying moisture content and grain size, is mapped as the first layer along the line. The layer thickness varies from 2.2m at VES-6 to 7m at VES-9 and interpreted as clay soil. This layer is underlain by a high resistivity (200-719 Ω-m) layer which thickens from about 5m at VES-9 to about 40m at VES-19. The resistivity response of this horizon is interpreted as dry weather and fractured ignimbrite, presumably devoid of water.

The next geoelectric layer with intermediate resistivity responses (100-146Ω-m) were mapped as the third layer. The layer thickness varies from 41m at VES-8 to 75m at VES-19. Based on the geology of the area it could be resistivity response of highly weathered and fractured ignimbrite with clay. This conductive horizon may contain good groundwater potential.

This is underlain by highly resistive (260-311Ω-m) layer which has thickness that ranges from 30m at VES-9 to 80m at VES-20. According to lithology log of nearby borehole (appendix-3) moderately weathered pumice unit covers this depth range. The bottom layer of this section with relatively low resistivity signature ranging from 48-81Ω-m corresponds to volcanic ash.

In figure 5.11 above, inferred geological structure is shown by broken line. The magnetic curve and geoelectric section reflects the same pattern which may concluded as geological structures (fault) that exist at approximate horizontal distance of 800m along the projected survey line.

5.4.5. Geoelectric Section of Profile Five and Magnetic Profile Plot Two

The resulting geoelectric section constructed from the interpreted layer parameters of VES-10, VES-11 and VES-12 lying on this profile line is given in figure 1.12. The subsurface, beneath the projected line is represented by four distinct geoelectric layers.

Near- surface very thin geoelectric layer, with resistivity range of 13-34Ω-m, reflects presence of top clay soil. The thickness of this top layer reaches about 5m at VES-11. This is underlain by a geoelectric layer with resistivity rang of 70-151Ω-m and thickness varying from 30m at VES-12 to 80m at VES-11 and inferred as highly weathered ignimbrite with sand.

The third geoelectric layer in the sequence has resistivity that ranges 75-180Ω-m. It thickness reaches up 60m. According to the geology of the area this resistivity respond is interpreted as weathered ignimbrite. Similarly, the bottom layer with resistivity range of 4-60Ω-m stands for paleosol with ignimbrite. This highly conductive layer is water bearing horizon which has good potential of ground water as compared to the above layers.

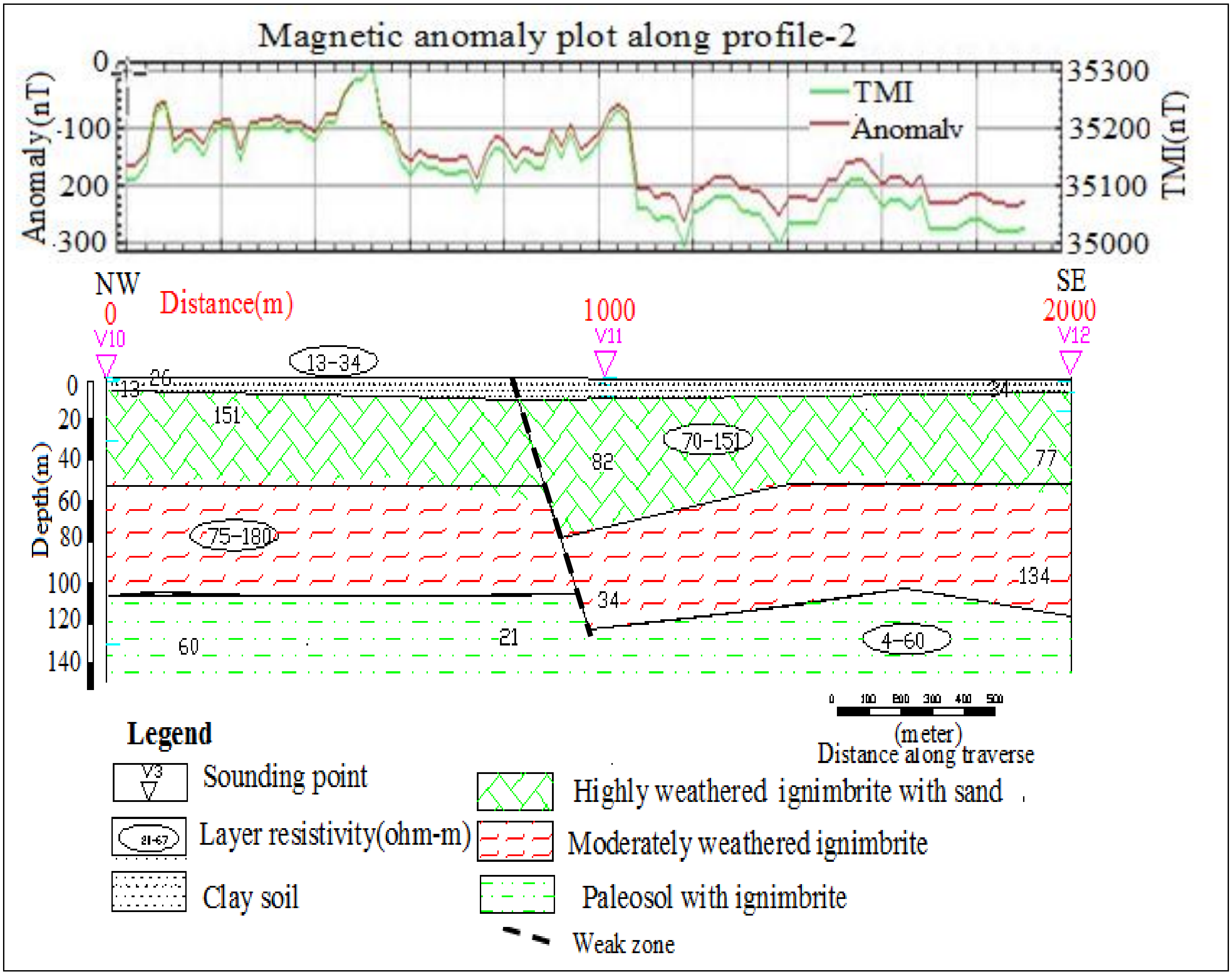

Figure 5.12: Geoelectric section of profile five and its magnetic anomaly plot.

Similar to the above geoelectric sections, geoelectric section of this profile reflects the same lithologic units of the area except small variation in thickness of the layer's depth of the burial.

However, resistivity value of the layers in this profile is relatively low as compared to other profiles.

As shown in the figure 5.12. above, weak zone is mapped. The magnetic anomaly plot and geoelectric section reflects similar pattern in geological structure which may represent lithologic contact or fault. The fault is mapped at an approximate distance of 750m along the profile line.

5.5. 2D Modeling

2D modeling is very essential to estimate the physical properties of the subsurface geological units and structures. The modeling is done by using the GM-SYS software. It is interactive forward modeling which calculates the magnetic response from a user defined hypothetical geological model. It should be noted that magnetic model is non-unique, many earth materials can produce the same magnetic response and several lithologies may be interpreted from a given model block's magnetic susceptibility. Therefore, it is important to use many independent source of information as much as possible to constrain the model.

5.5.1. 2D Modeling along Magnetic Profile One

The magnetic 2D model is developed from magnetic anomaly of profile one with interpreted VES curve parameters of VES-19, VES-20, VES-6, VES-7, VES-8 and VES-9, and borehole data (Faji sole borehole which is found in Annex-3 (1)). As shown in figure 5.13, the model reflects that existence of normal fault below depth of 10m that extend to 300m depth. Lithologic unite that are described in the model includes: top soil, ignimbrite, pumice, volcanic ash and underlying scoracious basalt.

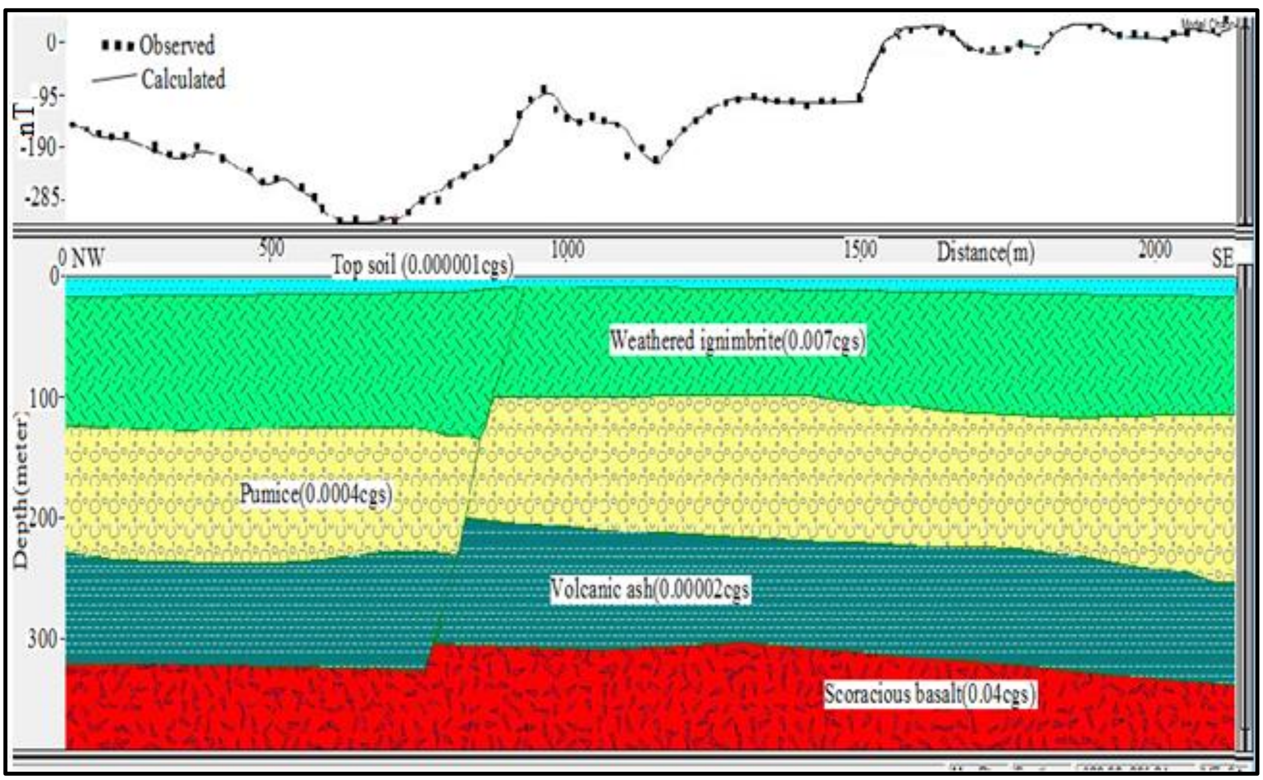

Figure 5.13: 2D model of magnetic profile one

Geoelectric section along this profile as shown in figure 5.11 reflects the same lithologic units and geological structures except slight variation in thickness. Based on the geoelectric section and lithologic log of the borehole ignimbrite, pumice and basalt are varying in their degree of weathering and fracture. Groundwater system of the area is controlled by highly weathered and fractured horizons and geological structures.

CHAPTER SIX

6. Conclusions and Recommendations

6.1. Conclusions

Randomly distributed vertical electrical soundings (VES) and magnetic survey have been used to investigate ground water potential along the Shashemene-Kofele road. A total of 20 VES points along five traverse with maximum current electrode spacing (AB/2) of 1000m have been conducted in the study area. Magnetic data of about 200 reading points are also collected in systematic manner along two profiles that run over fourth and fifth resistivity (VES) traverses. Based on the results of the geophysical surveys, their respective interpretations and available information from varies source, the following conclusions are drawn by using the integrated data presentation approaches.

The apparent resistivity pseudo-depth section, sliced-stacked map and the geoelectric sections show presence of low resistivity horizons at different depth with their physical suitability to act as aquifer beds. The aquifer thickness in the area is obtained to range between 70m and 160m. The study result revealed that highly weathered and fractured ignimbrite with sandy soil is the main water bearing horizon which has good groundwater potential.

Sliced-stacked section constructed from VES data showed the presence of highly conductive horizons (saturated zone), especially in eastern direction of the study area.

As shown in the geoelectric sections and magnetic profile plots, the area is transected by several subsurface geological structures (discontinuities) that are important for groundwater flow and occurrence. 2D magnetic model reflects existence of normal fault below depth of 10m that extend to 300m due to tectonic activity of Main Ethiopian Rift.

Comparison of the geophysical results with borehole lithologic data shows that results of geophysical interpretations are well correlated with the borehole lithologic log.

Magnetic anomaly plots and geoelectric sections highly reflects the same pattern that concluded as geological structures. Integrated geophysical method has facilitated the data interpretation and greatly reduced the ambiguity in each method.

6.2. Recommendations

Based on the limitation and results obtained from this study, the following points are recommended.

- Based on the data analysis eight well sites are recommended for drilling at VES-2, VES-10, VES-5, VES-17, VES-6, VES-8, VES-11 and VES-14, which are listed according to their priority order.
- Pumping test should be conducted on the proposed site to determine well yield and other parameters.
- Groundwater system of the area is highly controlled by geological structures, so that drilling should be done at low resistivity zones that continue to depth.
- Geochemical analysis is recommended along the proposed sites in order to determine its water quality.
- It is recommended to collect more data sets using deep VES and time domain electromagnetic methods for more analysis of the aquifer in the study area.
- Detailed magnetic survey parallel and perpendicular to the profile lines and outside of the study area is recommended to identify extension of geological structures(faults) that behaved to act as barrier for groundwater occurrence or conduit for groundwater flow.
- It is also recommended to map detail geological structures of the area, with their orientation.

References

Antonio,L, Invan,Z. and Marcelo, A. (2009). Inversion of teleseismic receiver function and magnetotelluric sounding to determine basement depth in the parama basin, SE Brazil. *App. geop*.**68**:231-242.

Ariyo, S.O., and Banjo, A.A. (2008). Application of electrical resistivity method for groundwater exploration in a sedimentary terrain: A case study of Ilara-Remo, Southwest Nigeria: *Conti. J. of Earth Sci.* **3**: 53 – 58.

Barker, R. D. (1992). The Offset Systems of Resistivity Sounding and its use with a Multicore cable. Geophs. Prospecting.**29**: 128-143.

Barker, R.D. (1996). Recent Application of Electrical Imaging Surveys in the United Kingdom, Sageep, pp.1289.

Baker R. D. (1996). Application of electrical tomography in groundwater contamination studies: 61st Mtg. Eur.Assoc. Expl geophysics., Extended Abstracts, European Association of Geophysical Exploration.session: pp.82.

Berhanu, B., Čížek, D., Žáček, V., Rapprich, V., Aman, Y., Dereje, K., Erban, V., Ezra, T., Firdawok, L., Habtamu, M., Hroch, T., Kopačková, V., Málek, J., Malík, J., Mišurec, J., Orgoň, A., Pécskay, Z., Šíma, J., Tarekegu, D., and Verner, K. (2014): Explanation booklet to the Set of Geoscience maps of Ethiopia at a scale 1: 50,000: sub-sheet 0738-D3 Shashemene. Czech Geological Survey, Prague; aquates; Geological Survey of Ethiopia, Addis Ababa,Ethiopia. pp 29-33.

Bernard, J., Vachette, C. and Valla, P. (1990). Deep groundwater survey with audio-magnetottelluric soundings: Annual Meeting Abstracts, Society of Exploration Geophysics, 528531.

Bernard, J. (2003). Short notes on the principles of geophysical methods for groundwater investigations.

Bekele A., Acocella, V., Korme T. and Ayalew, D. (2007). Quaternary faulting and volcanism in the Main Ethiopian Rift. *J. Afr. Earth sci.* **48**: 115-124.

Bekele A., Tsegaye, Manetti, P., Bonini,M., Corti, G., Innocenti, F., Mazzarini,F. and Pecskay, Z. (2005). Geological map(Scale 1: 200000) of the northern main Ethiopian rift and its implication for the volcano-tectonic evolution of the rift, Geological Society of America.

Blakely, R.J. (1995). *Potential theory in gravity and magnetic application*. Cambridge University press, NY, Cambridge, 441pp.

Caroline L., (1999). Ziway-Shala lake basin system, Main Ethiopian Rift: Influence of volcanism, Tectonics and climate forcing on basin formation and sedimentation. Paleo-geography, paleo-climatology and paleo-ecology 150(1999) 135-177.

Carruthers, R. M. and Smith, I. F. (1992). The use of ground electrical methods for sitting water supply boreholes in shallow crystalline basement terrains. **In:** *E.P. Wight and W.G. Burgess.* The Hydrogeology of crystalline basement aquifers in Africa. *Geological Society Special Publication*. **66:**203-220.

Craig, H. (1977). Isotope geochemistry and hydrology of geothermal waters in the Ethiopian Rift Valley. Scripps Insi. Oceanography, pp 77–14.

Darling, W.G., Berhanu Gizaw, and Arusei, M.K. (1996). Lake-groundwater relationships and fluid-rock interaction in the African rift valley: Isotopic evidence. *J. African Earth Sci.*, **22:**423–431.

Debebe, N., Yakoye B., Vladislav R. (2014). Geological hazards and engineering geology maps of Hosaina. Explanatory notes. Czech Geological Survey, Ethiopian Geological Survey and Aquatest a.s. Czech Republic. First edition.

Ebinger, C. (2005). Continental break-up: The East African perspective. Astronomy and Geophysics. **46:** 216-221.

EIGS (Ethiopian Institute of Geological Survay) (2012). A report on Geology, geochemistry and gravity survey of Hossaena area (Memoer No. 36). Unpublished report, Addis Ababa, Ethiopia.

Elizabeth, K., Zinabu Gebremariam and Ahlgren, A. (1989). The Ethiopian Rift Valley lakes: Chemical characteristics along a salinity-alkalinity series. Hydrobiologia 288 Addis Ababa, Ethiopia.pp:.1–12.

Hofmann, C., Courtillot, V., Feraud, G., Rochette, P., Yirgu, G., Ketefo, E. and Pik, R. (1997). Timming of the Ethiopian flood basalts events and implications for plume birth and global change, *Nature.* **389:** 838-840.

Igor, S. Zektser and Lome, G. Everett, (2004). Groundwater resources of the world and their use, UN. pp:20.

Jepsen, D. H. and Athearn, M.J. (1997). East-West Geologic Sections. Blue Nile River Basin, Drawing 5.2 BN-3, Department of Water Resources, Addis Ababa.

Kazmin, V. (1972). Geological map of Ethiopia. Scale (1: 2000,000). Geological survey of Ethiopia, Ministry of Mines, Addis Ababa.

Kazmin, V. (1980). Transform faults in the East African Rift System. *Atti. Conv. Lincei*,**47:**65-73.

Kearey, p., Brooks, M. and Hill, I. (2002). An Introduction to Geophysical Exploration. Blackwell Science, London. **3:**281.

Loke, M. (2004). Tutorial: 2-D and 3-D electrical imaging surveys. 136pp.

Mazac, O., Benes, L., Landa, I. and Maskova, A. (1990). Determination of the extent of oil contamination in groundwater by geophysical methods. In Ward. S. H., ED., Geotechnical and environmental geophysics, **02**:107-112.

Merla, G., Abbate, E., Azzaroli, A., Bruni, P., Canuti, P., Fazzuali, M., Sagri, M. and Tacconi, P. (1979). A geological map of Ethiopia and Somalia, and comment, CNR, Firenze.

Milsom, J. (2003). *Field Geophysics*. John Wiley & Sons Ltd, London, England, 3rd edi., 249pp.

Ministry of Water and Energy(MOWE) (2014). Water Source Assessment, Feasibility Study and Preliminary Design for 12 Rural Kebeles and 3 Rural Towns Water Supply in Wendo and Shashamane Woredas. V-I. Unpublished technical report. Addis Ababa, Ethiopia.

Mohr, P. (1962). The Ethiopian Rift system. *Bull. Geol. Obs*. **5:** 33-62.

Nicholson, S.E., (1996). A review of climate dynamics and climate variability in eastern Africa. **In:** *Johnson, T.C., Odada, E.O. (Eds*). The Limnology, Climatology and paleoclimatology of the Easter Africa lakes. Amsterdam, pp. 25-56.

Olayinka, A.I., and C.N.C. Mbachi, (1992). A technique for the interpretation of electrical sounding from crystalline basement areas of Nigeria: *J. Mining and Geol.*, **27:** 63-69.

Reynolds, J.M. (1997). *An Introduction to Applied and Environmental Geophysics*.

Sharma, P.V. (1997). *Environmental and Engineering Geophysics*, Cambridge University press, viewed 23 December 2017, http://books.google.com/books?hl=en&lr=&id=ic-sOMgM-rEC&pgis=1.

Shaaban, F. (2002). Vertical electrical for groundwater investigation in northwestern Egypt: a case study in a coastal area, *J. African Earth Sci*., **33:** 673-686.

Shimels Fikre (2006). Hydrogeological system analysis in Ziway–Shalla lakes area using hydrochemistry and isotope techniques, central Ethiopia**.** Unpublished M.Sc. Thesis Addis Ababa University, Addis Ababa, Ethiopia. pp 33.

Ukstins, I.A., Renne, P.R., Wolfenden, E., Baker, J., Ayalew, D. and Menzies, M. (2002). Matching conjugate volcanic rifted margins: $^{40}Ar/^{39}Ar$ chronostratigraphy of pre- and syn-rift bimodal flood volcanism in Ethiopia and Yemen. *Earth planet Sci. Lett*.,**98:** 289-306.

Vander Velpen B.P.A., (1995). RESIXIP and Win Resist software, 1st version; Interpex limited company.

WoldeGebriel, G., Aronson J.C., and Walter R.C. (1990). Geology, Geochronology and Rift Basin Development in the Central Sector of the Main Ethiopian Rift. Geological Society of America, bulletin.; **13**:439- 458.

Yahya, A. (2011). Geophysical Investigation of the Gergedi thermal springs, north west of wonji, Main Ethiopian Rift. Unpublished Msc. thesis. Adiss Ababa University, Addiss Ababa, Ethiopia.

Young, M.E., de Bruijin, R.G.M. and Al-Ismaily, S. (1998). Reports: exploration of an alluvial aquifer in Oman by time-domain electromagnetic sounding. *Hydrogeol. J.*,**6:**383-393.

Yungul, S. H., (1996). *Electrical methods in geophysical exploration of deep sedimentary basin*, Publ., Champan and Hall, London., 208 p.

Zinabu Gebre-Mariam and Elias Dadebo, (1989). Water resources and Fisheries management in the Ethiopian rift valley lake. SINET: *Ethiopian J. of Sci*.,**12 (2):**95-109.

Zohdy, A., Eaton, G.P. & Mabey, D. R. (1990*). Application of Surface Geophysics to Groundwater Investigations*. In Techniques of Water Resource Investigations of the United States Geophysical Survey, Denver: USGS publications.p116, viewed 21 December 2017http://pubs.usgs.gov/twri/twri2-d1/pdf/TWRI-2-D1.pdf.

http://www.weatherbase.com/weather/weathersummary.php3?s=601954&cityname=Shashemene %2C+Oromiya%2C+Ethiopia&units. viewed on 10 February 2018.

Appendix

Appendix 1: Interpreted VES curves of the each sounding points.

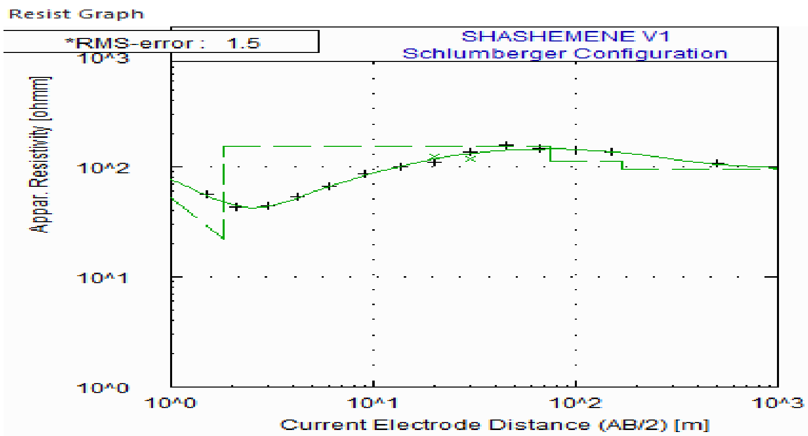

No	Res	Thick	Depth
1	108.1	0.6	0.6
2	22.0	1.2	1.8
3	155.0	73.0	74.8
4	112.0	95.0	169.8
5	95.0	-.-	-.-

* RMS on smoothed data

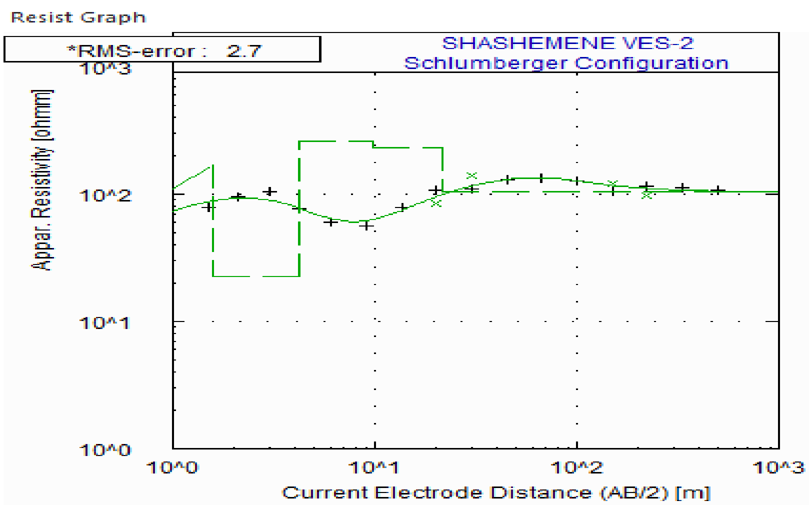

No	Res	Thick	Depth
1	48.7	0.4	0.4
2	168.0	1.1	1.6
3	22.4	2.7	4.3
4	260.0	5.4	9.7
5	231.9	11.8	21.4
6	104.3	-.-	-.-

* RMS on smoothed data

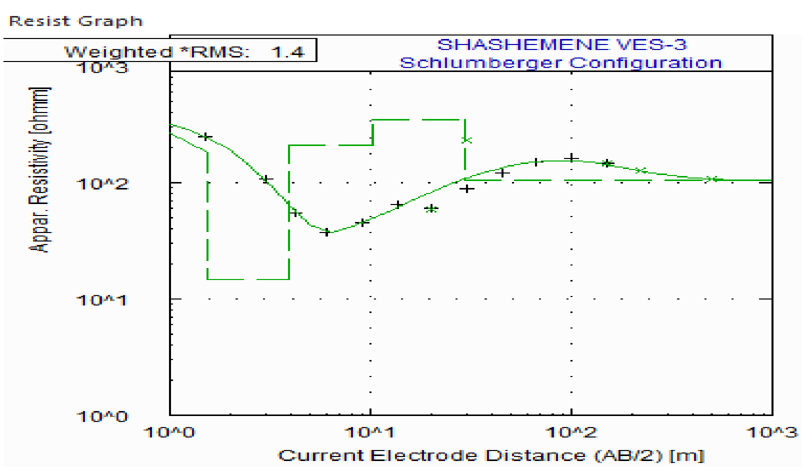

No	Res	Thick	Depth
1	368.6	0.7	0.7
2	180.4	0.8	1.5
3	14.6	2.4	3.9
4	209.7	6.2	10.2
5	351.5	19.3	29.5
6	103.7	-.-	-.-

* RMS on smoothed data

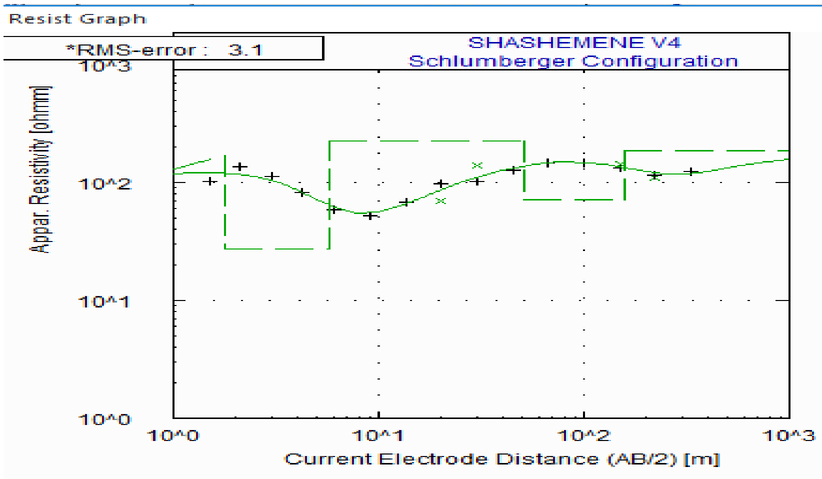

No	Res	Thick	Depth
1	111.3	0.7	0.7
2	168.8	1.1	1.8
3	27.1	3.9	5.7
4	223.9	45.7	51.4
5	72.1	105.9	157.4
6	186.8	-.-	-.-

* RMS on smoothed data

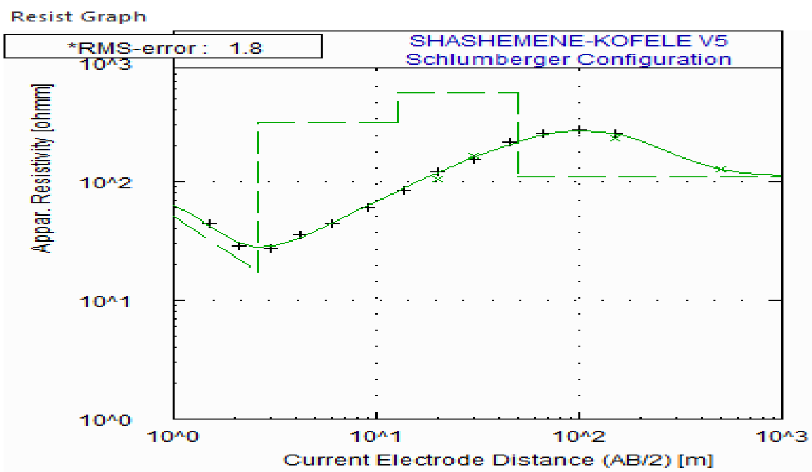

No	Res	Thick	Depth
1	95.8	0.6	0.6
2	17.6	2.0	2.6
3	316.6	10.2	12.8
4	564.5	36.8	49.6
5	109.6	-.-	-.-

* RMS on smoothed data

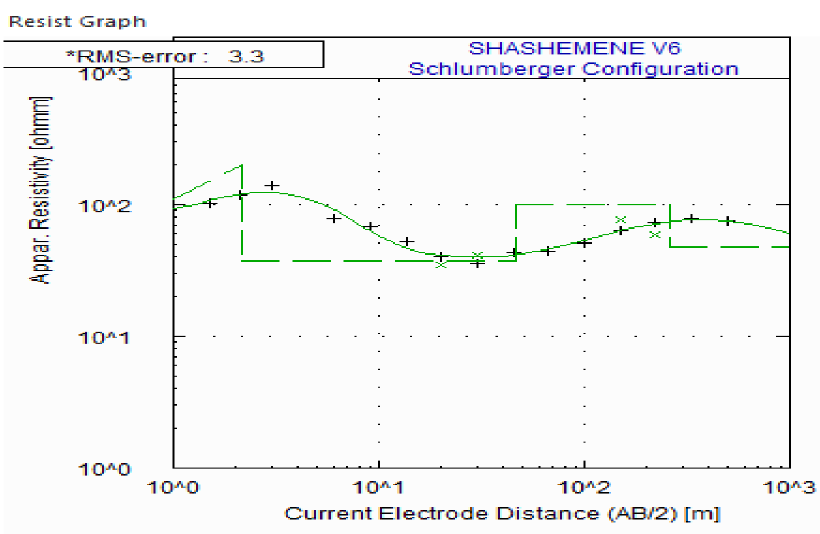

No	Res	Thick	Depth
1	70.6	0.6	0.6
2	199.1	1.6	2.2
3	37.6	44.4	46.6
4	100.3	214.5	261.1
5	47.9	-.-	-.-

* RMS on smoothed data

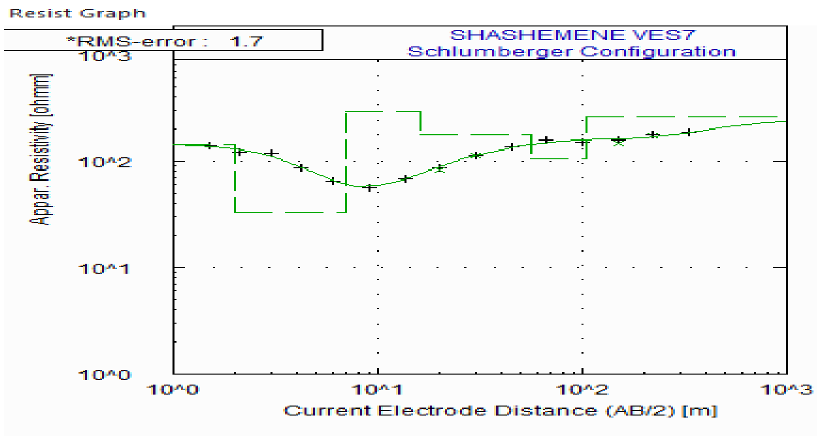

No	Res	Thick	Depth
1	144.4	2.0	2.0
2	33.3	5.0	7.0
3	296.8	9.0	16.0
4	179.2	40.6	56.6
5	105.5	49.2	105.8
6	260.7	-.-	-.-

* RMS on smoothed data

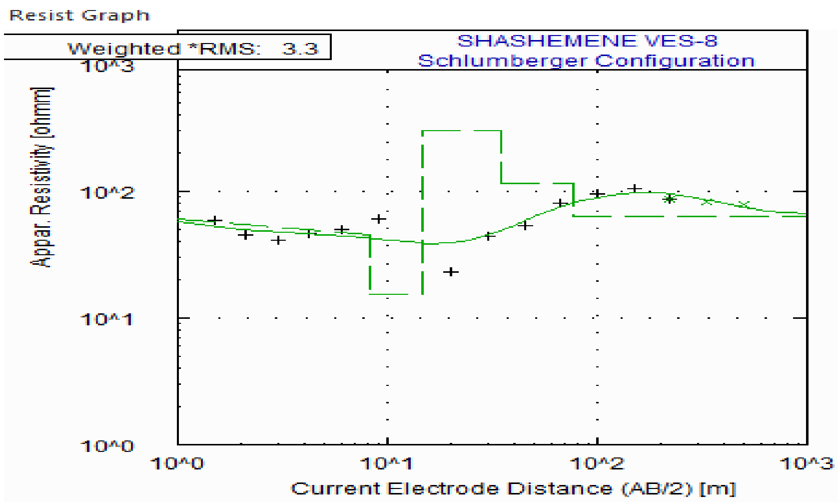

No	Res	Thick	Depth
1	64.5	0.6	0.6
2	45.0	7.7	8.3
3	15.4	6.4	14.7
4	304.0	20.0	34.7
5	114.5	41.3	76.0
6	63.8	-.-	-.-

* RMS on smoothed data

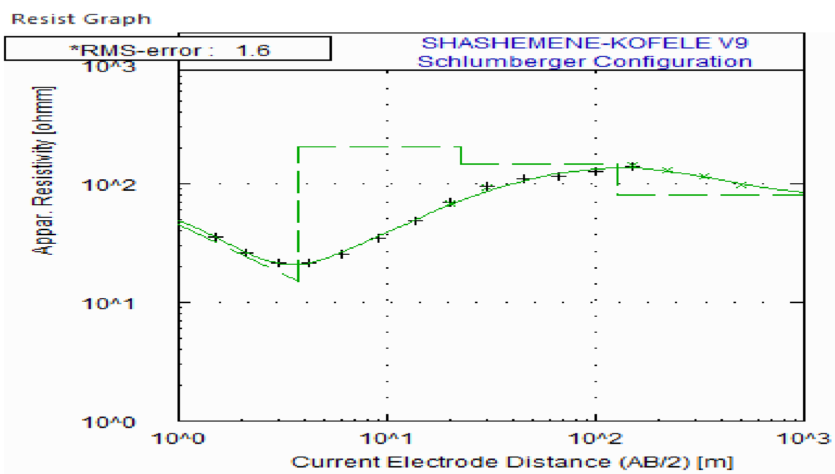

No	Res	Thick	Depth
1	63.2	0.7	0.7
2	14.9	3.0	3.7
3	205.8	18.9	22.6
4	146.6	104.8	127.4
5	81.0	-.-	-.-

* RMS on smoothed data

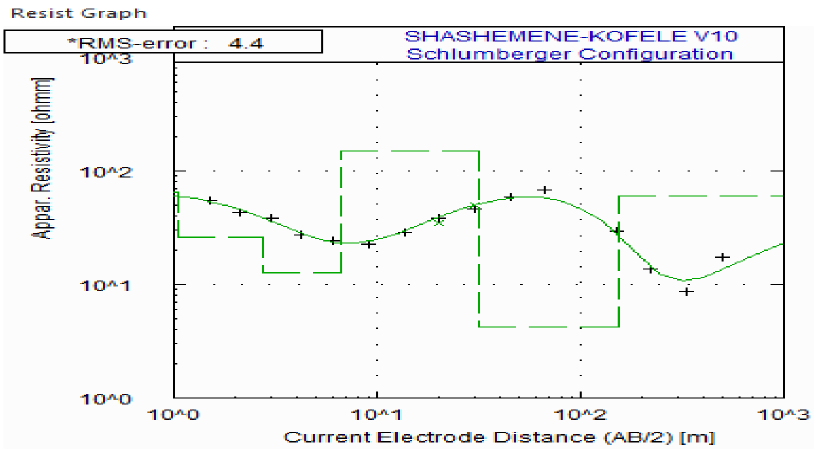

No	Res	Thick	Depth
1	64.2	1.1	1.1
2	26.1	1.7	2.8
3	12.8	3.8	6.6
4	150.8	24.7	31.3
5	4.2	123.2	154.5
6	60.4	-.-	-.-

* RMS on smoothed data

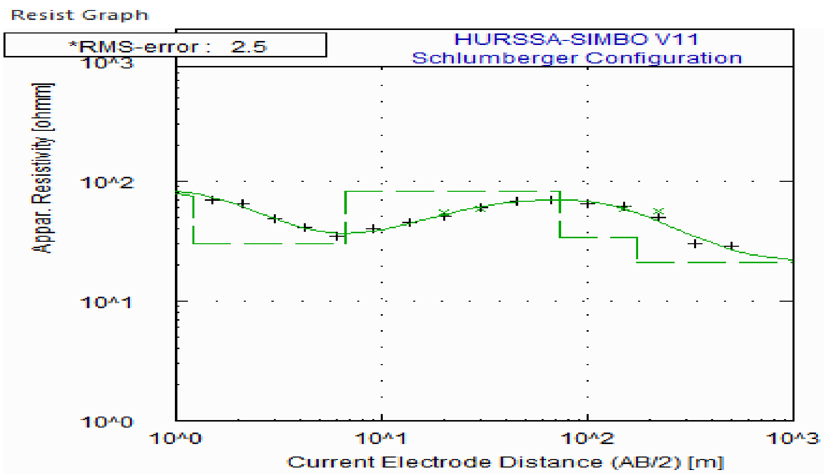

No	Res	Thick	Depth
1	95.6	0.5	0.5
2	74.4	0.7	1.2
3	30.1	5.4	6.6
4	82.0	66.1	72.7
5	34.0	100.4	173.1
6	21.0	-.-	-.-

* RMS on smoothed data

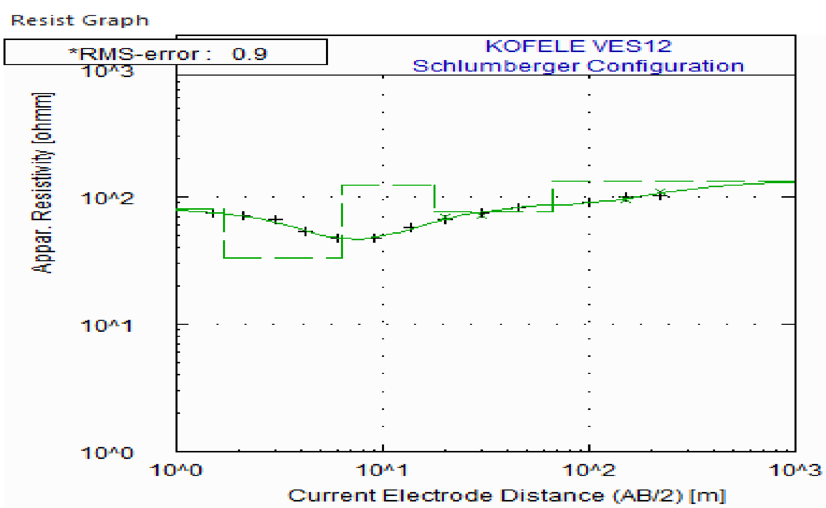

No	Res	Thick	Depth
1	79.7	1.7	1.7
2	33.5	4.7	6.4
3	123.0	11.2	17.6
4	77.1	48.2	65.9
5	134.3	-.-	-.-

* RMS on smoothed data

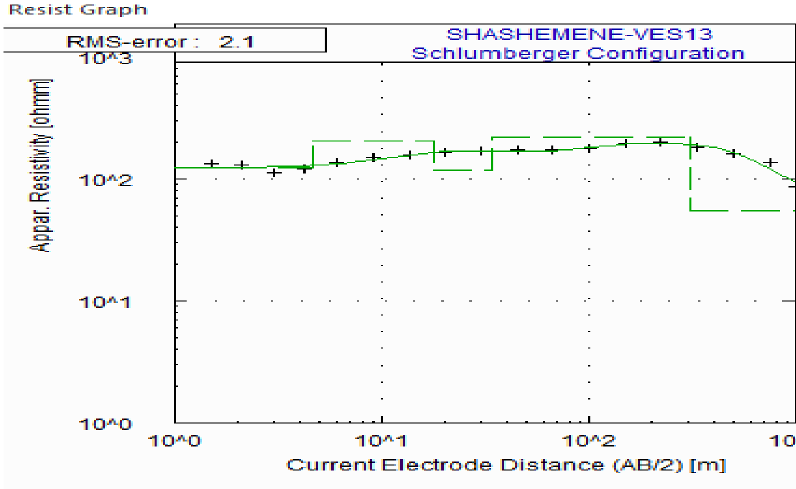

No	Res	Thick	Depth
1	123.6	4.7	4.7
2	204.2	13.3	18.0
3	118.3	16.0	34.0
4	221.6	276.7	310.7
5	55.0	-.-	-.-

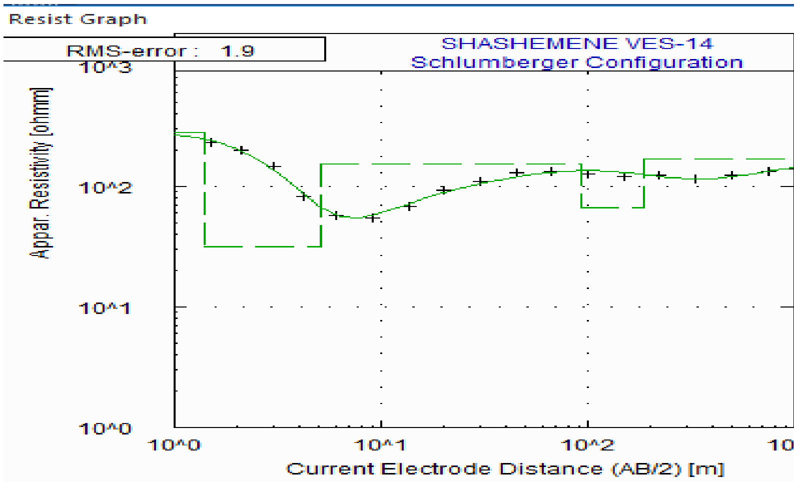

No	Res	Thick	Depth
1	283.8	1.4	1.4
2	31.7	3.7	5.1
3	154.2	88.8	93.9
4	65.9	94.8	188.7
5	167.9	-.-	-.-

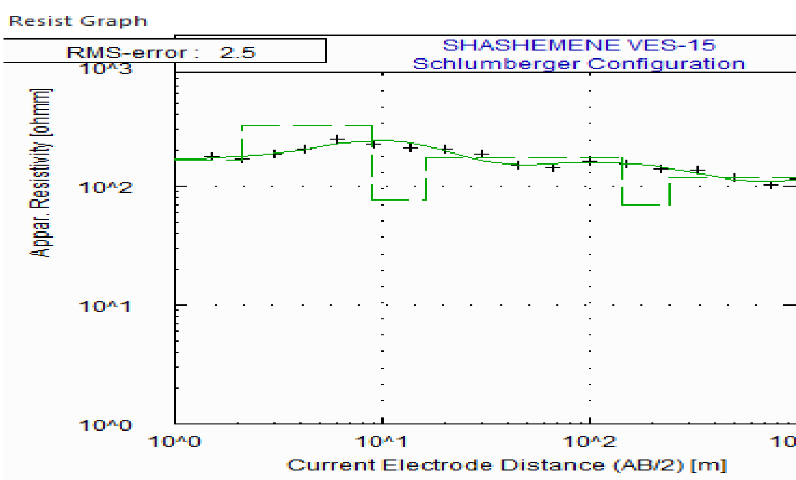

No	Res	Thick	Depth
1	167.4	2.1	2.1
2	326.1	6.7	8.8
3	76.0	7.5	16.3
4	174.5	126.5	142.8
5	69.1	99.8	242.6
6	117.9	-.-	-.-

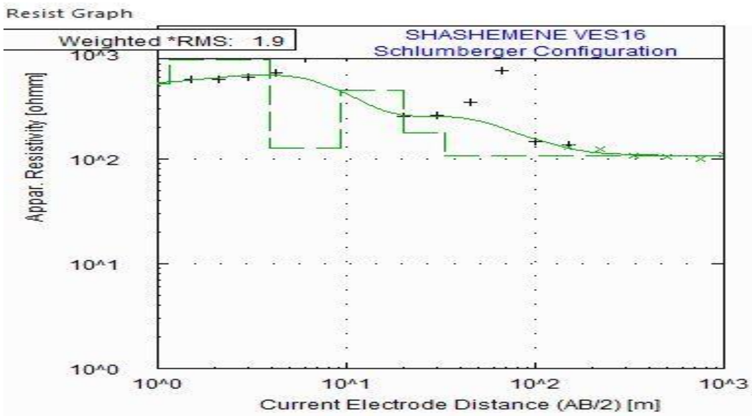

No	Res	Thick	Depth
1	523.7	1.1	1.1
2	885.1	2.8	4.0
3	127.2	5.4	9.4
4	457.3	10.7	20.0
5	176.2	13.3	33.3
6	107.0	-.-	-.-

* RMS on smoothed data

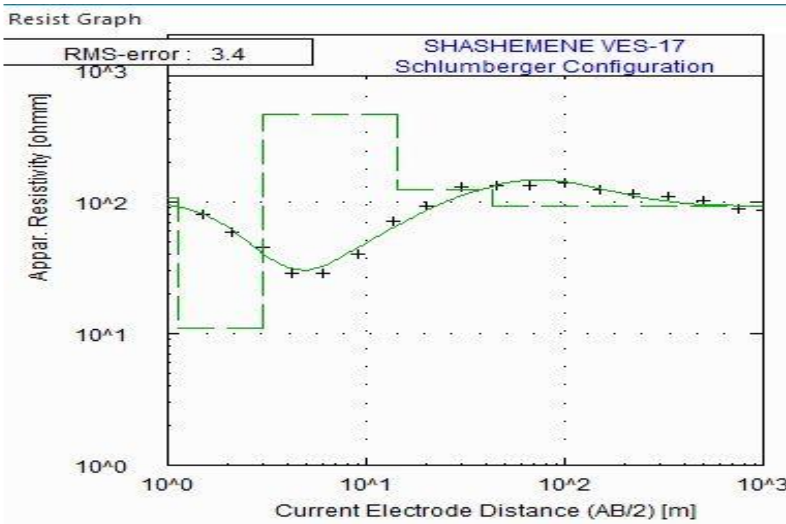

No	Res	Thick	Depth
1	106.3	1.1	1.1
2	10.9	1.9	3.0
3	467.2	11.4	14.3
4	123.2	29.1	43.4
5	92.5	-.-	-.-

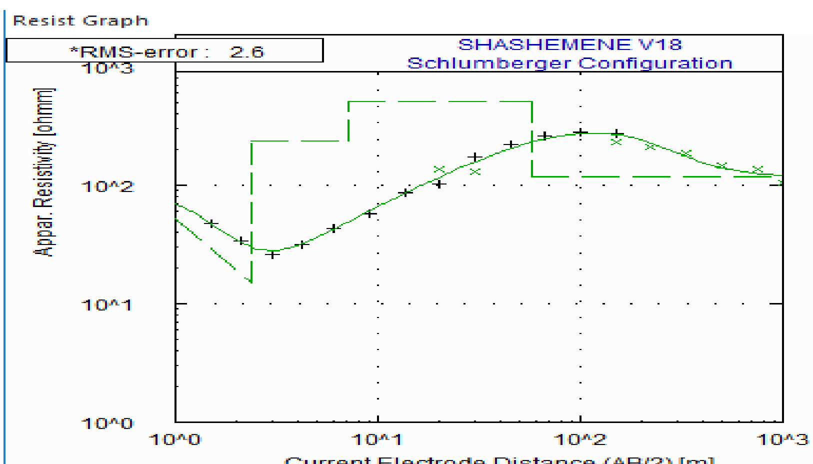

No	Res	Thick	Depth
1	97.5	0.6	0.6
2	15.1	1.7	2.4
3	238.8	4.8	7.2
4	516.2	50.2	57.4
5	117.6	-.-	-.-

* RMS on smoothed data

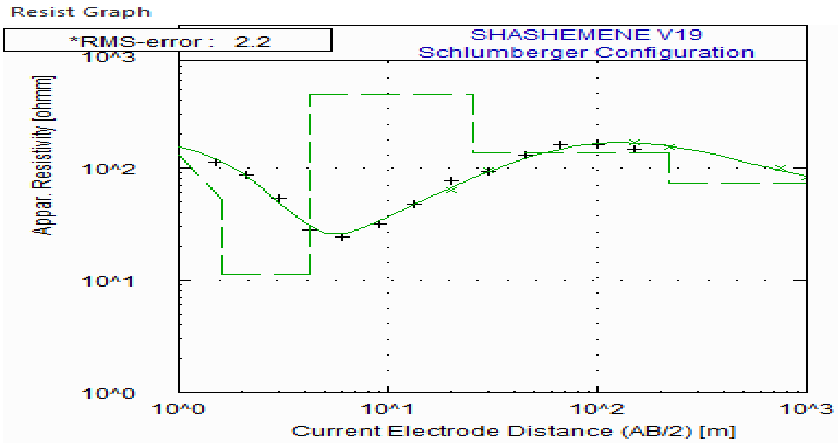

No	Res	Thick	Depth
1	178.2	0.9	0.9
2	52.1	0.8	1.6
3	11.2	2.6	4.2
4	457.4	21.3	25.5
5	136.5	193.4	218.9
6	72.6	-.-	-.-

* RMS on smoothed data

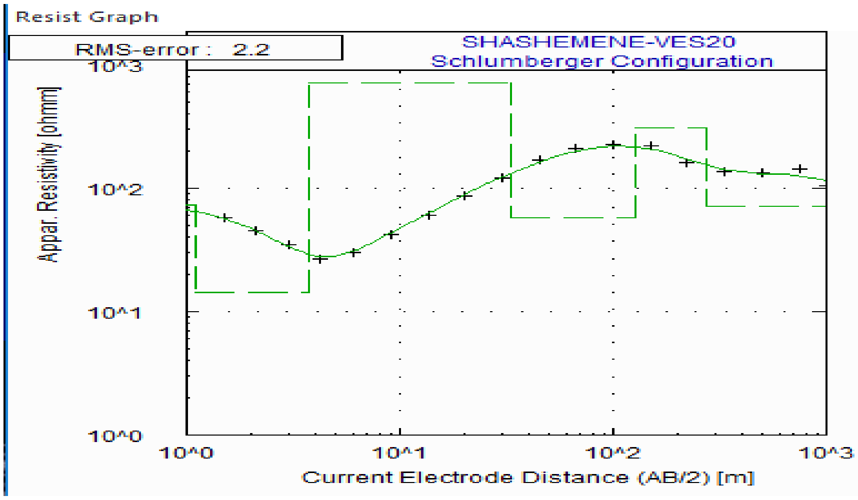

No	Res	Thick	Depth
1	72.5	1.1	1.1
2	14.4	2.6	3.7
3	719.5	29.4	33.1
4	57.1	93.5	126.6
5	311.5	145.6	272.1
6	71.3	-.-	-.-

Appendix 2: Table-1. Water Source Inventory Data

ID	Site	X UTM	Y UTM	Elevation [m]	Depth [m]	SWL [m]	Yield [l/s]	Geological unite	Source
1	Shashemene	455083	795184	1879	24			Dino formation	Halcrow
2	Shashemene	456242	795091	1927	145	91	2.17	Dino formation	Tesfay
3	Shashemene-Bekele Mola	454470	797355	1925	36	21		Dino formation	Tesfay
4	Kofele	476349	782867	2650	51	21	0.3	Nazret group	Tesfay
5	Sole no.1	461905	793072	2151	240			Ignimbrite	DH consultant
6	Goba	462767	786881	2334	42	35	3	Ignimbrite	DH consultant
7	Watera Haro	462049	787412	2325	54	30	5	Ignimbrite	DH consultant
8	Edola	458543	792168	2048				Ignimbrite	DH consultant
9	Sole no.2	461550	793334	2148	250	88	8.8	Ignimbrite	DH consultant
10	Burka-Bachilegesa	464817	784783	2445			2.5	Ignimbrite	DH consultant
11	Watera-Wage	463848	787222	2366				Ignimbrite	DH consultant
12	Bele	457263	785751	1754				Lacustrine sediments	DH consultant
13	Deye	465618	789609	2345			3	Ignimbrite	DH consultant
14	Denku	461769	793958	2128	162			Ignimbrite	DH consultant
15	Bekele Adem	458203	791792	2041	316	94.5	6	Ignimbrite	DH consultant
16	Abaro	462876	786900	2075				Ignimbrite	Tadese and Zenaw(2003)
17	Wondo G.F. College	460747	784454	1642				Rhyolite	Tadese and Zenaw(2003)
18	Bele hot spring	456965	786018	2532				Lacustrine sediments	Tadese and Zenaw(2003)

Description of geologic units

Dino formation: Ignimbrites, tuffs, pyroclastics, occasional lacustrine beds

Lacustrine sediments: Lacustrine sediments, silts, clays, diatomite, minor ignimbrites

Nazret group: Stratified silicic rocks, ignimbrites, unwelded tuffs, ash-flows, rhyolites

APPENDIX-3: Borehole logs (adopted from MOWE, 2014)

1. Faji sole borehole (461550E, 793334N)

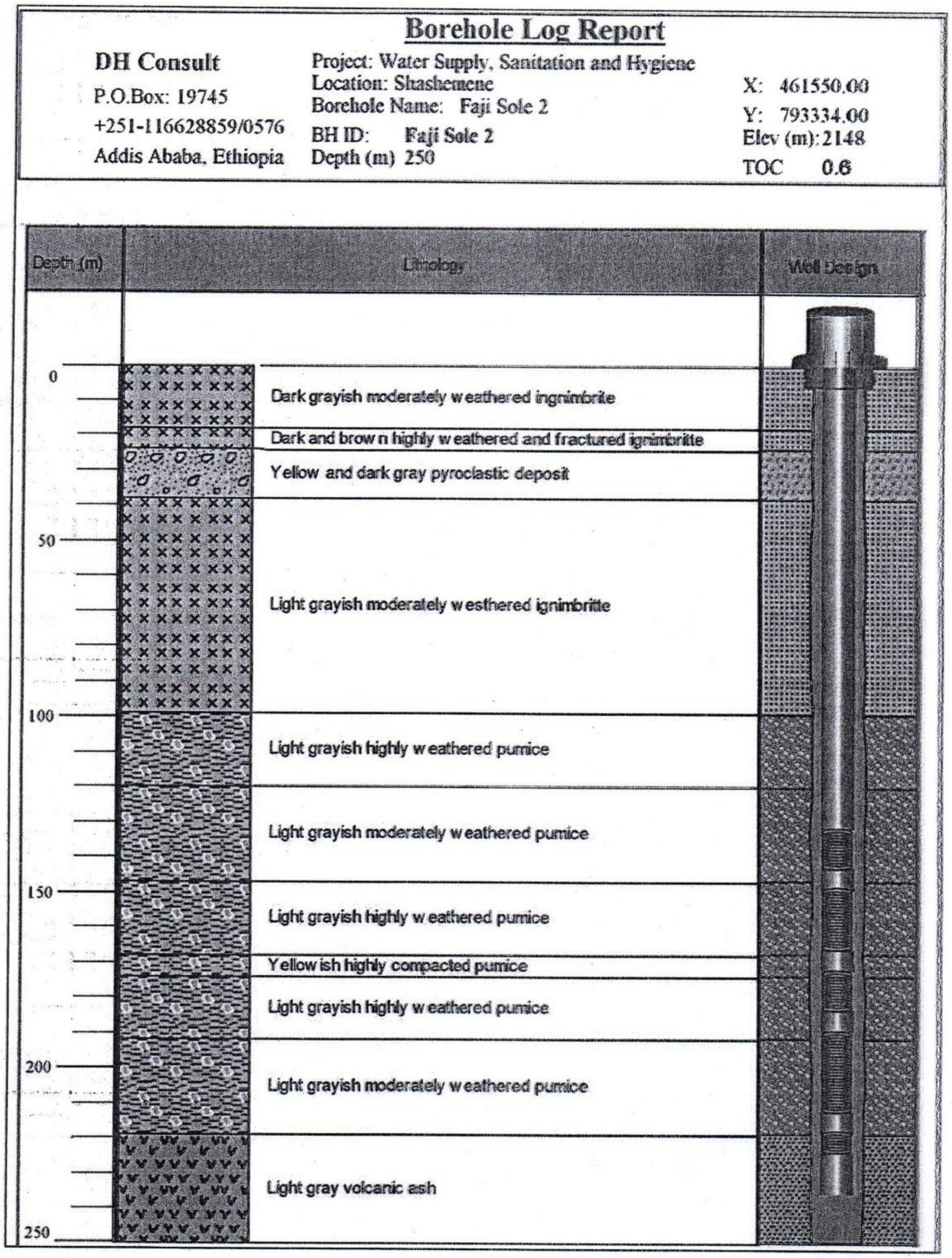

2. Mullata borehole (458203E, 791793N)

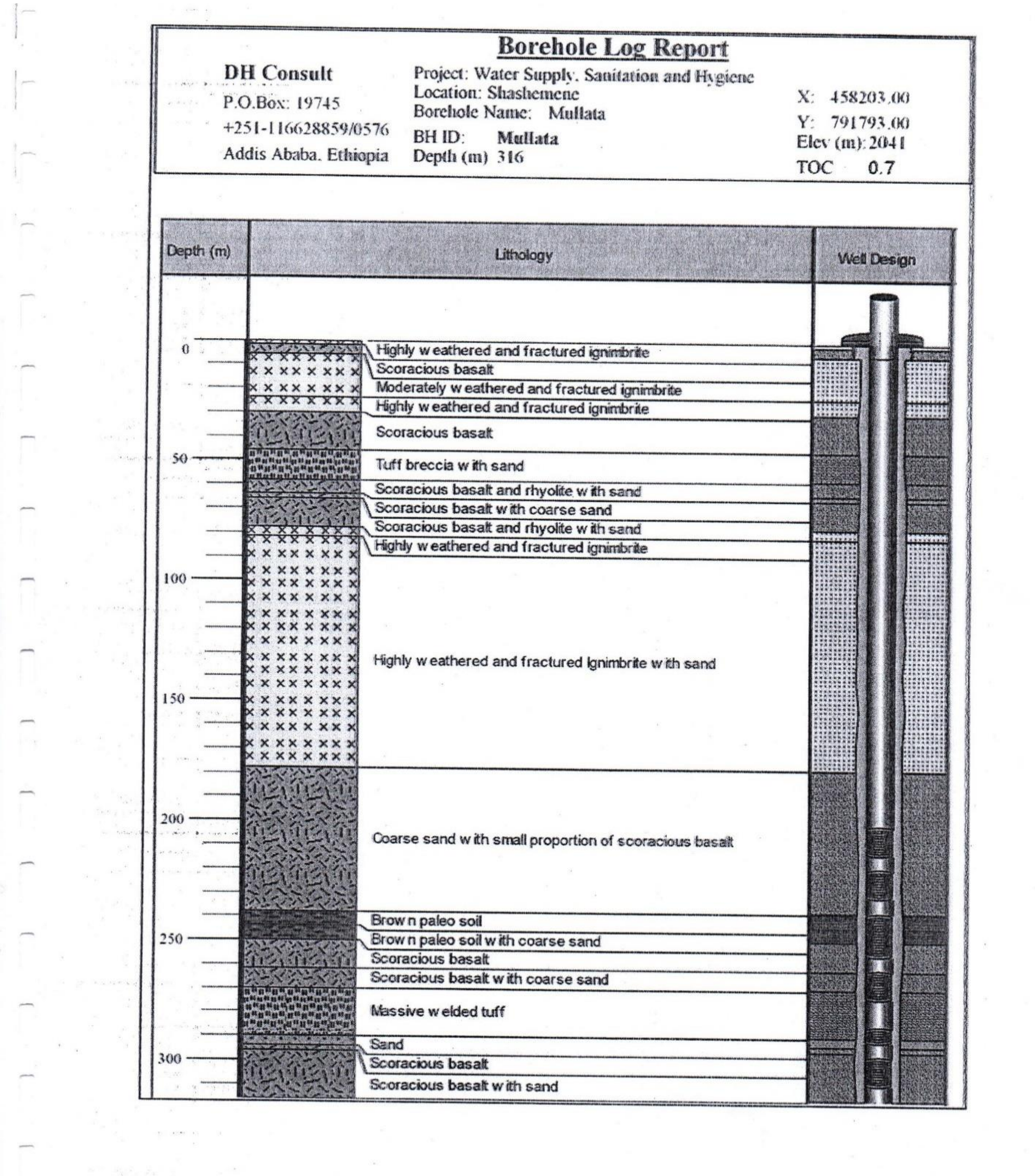

3. Shashemene new borehole (460822E, 794230N)

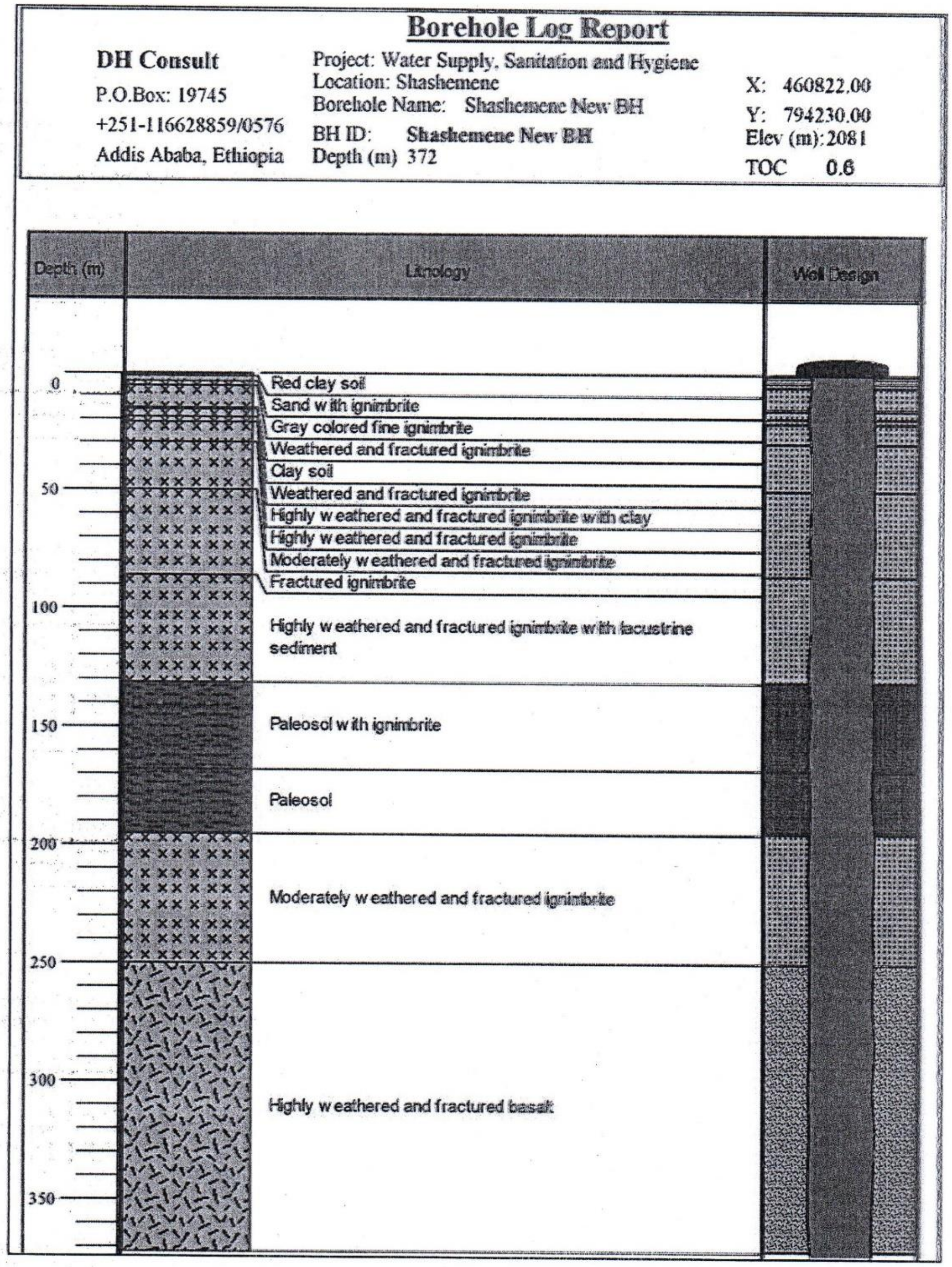

Figure 6-7a-c: Lithological logs of Faji Sole borehole number2, Mullata and Shashamane new boreholes.

Declaration

I hereby declare that the work which is being presented in this thesis is original work of my own, which has not been presented for any degree or diploma in any other university or institution, except where acknowledgement has been made in the text.

Tariku Degife Signature___________________

Date: 6/22/2018

This thesis has been submitted for examination with approval as university advisor.

Prof. Tigistu Haile Signature___________________

Advisor Date: 6/22/2018

Dr. Bekele Abebe Signature__________________

Co- Advisor Date: 6/22/2018